ZANCO (Print Version: ISSN 2218-0230)
(Online Version: ISSN 2412-3986)
(DOI : 10 . 21271 / ZJPAS)

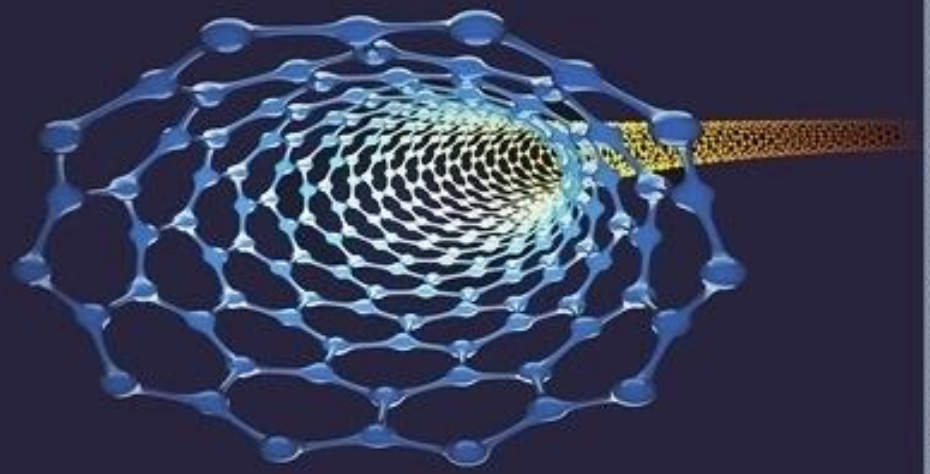

زانکۆی سەلاحەدین - هەولێر
Salahaddin University-Erbil

Volume 31, Number 2, 2019

ZANCO Journal of Pure and Applied Sciences

ZANCO

Journal of Pure and Applied Sciences

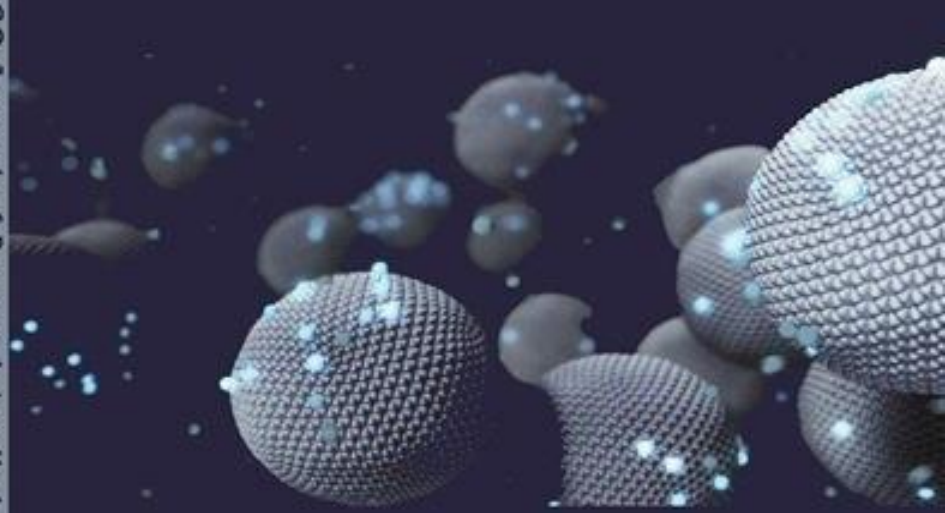

زانکۆی سەلاحەدین - هەولێر
Salahaddin University-Erbil

Volume 31, Number 2, 2019

ZANCO Journal of Pure and Applied Sciences
The official scientific journal of Salahaddin University-Erbil
https://zancojournals.su.edu.krd/index.php/JPAS

ISSN (print):2218-0230**, ISSN (online):** 2412-3986**, DOI: http://dx.doi.org/10.21271/zjpas**

RESEARCH PAPER

The Graph Based on a Given Ideal of a Ring

Fryad H. Abdulqadr

Department of Mathematics, College of Education, Salahaddin University - Erbil, Kurdistan Region, Iraq

A B S T R A C T:
In this paper we introduce a new kind of graph associated with a commutative ring with identity, and we discover some of its characterizations and properties. Let R be a commutative ring with identity and K be a non-trivial ideal of R. The graph-based on an ideal K, denoted by $\chi_K(R)$, is the undirected graph whose vertices are non-trivial ideals of R and two of its vertices are adjacent if and only if IJ⊂K.

KEY WORDS: Graphs, Annihilating-Ideal Graphs, Zero Divisor Graphs,Graphs based on the ideals.
DOI: http://dx.doi.org/10.21271/ZJPAS.31.2.1
ZJPAS (2019) , 31(2);1-8 .

1. INTRODUCTION :

In the recent years, many kinds of graphs associated with a ring were introduced. The concept of zero divisor graphs was introduced by (Beck, 1988) but his motive was in graph coloring. The diameter of zero divisor graph of a commutative ring with identity was studied by (Anderson, 1999). The concept of the annihilating-ideal graph AG(R) of a commutative ring R was introduced by (Behboodi, 2011) as a graph whose vertices are non-trivial ideals of R, and two distinct vertices I and J are adjacent if and only if IJ=(0). Many of its properties and characteristics were discovered by (Behboodi, 2011), (Lalchandani, 2017) and (Selvakumar, 2018). The Girth of the annihilating-ideal graph of commutative rings was studied by (Ahrari, 2015).

In this paper, we introduce and study a new kind of graph called graph-based on non-trivial ideals of R. The rings considered in this paper are commutative with identity. Also we use K, Max(R) and Min(R) to denote a non-trivial ideal, the set of maximal and minimal ideals of R respectively.

2. BACKGROUNDS

In this section, we recall some definitions and theorems that we need in our work.
According to (Gary, 1986), we will need the following definitions.

Definition2.1:
1. The degree of a vertex v in a graph G is the number of edges of G incident to v. The degree of a vertex v and the set of all vertices incident to v

* **Corresponding Author:**
Frya H. Abdulqadr
E-mail: fryad.abdulqadr@su.edu.krd
Article History:
Received:27/06/2018
Accepted:07/02/2019
Published:23/04/2019

in G are denoted by $\deg_G(v)$ and $N_G(v)$ respectively.

2. A graph G is complete if every two of its vertices are adjacent. A complete graph of order n is denoted by K_n. A clique number cl(G) of G is the greatest positive integer n such that K_n is a subgraph of G.

3. A vertex u is said to be connected to a vertex v in a graph G if there exists a u-v path in G. A graph G is connected if every two of its vertices are connected.

4. The distance d(x, y) between two vertices u and v in a connected graph G is the minimum of lengths of the u-v paths of G.

5. The eccentricity e(v) of a vertex v of a connected graph G is the number $\mathrm{Max}_{u\in V(G)}d(u,v)$.

6. The radius radG of a connected graph G is defined as $\mathrm{Min}_{u,v\in V(G)}e(v)$.

7. A vertex v of a connected graph G is a central vertex if e(v)=radG.

8. The diameter of a connected graph G is $\mathrm{Max}_{u,v\in V(G)}d(u,v)$.

9. A vertex v of a connected graph G is a cut-vertex if its removal produces a disconnected graph.

10. An acyclic graph G has no cycles. A tree is an acyclic connected graph.

11. The length of the shortest cycle in a graph G that contains cycles is called the girth of G and denoted by g(G).

12. A graph G is embeddable on a surface S if G can be drown on S so that edges intersect only at a vertex mutually incident with them. A graph is planar if it can be imbedded in the plane.

13. A dominating set for a graph G is a subset D of a vertex set of G such that every vertex not in D is adjacent to at least one member of D. The domination number $\gamma(G)$ is the number of vertices in a smallest dominating set for G.

14. An assignment of colors to the vertices of a graph G, one color to each vertex, so that adjacent vertices are assigned different colors is called a coloring of G; a coloring in which n colors are used is an n-coloring. The minimum n for which a graph G is n-colorable is called the chromatic number, and is denoted by X(G).

15. A graph G_1 is isomorphic to a graph G_2if there exists a one to one mapping f, called an isomorphism, from $V(G_1)$ onto $V(G_2)$ such that f preserves the adjacency.

According to (Gary, 1986), we need the following results.

Theorem2.2: (Kuratowsky Theorem)

A graph G is planar if and only if it does not contain a graph homeomorphic with K_5 or $K_{3,3}$.

According to (Behboodi, 2011), we will need the following results.

Proposition2.3: Let R be an Artinian ring. Then every non-zero proper ideal I of R is a vertex of AG(R).

Theorem2.4: For every ring R, the annihilating-ideal graph AG(R) is connected and diam(AG(R))≤3. Moreover, if AG(R) contains a cycle, then $g(AG(R)) \leq 4$.

3. THE GRAPH BASED ON AN IDEAL K

We start this section with the following definition.

Definition3.1: Let R be a commutative ring with identity and K be a non-trivial ideal of R. The graph based on an ideal K, denoted by $\chi_K(R)$, is the undirected graph whose vertices are non-trivial ideals of R and two of its vertices are adjacent if and only if IJ⊂K.

Before starting our main results, we give the following example.

Example3.2: Consider rings z_{24} and z_{64}. The following figures show the graphs $\chi_{(16)}(z_{64})$ and $\chi_{(6)}(z_{24})$.

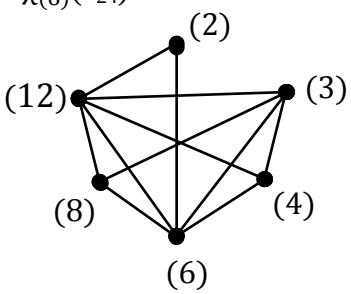

The graph $\chi_{(6)}(z_{24})$

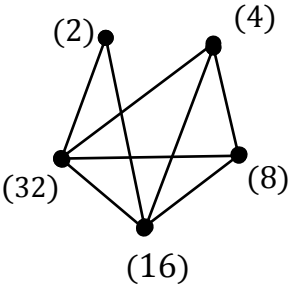

The graph $\chi_{(16)}(z_{64})$

Fig.1

Remark3.3:
1. IJ=(0)⊂K, for every edge {I, J} of AG(R). Thus AG(R) is a subgraph of $\chi_K(R)$.
2. If P is a proper ideal of R such that K⊂P, then $\chi_K(R)$ is a subgraph of $\chi_P(R)$.

We begin our results of this section with the following Lemma.

Lemma3.4:
1. If R is Artinian, then every non-trivial ideal of R is an ideal vertex of $\chi_K(R)$.
2. If I is an ideal of R such that 0≠I⊂K, then I is an ideal vertex adjacent to each other ideal vertices in $\chi_K(R)$.
3. If K∈Max(R), then degK is finite if and only if $\chi_K(R)$ is a finite graph.

Proof: The prove is trivial.

The next result illustrates the completeness of $\chi_K(R)$.

Theorem3.5: Let |Max(R)|≤2. If K∈Max(R) and every ideal vertex I∉Max(R) of $\chi_K(R)$ contains properly in K, then $\chi_K(R)$ is a complete graph.

Proof: Let I and J be any two distinct ideal vertices of $\chi_K(R)$. Then either I≠K or J≠K. Suppose that I≠K. If Max(R)={K}, then IJ⊆I⊂K. Suppose that Max(R)={K, M} with M≠K. If I, J∈Max(R), then the maximally of M gives that IJ=MK⊂K. Now assume that at least one of I and J is not maximal ideal, let be I. Then IJ⊆I⊂K. From each case, we have shown that I and J are adjacent in $\chi_K(R)$. Hence $\chi_K(R)$ is a complete graph.

In general, if K is a maximal ideal of R and $|Max(R)| > 2$, the graph $\chi_K(R)$ may not be complete, as the following example shows.

Example3.6: Consider a ring z_{30}.

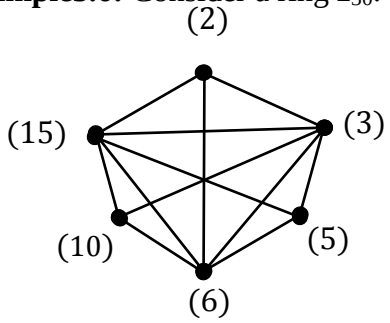

Fig.2: The graph $\chi_{(3)}(z_{30})$

Obviously, $\chi_{(3)}(z_{30})$ is incomplete.

We are now in a position to give the following main result of this section.

Theorem3.7:
1. Every two minimal ideals of R are adjacent ideal vertices in $\chi_K(R)$.
2. If K is a minimal ideal of R, then $\chi_K(R)$ and AG(R) are identical graphs.
3. Let Min(R)≠ ∅ be finite. Then every ideal vertex I∉Min(R) of $\chi_K(R)$ is adjacent to a minimal ideal of R. Moreover, the domination of $\chi_K(R)$ is at most |Min(R)|.

Proof:
1. Let I, J∈ Min(R) with I≠J. If IJ≠(0), then the minimally of I and J gives that IJ=I=J, which is impossible. Thus IJ=(0)⊂K. Hence I and J are adjacent ideal vertices in $\chi_K(R)$.
2. Let K∈ Min(R) and {I, J} be any edge of $\chi_K(R)$. It follows that IJ⊂K. Since K is a minimal ideal of R, IJ=(0). Thus {I, J} is an edge of AG(R). It follows from Remark3.3 that $\chi_K(R)$ and AG(R) are identical graphs.
3. Let I∉Min(R) be any ideal vertex of $\chi_K(R)$. If K∉Min(R), then there exists a minimal ideal L such that L⊂K. It follows from Lemma3.4 that I is adjacent to L in $\chi_K(R)$. Assume that K∈Min(R). Since I is an ideal vertex of $\chi_K(R)$, there exists an ideal vertex J≠I of $\chi_K(R)$ such that IJ⊂K. If J∈Min(R), the prove is completed, otherwise J contains a minimal ideal say N. This gives that IN⊆IJ⊂K. Thus I is adjacent to N in $\chi_K(R)$. From each case, we have shown that every ideal vertex of $\chi_K(R)$ is adjacent to at least one minimal ideal of R. This shows that $\gamma(\chi_K(R))\leq |Min(R)|$.

In the next result, we illustrate the incidence of edges of $\chi_K(R)$.

Proposition3.8: Let K be a prime ideal of R. For every edge {I, J} of $\chi_K(R)$ with I and J different from K, either I or J is a central ideal vertex $\chi_K(R)$.

Proof: Let {I, J} be an edge in $\chi_K(R)$ such that I, J≠K. Since IJ⊂K and K is a prime ideal of R, either I⊂K or J⊂K. It follows from the second part of Lemma3.4 that either I or J is a central ideal vertex of $\chi_K(R)$.

In the next result, we find the lower bound of the clique number of $\chi_K(R)$.

Theorem3.9: Let K∉Min(R) be a non-idempotent ideal of a non-domain R. Then the clique number of $\chi_K(R)$ is at least $|\{aK\in V(\chi_K(R))\backslash Min(R): a\in R\}| + |Min(R)|$.

Proof: Suppose that $A = S \cup Min(R)$, where $S=\{aK\in V(\chi_K(R))\backslash Min(R): a\in R\}$. Let I and J be any two distinct elements in A. If I, J∈Min(R), then by Theorem3.7, I and J are adjacent ideal vertices in $\chi_K(R)$. If I∈Min(R) and J∈S, then there exists $a\in R$ such that $a \notin Ann(K)$ and $J=aK \notin Min(R)$. Obviously, IJ⊆ K. If IJ=K, then K⊆I. This contradicts that I∈Min(R) and $K \notin Min(R)$. Therefore IJ contains properly in K. Suppose that I, J∈S. Then there exists $b, c \notin Ann(K)$ such that I=bK and J=cK are not minimal ideals of R. Since IJ⊆K^2⊆K and K is not idempotent ideal of R, IJ⊂K. From each case, we have shown that I and J are adjacent in $\chi_K(R)$. Thus the induced subgraph of $\chi_K(R)$ by the vertex set A is a complete. Hence $cl(\chi_K(R)) \geq |A|$.

We are now in a position to give the following main result of this section.

Theorem3.10: The graph $\chi_K(R)$ is connected and $diam\chi_K(R) \leq 3$.

Proof: Let I and J be any two distinct ideal vertices of $\chi_K(R)$. If I and J are adjacent in $\chi_K(R)$, we are done. Suppose that I and J are not adjacent in $\chi_K(R)$. Then there exist ideal vertices L and Q adjacent to I and J in $\chi_K(R)$, respectively. If L=Q, then P_2: I, L, J is a path in $\chi_K(R)$ of length 2. Suppose that L≠Q. If LQ⊂K, then P_3: I, L, Q, J is a path in $\chi_K(R)$ of length 3. If LQ⊄K, then LQ is a non-trivial ideal of R. Since I and J are not adjacent in $\chi_K(R)$, the ideals I , LQ and J are distinct. Obviously, ILQ, JLQ⊂K. Thus P'_2: I, LQ, J is a path in $\chi_K(R)$ of length 2. From each case we have shown that I and J are connected by a path of length at most 3. Thus $\chi_K(R)$ is a connected graph and $diam\chi_K(R) \leq 3$.

In the next result, we find the girth of $\chi_K(R)$.

Theorem3.11: Let $\chi_K(R)$ contains a cycle. If K∈Min(R), then the girth of $\chi_K(R)$ is less than or equal to 4, otherwise the girth is exactly 3.

Proof: If K∈Min(R), then by Theorem3.7 and Theorem2.4, $g(\chi_K(R))\in\{3, 4\}$. Suppose that K∉Min(R). Then there exists a non-zero ideal L such that L⊂K. By Lemma3.4, L is adjacent to every ideal vertex of $\chi_K(R)$. To find the girth of $\chi_K(R)$, assume that $\chi_K(R)$ contains a cycle C_n:I_1, I_2 , …, I_n, I_1 of length n. We have to show that n=3. Assume that n>3. Now we have two cases for L:

Case1: Let L be a vertex of C_n. If $L=I_1$, then by Lemma3.4, L is adjacent to I_3. Thus C_3: L, I_2, I_3, L is a cycle in $\chi_K(R)$ of length three. Similarly, if $L=I_r$, then we can obtain a cycle in $\chi_K(R)$ of the same length, for every r=2, 3, …, n.

Case2: Let $L\neq I_r$, for every r=1, 2, 3, …, n. By the same way of the first case, we can show that C_3: L, I_2, I_3, L is a cycle in $\chi_K(R)$ of length three.

Both cases contradict the fact that n>3. Therefore $g(\chi_K(R))=n=3$.

The following result shows that all ideal vertices which are not minimal ideals of R, will not be cut-vertices of $\chi_K(R)$.

Theorem3.12: Every cut-vertices of $\chi_K(R)$ is a minimal ideal of R.

Proof: Let I be any cut-vertex of $\chi_K(R)$. If we assume that I∉Min(R), then there exists a non-zero ideal L of R such that L⊂I. Since I is an ideal vertex of $\chi_K(R)$, there exists an ideal vertex J of $\chi_K(R)$ such that IJ⊂K. Obviously, LJ⊆IJ⊂K. This yields that L is an ideal vertex of $\chi_K(R)$. Suppose that S is an adjacent ideal vertex with I in $\chi_K(R)$ such that S belongs to a component of $\chi_K(R)$-{I} which does not contains L. This gives that LS⊆IS⊂K. Thus L and S are adjacent in $\chi_K(R)$. This contradicts the fact that S and L are in

different components of $\chi_K(R)$-{I}. Therefore I must be a minimal ideal of R.

Proposition3.13: Let K∉Min(R). If either $|Min(R)|>1$ or $|\chi_K(R)|>2$, then $\chi_K(R)$ is not a tree.
Proof: Suppose that $|Min(R)|>1$. Let S and T be two distinct minimal ideals of R. From Theorem3.7, S and T are adjacent ideal vertices in $\chi_K(R)$. On the other hand the minimally of S and T gives that neither K⊆S nor K⊆T. This yields that neither KS=K nor KT=K. It follows that KS, KT⊂K. Thus $\chi_K(R)$ contains a cycle C_3:S, T, K, S. Hence $\chi_K(R)$ is not a tree. It is easy to show that $\chi_K(R)$ is not a tree, when $|\chi_K(R)|>3$.

The graph $\chi_K(R)$ may be a tree, where K∈Min(R). We explain it in the following example.
Example3.14: Consider a ring z_{12}.

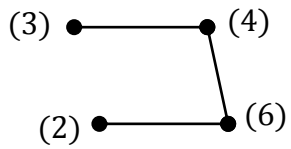

Fig.3: The graph $\chi_{(4)}(z_{12})$

We next turn to give the following result.
Proposition3.15:
1. If J and S are not co-maximal ideals of R and $|N_{AG(R)}(J) \cap N_{\chi_K(R)}(S)|>1$, then J+S is an ideal vertex of $\chi_K(R)$.
2. If AG(R)≠ ∅, then K is either an ideal vertex of AG(R) or adjacent to all ideal vertices I∈AG(R) in $\chi_K(R)$.
3. If R is Artinian ring, then $diamAG(R)\geq diam\chi_K(R)$.
Proof:
1. The ideal J+S is a non-trivial ideal, because J and S are not co-maximal ideals of R. Since $|N_{AG(R)}(J) \cap N_{\chi_K(R)}(S)|>1$, there exists I∈ $N_{AG(R)}(J) \cap N_{\chi_K(R)}(S)$ and J+S≠I. This gives that IJ=(0) and IS⊂K. It follows that I(J+S)⊂K. Thus J+S is an ideal vertex of $\chi_K(R)$.
2. Let AG(R)≠ ∅ and let I be any ideal vertex of AG(R). Then there exists an ideal vertex J of AG(R) such that IJ=(0). If either K=I or K=J, then K is an ideal vertex of AG(R). Suppose that neither K=I nor K=J. If KI=K, then K⊆I. It follows that KJ⊆IJ=(0). Thus K is an ideal vertex of AG(R). If KI≠K, then KI⊂K. Thus K is adjacent to I in $\chi_K(R)$.
3. The prove follows from Remark3.3 and Proposition2.3.

In the following result, we find the diameter of $\chi_K(R)$.
Proposition3.16: Let I be a non-trivial ideal of R such that {I, I^2, I^3, …, I^n} represents the set of all ideals of R. Then:

$$diam\chi_{I^s}(R)=\begin{cases} 1 & , \text{ if } s \in \{1,2\} \\ 2 & , \text{if } s \in \{3,4,\dots,n-1\} \end{cases}.$$

Proof: Let $s \in \{1,2\}$. Since $I^iI^j \subset I$, for every i and j with i<j, the graph $\chi_{I^s}(R)$ is a complete graph. In this case $diam\chi_{I^s}(R)=1$ and $cl(\chi_{I^s}(R))=|\chi_{I^s}(R)|$. If $s\in \{3,4,\dots,n-1\}$, then $I^sI^j \subset I^s$, for every j∈{1, 2, …, n−1}\{s}. Thus I^s is adjacent to each ideal vertex of $\chi_{I^s}(R)$. This yields that $diam\chi_{I^s}(R)\leq 2$. On the other hand $I^2I \not\subset I^s$, therefore $d(I^2, I)>1$. Hence $diam\chi_{I^s}(R)=2$.

4. THE GRAPH $\chi_K(z_{p^n})$

In this section we explore some characterizations of the graph-based on an ideal K=(p^s) of a ring z_{p^n}, where p is a prime number, and s and n are positive integers with $1 \leq s<n$. Obviously, n>1. If n=2, then the graph $\chi_{(p^s)}(z_{p^n})$ is empty. Through this section we assume that n>2.

We start this section with the following main result.
Proposition4.1: The graph $\chi_{(p^s)}(z_{p^n})$ is complete if and only if either s=1 or s=2.
Proof: Suppose that $\chi_{(p^s)}(z_{p^n})$ is a complete graph. Clearly, (p)(p^2) ⊄ (p^s), for every s>2. On the other hand (p^i)(p^j)⊂(p)∩(p^2), for every i≠j. This gives that s∈{1, 2}.

Conversely, suppose that s∈{1, 2}. Since i+j>2, for every i, j=1, 2, …, n−1 with i≠j, $(p^i)(p^j)\subset(p^s)$, for every i≠j. Hence the graph $\chi_{(p^s)}(z_{p^n})$ is complete.

In the next result we find the radius and central of $\chi_{(p^s)}(z_{p^n})$.

Proposition4.2: The radius of $\chi_{(p^s)}(z_{p^n})$ is equal to 1, and the central vertices of $\chi_{(p^s)}(z_{p^n})$ are (p^s), (p^{s+1}), …, (p^{n-1}) if s>2, otherwise all ideal vertices are central vertices of $\chi_{(p^s)}(z_{p^n})$.

Proof: Since $(p^b)(p^{n-1})\subset(p^s)$, for every ideal vertex (p^b), every ideal vertex (p^b) is adjacent to (p^{n-1}) in $\chi_{(p^s)}(z_{p^n})$. Thus the eccentricity of (p^{n-1}) is $e((p^{n-1}))=1$. This gives that $rad\chi_{(p^s)}(z_{p^n})=1$. If s≤2, Proposition4.1 follows that all ideal vertices are central vertices of $\chi_{(p^s)}(z_{p^n})$. Suppose that s>2. Let a be an integer with 0<a<n. If a≥s, then $(p^a)(p^m)\subset(p^s)$, for every m=1, 2, …, n−1 with m≠a. In this case $e((p^a))=1$. Assume that a<s. Obviously, $(p^a)(p^2)\not\subset(p^s)$, where a=1 and $(p^a)(p^1)\not\subset(p^s)$, where a>1. Thus $e((p^a))>1$. From both cases we have $rad\chi_{(p^s)}(z_{p^n})=1$ the central ideal vertices of $\chi_{(p^s)}(z_{p^n})$ are (p^s), (p^{s+1}), …, (p^{n-1}).

The next result demonstrates the relationship between two graphs-based on distinct ideals of z_{p^n}.

Theorem4.3: For every two distinct non-trivial ideals I and J of z_{p^n}, the graphs $\chi_I(z_{p^n})$ and $\chi_J(z_{p^n})$ are not isomorphic, otherwise they are identical complete graphs.

Proof: Let I=(p^a) and J=(p^b) be two distinct non-trivial ideals of z_{p^n}. If $a,b\in\{1, 2\}$, then by Proposition4.1, $\chi_I(z_{p^n})$ and $\chi_J(z_{p^n})$ are complete. From Proposition2.3, $\chi_I(z_{p^n})$ and $\chi_J(z_{p^n})$ have the same vertex set. In this case $\chi_I(z_{p^n})$ and $\chi_J(z_{p^n})$ are isomorphic. Suppose that a>2. If $b\in\{1, 2\}$, then $\chi_J(z_{p^n})$ is a complete graph but $\chi_I(z_{p^n})$ is incomplete graph. In this case $\chi_I(z_{p^n})$ and $\chi_J(z_{p^n})$are not isomorphic graphs. Suppose that a, b>2. Clearly, $\chi_I(z_{p^n})$ and $\chi_J(z_{p^n})$have the same vertex set including the maximal ideal (p). Obviously, the set of all ideal vertices adjacent to (p) in $\chi_I(z_{p^n})$ and $\chi_J(z_{p^n})$ are $\{(p^a), (p^{a+1}), (p^{a+2}), \ldots, (p^{n-1})\}$ and $\{(p^b), (p^{b+1}), (p^{b+2}), \ldots, (p^{n-1})\}$ respectively. This shows that $deg_{\chi_I(z_{p^n})}(p)\neq deg_{\chi_J(z_{p^n})}(p)$. Thus $\chi_I(z_{p^n})$ and $\chi_J(z_{p^n})$ are not isomorphic.

Example4.4: The following figures show that the graphs $\chi_{(2)}(z_{32})$ and $\chi_{(4)}(z_{32})$ are isomorphic, but $\chi_{(8)}(z_{32})$ and $\chi_{(16)}(z_{32})$ are not isomorphic.

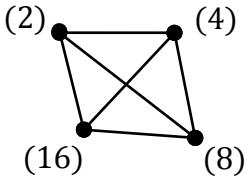

The graphs $\chi_{(2)}(z_{32})$ and $\chi_{(4)}(z_{32})$

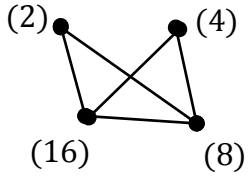

The graph $\chi_{(8)}(z_{32})$

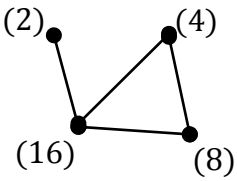

The graph $\chi_{(16)}(z_{32})$

Fig.4

In the next main result, we find the clique number of $\chi_{(p^s)}(z_{p^n})$.

Theorem4.5: Let $|\chi_{(p^s)}(z_{p^n})|>2$. Then the clique number of $\chi_{(p^s)}(z_{p^n})$ is $cl(\chi_{(p^s)}(z_{p^n}))=n-\left\lfloor\frac{s}{2}\right\rfloor$.

Proof: Let s∈{1, 2}. Then by Proposition4.1, $cl(\chi_{(p^s)}(z_{p^n}))=n-1$. If s∈{3, 4}, then a subgraph of $\chi_{(p^s)}(z_{p^n})$ induced by ideal vertices (p^2), (p^3), …, (p^{n-1}) is complete. In general, if s∈{l, l+1}, then a subgraph of $\chi_{(p^s)}(z_{p^n})$ induced by a set of ideal vertices

W={$(p^{\left\lceil\frac{l}{2}\right\rceil})$, $(p^{\left\lceil\frac{l}{2}\right\rceil+1})$, $(p^{\left\lceil\frac{l}{2}\right\rceil+2})$ …, (p^{n-1})} is complete, where 0<l<n. To show that W is a maximal complete subgraph of $\chi_{(p^s)}(z_{p^n})$, let I∉W be any ideal vertex of $\chi_{(p^s)}(z_{p^n})$. Then

I=(p^r) fore some r≤ $\left\lfloor\frac{l}{2}\right\rfloor - 1$. Since r+$\left\lfloor\frac{l}{2}\right\rfloor \leq 2\left\lfloor\frac{l}{2}\right\rfloor - 1 \leq s$, then $(p^r)(p^{\left\lfloor\frac{l}{2}\right\rfloor}) \not\subset (p^l)$. This means that a graph obtained by adding any ideal vertex of W will not be complete. Therefore W is a maximal complete subgraph of $\chi_{(p^s)}(z_{p^n})$. From each case we have shown that cl($\chi_{(p^s)}(z_{p^n})$)=n− $\left\lfloor\frac{s}{2}\right\rfloor$.

The next result illustrates the planarity of $\chi_{(p^s)}(z_{p^n})$.

Theorem4.6: Let $|\chi_{(p^s)}(z_{p^n})|$>5. Then the graph $\chi_{(p^s)}(z_{p^n})$ is planar if and only if (n, s)∈{(7, 5), (7, 6), (8, 7)}.

Proof: Assume that $\chi_{(p^s)}(z_{p^n})$ contains a complete bipartite subgraph with partite V={(p^{a_1}), (p^{a_2}), (p^{a_3})} and W={(p^{b_1}), (p^{b_2}), (p^{b_3})}. Since $(p^{a_i})(p^{b_j}) \subset (p^s)$, for every i, j=1, 2, 3 with i≠j, therefore (a_i+b_j)>s. On the other hand $(p^{a_i})(p^{a_j})$, $(p^{b_i})(p^{b_j}) \not\subseteq (p^s)$, for every i, j=1, 2, 3 with i≠j, then a_i+a_j, b_i+b_j≤s. Thus 2s<(a_i+b_i)+(a_j+b_j)≤2s. which is impossible. Hence $\chi_{(p^s)}(z_{p^n})$ does not contain a complete bipartite subgraph $K_{3,\,3}$. Suppose that (n, s)=(8, 7), then $\chi_{(p^s)}(z_{p^n})$ is:

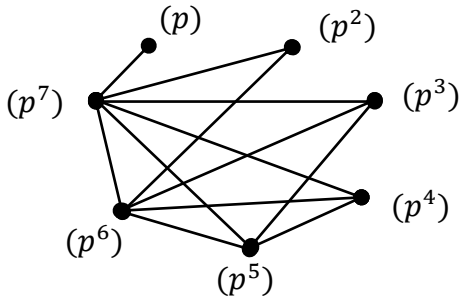

Fig.5: The graph $\chi_{(p^7)}(p^8)$

Obviously, $\chi_{(p^7)}(z_{p^8})$ does not contain K_5. Then by Koratowsky Theorem $\chi_{(p^s)}(z_{p^n})$ is a planar graph. Similarly, we can prove that $\chi_{(p^s)}(z_{p^n})$ is a planar graph, when (n, s)∈{(7, 5), (7, 6)}. Now suppose that (n, s)∉{(7, 5), (7, 6), (8, 7)}. If s∈{1, 2}, then Proposition4.1 and $|\chi_{(p^s)}(z_{p^n})|$>5 give that $\chi_{(p^s)}(z_{p^n})$ is a non-planar graph. Suppose that s>2. Clearly, n>6. If n=7, then s∈{3, 4} and hence $\chi_{(p^s)}(z_{p^n})$ contains K_5 of ideal vertices (p^2), (p^3), (p^4), (p^5) and (p^6). If n=8, then s∈{3, 4, 5, 6}. Similarly, we can find a complete subgraph K_5 of $\chi_{(p^s)}(z_{p^n})$. Suppose that n≥9. It is not hard to show that (p^{n-i}) $(p^{n-j}) \subset (p^s)$, for every i, j=1, 2, 3, 4, 5 with i≠j. Thus $\chi_{(p^s)}(z_{p^n})$ contains K_5 of ideal vertices (p^{n-1}), (p^{n-2}), (p^{n-3}), (p^{n-4}) and (p^{n-5}). From each case $\chi_{(p^s)}(z_{p^n})$ is a non-planar graph.

In the next we find the chromatic number of $\chi_{(p^s)}(z_{p^n})$.

Theorem4.7: For every s=1, 2, …, n−1, the chromatic number of $\chi_{(p^s)}(z_{p^n})$ is $\chi(\chi_{(p^s)}(z_{p^n})) = |\chi_{(p^s)}(z_{p^n})| - \left\lfloor\frac{s-1}{2}\right\rfloor$.

Proof: Let s∈{1, 2}. Then by Proposition4.1, $\chi_{(p^s)}(z_{p^n})$ is a complete graph. Thus the ideal vertex set of $\chi_{(p^s)}(z_{p^n})$ can be colored in $|\chi_{(p^s)}(z_{p^n})|$ different colors. In this case, the chromatic number of $\chi_{(p^s)}(z_{p^n})$ is equal to $\chi(\chi_{(p^s)}(z_{p^n})) = |\chi_{(p^s)}(z_{p^n})|$. Suppose that s∈{3, 4}. Clearly, a subgraph of $\chi_{(p^s)}(z_{p^n})$ induced by the set of ideal vertices A={(p^2), (p^3), …, (p^{n-1})} is complete. Then the set A can be colored in $|\chi_{(p^s)}(z_{p^n})| - 1$ different colors. Since (p^1) and (p^2) are not adjacent ideal vertices in $\chi_{(p^s)}(z_{p^n})$, we can color (p^1) in the same color of (p^2). Thus $\chi(\chi_{(p^s)}(z_{p^n})) = |\chi_{(p^s)}(z_{p^n})| - 1$. Suppose that s∈{5, 6}. Obviously, a subgraph of $\chi_{(p^s)}(z_{p^n})$ induced by the set B={(p^3), (p^4), …, (p^{n-1})} is a complete graph. Then the set B can be colored in $|\chi_{(p^s)}(z_{p^n})| - 2$ different colors. Since (p^1), (p^2), (p^3) are not adjacent to each others in $\chi_{(p^s)}(z_{p^n})$, we can color (p^1) and (p^2) in the same color of (p^3). Thus $\chi(\chi_{(p^s)}(z_{p^n})) = |\chi_{(p^s)}(z_{p^n})| - 2$. We continue on this process to get the general form $\chi(\chi_{(p^s)}(z_{p^n})) = |\chi_{(p^s)}(z_{p^n})| - \left\lfloor\frac{s-1}{2}\right\rfloor$.

Before closing this section we give the following result.

Proposition4.8: A graph $\chi_{(p^s)}(z_{p^n})$ is a tree if and only if (n, s)∈{(4, 3), (3, 1), (3, 2)}.

Proof: Suppose that (n, s)=(4, 3). Then $\chi_{(p^s)}(z_{p^n})$ consists of a path P_2: (p), (p^3), (p^2). Thus $\chi_{(p^3)}(z_{p^4})$ is a tree. Similarly, we can show that $\chi_{(p^s)}(z_{p^n})$ is a tree, when (n, s)∈{(3, 1), (3, 2)}. We now assume that (n, s)∉{(4, 3), (3, 1), (3, 2)}. Since s<n, then n≠3. If n=4, then s∈{1, 2}. By Proposition4.1, $\chi_{(p^s)}(z_{p^n})$ consists of a cycle of vertices (p), (p^2) and (p^3). Suppose that n>4. Since $(p^{n-i})(p^{n-j})\subset (p^s)$, for every s=1, 2, …, n−1 and every i, j=1, 2, 3 with i≠j, the graph $\chi_{(p^s)}(z_{p^n})$ contains a cycle C_3: (p^{n-1}), (p^{n-2}), (p^{n-3}), (p^{n-1}). From all cases we have shown that $\chi_{(p^s)}(z_{p^n})$ will not be a tree.

REFERENCES

Ahrari, M., Safari, S. and Amini, B.2015. On the Girth of the Annihilating-Ideal Graph of Commutative Rings, J. of Linear and Topological Algebra, Vol.4, No.3, pp.209-216.

Anderson, D. F. and Livingston, P. S. 1999 , The zero divisor graph of a commutative ring, Journal of Algebra, 217, 434-447.

Beck, I. 1988. Coloring of commutative rings, J. Algebra, 116, pp. 208–226.

Behboodi, M. and Rakeei, Z. 2011. The Annihilating-Ideal Graph of Commutative Rings I, J. of Algebra and Appl., Vol.10, No.4, pp.727-739.

Behboodi, M. and Rakeei, Z. 2011. The Annihilating-Ideal Graph of Commutative Rings II, J. of Algebra Appl., Vol.10, pp.741-753.

David, S. and Richard, M. 1991. Abstract Algebra, Prentice-Hall Inc. U. S. A.

Gary, C. and Linda, L. 1986. Graphs and Digraphs, 2nd ed., Wadsworth and Brooks/Cole, California.

Lalchandani, T. P. 2017. Exact Annihilating-Ideal Graph of Commutative Rings, J. of Algebra and Related Topics, Vol.5, No.1, pp. 27-32.

Selvakumar, K. and Subbulakshmi, P. 2018. On the Crosscap of the Annihilating-Ideal Graph of a Commutative Ring, Palestine Journal of Mathematics, Vol.7, No.1, pp.151-160.

ZANCO Journal of Pure and Applied Sciences
The official scientific journal of Salahaddin University-Erbil
https://zancojournals.su.edu.krd/index.php/JPAS

ISSN (print):2218-0230**, ISSN (online):** 2412-3986**, DOI: http://dx.doi.org/10.21271/zjpas**

RESEARCH PAPER

Facial Expression Identification System Using fisher linear discriminant analysis and K- Nearest Neighbor Methods.

Abdulqadir Ismail Abdullah[1]

[1]Department of Computer Science, College of Science, Knowledge University, Erbil, Kurdistan Region, Iraq

A B S T R A C T:

Facial expression system has become an important and effective research area in many fields such as cognitive processes, medical care and interaction between man and computer. A facial expressions recognition system using each of FLDA with K-nearest neighbors (K-NN) classifier is introduced in this research. The system is applied to recognize various basic facial expressions such as happy, neutral, angry, disgust, sad, fear and surprise, in the Karolinska Directed Emotional Faces (KDEF) and Japanese Female Facial Expressions (JAFFE) database. The experimental results on JAFFE database proved that the proposed method is robust with good accuracy compared to other approaches. The accuracy rate of the system achieved 95.٠9% and 94% when the proposed method was tested.

KEY WORDS: Face Expression, Expression Recognition, Fisher Linear Discriminant Analysis, K-Nearest Neighbors.
DOI: http://dx.doi.org/10.21271/ZJPAS.31.2.2
ZJPAS (2019) , 31(2); 9-13.

1. INTRODUCTION:

One of the goals of intelligent systems is to create systems that have the ability to effectively interact with humans in many ways. Many systems have been developed that carry out human facial expressions recognition to understand, interact, and recognize human emotions. However, the realization of the balance between speed and accuracy of each method in these systems is a challenging task (Chakraborty *et al*., 2017). Depending on the purpose of the system each system tries to use a methodology that reaches a level of accuracy and speed that is needed by the system.

* **Corresponding Author:**
Abdulqadir Ismail Abdullah
E-mail:abdulqadir.abdullah@knowledge.edu.krd
,abdulkhoshnaw@gmail.com
Article History:
Received: 06/11/2018
Accepted: 13/03/2019
Published: 23/04/2019

In general, most of facial expression systems contain three stages (preprocessing, feature extraction, and classification). In the feature extraction stage, the significant features of the face will be extracted to represent facial expressions (Abdullah *et al*., 2018).

There are two kinds of methods that can be implemented in this stage. The first type of method is used to extract the geometric features of the face while the second method is used to extract the appearance features (Sadeghi *et al*., 2013).

Geometric features methods aim to extract the shape and location of face component such as mouth, nose, eyes and eyebrow. However, using these kinds of methods in real time systems is very difficult because it needs more computational power but they are more robust compared to the appearance features methods. On the other hand, appearance features methods such as PCA principal component analysis (PCA) (George *et*

al., 2017), linear discriminant analysis (LDA) (Otroshi-Shahreza, 2017), Gabor wavelet transform (Abdulrahman *et al*., 2014), they aim to extract significant features either whole-face or specific regions of the face image.

Classification stage is another important stage of face expression's recognition system. Many algorithms have been proposed in order to classify the features of the face. At first, binary classification was introduced such as support vector machines (SVM) (Senthikumar *et al*., 2017), and then a number of enhancement methods were introduced to obtain robustness and low computational cost (Burges *et al*., 1997).

The remainder of this paper is organized as follows. Section two provides description of the design of the proposed system including the mathematical description of the proposed methods such as fisher linear discriminant analysis and K-Nearest Neighbors method. Section three introduces the experiment results. Finally, the conclusions are presented in Section four.

2. SYSTEM DESIGN

The proposed system consists of three main stages. The first stage is preprocessing. In this stage some of preprocessing methods such as (Adjust the intensity of the image and, remove the noise and enhance the contrast of the face image) are applied to enhance the face image. In the second step, fisher linear discriminant analysis as a feature extraction method is applied to extract the unique features of the face image. Finally, K-Nearest Neighbors is used to classify the extract features to give the nearest classification of the input image. Figure 1 shows the description of the steps of the proposed system:

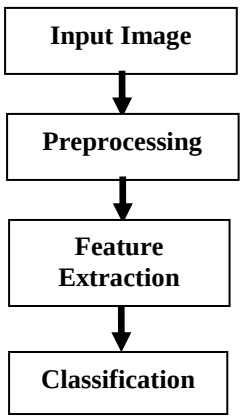

Figure (1): The design of the Proposed System

2.1. Preprocessing

Illumination is one of the important parameters that affect the quality of the image and the recognition rate. There are many preprocessing methods that can be applied to solve this problem and improve the quality of the input image and increase the recognition rate of the system. In this system, to enhance the contrast of the image, histogram equalization method was used in addition to Low Pass Filter to minimize the high frequency information. These two methods make the extract of the features from the image in the next stage easier and more effective.

2.2. Fisher Linear Discriminant Analysis

FLDA is a modification of Eigenfaces; therefore, it is based on Principal Components Analysis in its calculation. The main update to this method takes into consideration classes because Eigenfaccs does not find the variation among the two images from different classes during the training part. Each of the images was affected by the total average. FLDA uses the Linear Discriminant Analysis method to find the variation among different classes. It is aimed to minimize the variation within a class compared to the variation between classes. For that not only the total average of faces is used, but the average per class will also be an essential operation. The average is calculated according to the following equations (Atasoy *et al*., 2015):

$$\Psi_{c_l} = \frac{1}{q_i}\sum_{k=1}^{q_l} \Gamma_k \qquad (1)$$

Where C_i represents the class l and q_i represents the number of images in the class C. The average is also subtracted from each vector as in Eigentaces, but this time the average of the corresponding class is used.

$$\Phi_i = \Gamma_i - \Psi_{c_l} \qquad (2)$$

Then the scatter matrices are calculated. The Intra-class scatter matrix represented by Sw can be computed with the equation below:

$$s_w = \sum_{l=1}^{c}\sum_{\Gamma_k \in c_l} (\Gamma_k - \Psi_{c_l})(\Gamma_k - \Psi_{c_l})^T \qquad (3)$$

The Inter-class scatter matrix is represented by Sb which is computed using the following equation:

$$S_b = \sum_{i=1}^{c} q_i (\Psi_{c_i} - \Psi)(\Psi_{c_i} - \Psi)^T \quad (4)$$

The next formula is applied to get the total scatter matrix Sr.

$$S_T = \sum_{i=1}^{M} (\Gamma_i - \Psi)(\Gamma_i - \Psi)^T \quad (5)$$

After that, the aim is to find a projection of W which maximizes Fisher's optimization criteria.

$$W_{opt} = \arg max_w = \frac{|w^T S_b W|}{|w^T S_w W|} \quad (6)$$

Finally, the eigenvectors are found as follows:

$$S_b w_i = \lambda_i S_w w_i \, , i = 1,2, \dots m \quad (7)$$

Then the process is the same as Principal Components Analysis, the projection of the training image will be compared to the projection of a test image, and the class of the image which has the smallest distance will be the prediction of the algorithm.

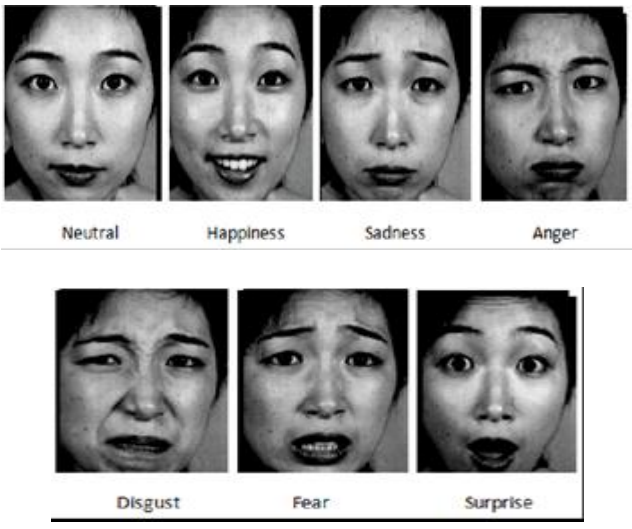

Figure 2: Different expressions of JAFFE Database

2.3 K-Nearest Neighbor

It is one of the famous and simple methods that is applied for classification and regression. It is applied to classify the extracted features based on closest training examples in the feature space. This method depends on Euclidian distance rule to calculate the similarity among the weight of the input facial image and the weights of the training data set. The Euclidean distance measuring is shown in equation below (Eyupoglu, 2016):

$$\mathrm{dist}(x, y) = \sqrt{\sum_{i=1}^{n} (x_i - y_i)^2} \quad (8)$$

Based on the equation (1), the smallest difference is selected and the input facial image is given the label of nearest neighbor class.

2.3. Implementation

The proposed system was implemented by developing a software application on a PC using MATLAB which allows us to program a code to process the input which are the images and also design a GUI in order to interact with the system. The system then will report the output to the user.

3. RESULTS AND DISCUSSION

MATLAB version 16th was used to implement the recognition system. All the experiments were simulated and implemented on a personal computer with 2.6MHz Core i5 CPU and 4 GB of memory running under Windows 7 64-bit operating system. A database called JAFFE (Dailey et al., 2010) (Japanese Female Facial Expressions) is a good example to evaluate the performance of this system by using it as a training set. This database is free and available on the Internet for academic and research purposes.

The database contains 213 images for 7 facial expressions (six basic facial expressions in addition to one neutral) are contained in this database and it is posed by 10 Japanese female models (Fig. 2).

These images are taken with a white homogeneous background in different lighting conditions. The size of each image is (256 x 256) pixels with 256 available gray levels per pixel and the accuracy rate of recognition reached up to 9°.٠9%. While, The KDEF (Goeleven et al., 2008) database consists of 239 colored images for s7 face expressions (one neutral pose and six different expressions) capture under different homogeneous background with different lighting conditions.

The database consists of 17 females and 17 males. The size of each image was (256 x 256) pixel. The accuracy rate of recognition reached up to 94%.

Table 1: Result accuracy by database

Seq.	Database	Number of Images	Accuracy
1	KDEF	239	94%
2	JAFFE	213	95.09%

In order to check the performance of our system in compare to other systems, a comparison was done to similar systems mentioned in (Shih et al., 2008). The comparison results are explained in Table 2 below.

Table 1: Comparison of results

#	Method	Database	Accuracy	Reference
1	Our proposed method	JAFFE	95.09%	
2	2D-LDA	JAFFE	94.13%	FRANK Y. SHIH, PATRICK S. P. WANG

As shown above that the proposed system in this research performed better than the other system and this can be due to the methods used.

A major disadvantage of this system is that some of the data used is non-linear and the methods described use linear descriptive analysis. A solution for this problem could be by using a Kernel method which allows to process non-linear data.

4. CONCLUSIONS

A facial expressions recognition system using each of FLDA with K-nearest neighbors (K-NN) classifier is proposed in this research. The system performance is computed by Extensive experiments conducted on databases called KDEF and JAFFE. The experimental results showed that the proposed system can work in different conditions such as facial details, different lighting exposure and facial expressions.

The results showed that the system has a high recognition rate with the accuracy up to 95.09% in JAFFE and 94 % in the KDEF database. In future work, a method like SVM (Support Vector Machine) or convolutional neural network (CNN) could be used to enhance the process of classification. Another method to enhance the lightening may be performed so as to improve the accuracy rate of the recognition. In the future the described method in this research could be improved by using some non-linear feature extraction methods and this will improve performance.

REFERENCES

CHAKRABORTY, S., SINGH, 2017. Local directional gradient pattern: a local descriptor for face recognition. Multimedia Tools Appl. 76, 1, pp. 1201-1216.

ABDULLAH, A. I., AL-DABAGH, M. Z. N. & ALHABIB, M.H.. 2018. Independent Component Analysis and Support Vector Neural Network for Face Recognition. International Journal of Applied Engineering Research, pp. 4802-4806.

SADEGHI, H., RAIE, A., & MOHAMMADI, M. 2013. Facial expression recognition using geometric normalization and appearance representation. 8th Iranian Conference on Machine Vision and Image Processing (MVIP), Zanjan, pp. 159-163.

GEORGE, G., ROBEN, R., RADHAKRISHNAN, B., & SURESH, L. P. 2017. Face recognition on surgically altered faces using principal component analysis. International Conference on Circuit ,Power and Computing Technologies (ICCPCT), Kollam, pp. 1-6.

OTROSHI-SHAHREZA, H. 2017. Frame-based face emotion recognition using linear discriminant analysis. 3rd Iranian Conference on Intelligent Systems and Signal Processing (ICSPIS), Shahrood, pp. 141-146.

ABDULRAHMAN, M., GWADABE, T. R, ABDU, F. J., & ELEYAN, A. 2014. Gabor wavelet transform based facial expression recognition using PCA and LBP.

22nd Signal Processing and Communications Applications Conference (SIU), Trabzon, pp. 2265-2268

SENTHILKUMAR, R. & GNANAMURTHY, R. K. 2017. Performance improvement in classification rate of appearance based statistical face recognition methods using SVM classifier. 4th International Conference on Advanced Computing and Communication Systems (ICACCS), Coimbatore, pp. 1-7.

BURGES, C., & SCHOLKOPF, B. 1997. Improving the Accuracy and Speed of Support Vector Machines.

ATASOY, H., YILDIRIM, S. & YILDIRIM, E. 2015. Emotion recognition from speech using Fisher's discriminant analysis and Bayesian classifier. 23nd Signal Processing and Communications Applications Conference (SIU), Malatya, pp. 2513-2516.

EYUPOGLU, C. 2016. Implementation of color face recognition using PCA and k-NN classifier, IEEE NW Russia Young Researchers in Electrical and Electronic Engineering Conference (EIConRusNW), St. Petersburg, pp. 199-202.

DAILY, M. N., JOYCE, C., LYONS, M. J., KAMACHI, M., ISHI, H., GYOBA, J. & COTTRELL EMOTION, G. W. 2010. Evidence and a computational explanation of cultural differences in facial expression recognition. Vol 10(6), 874-893.

GOELEVEN, E., DE RAEDT, R., LEYMAN, R, & VERSHUERE, B. 2008. The Karolinska directed emotional faces: a validation study. Cognition and Emotion, 22(6), pp. 1094-11189.

SHIH, F. Y. , WANG, P. S. P. , 2008. Performance comparisons of facial expression recognition in jaffe database. International Journal of Pattern Recognition and Artificial Intelligence 2008 22:03, 445-459.

.

ZANCO Journal of Pure and Applied Sciences
The official scientific journal of Salahaddin University-Erbil
https://zancojournals.su.edu.krd/index.php/JPAS

ISSN (print):2218-0230**, ISSN (online):** 2412-3986**, DOI: http://dx.doi.org/10.21271/zjpas**

RESEARCH PAPER

Model Reduction for Non-linear Protein Translation Pathways Using Slow and Fast Subsystems

Sarbaz H. A. Khoshnaw [1], Hemn M. Rasool [2]

[1] Department of Mathematics, University of Raparin, Kurdistan Region-Iraq
[2] Department of Mathematics, Koya University, Kurdistan Region-Iraq

A B S T R A C T:

This paper reviews the mechanisms of miRNA model where mathematical models of miRNA translation are suggested to describe the dynamics of protein synthesis. In this regard, we use the idea of quasi steady state approximation (QSSA) for separating model equations into slow and fast subsystems. This separation is based on a proper scaling that we have used in this study. The suggested technique provides one to minimize the model elements and gives some analytical approximate solutions. Accordingly, the equation of slow manifold can be calculated from the simplified model. The slow manifold is sufficiently close to the analytical solutions when the slow-fast parameter becomes smaller. We apply three types of model coefficient analysis including, elasticity coefficients, flux control coefficients and concentration control coefficients. These techniques have three main goals. The first goal quantifies the sensitivity of reaction rates to the change of concentrations or parameters. The second goal is to measure the change of a flux along model pathways in response to a change in model reaction rates. The third goal is to calculate the change of concentrations while responding to a change in reaction rates.

KEY WORDS: miRNA protein translation, Mathematical modeling, Slow and fast subsystems, Quasi steady state approximation, Elasticity and control coefficients.
DOI: http://dx.doi.org/10.21271/ZJPAS.31.2.3
ZJPAS (2019) , 31(2);14-24 .

1. INTRODUCTION :

Cells can be found in skin, muscles and bones. All of those cells include billions of proteins and enzymes. Indeed, proteins are fundamental of molecular for each living creature on the Earth (Cooper, 2000). There is an important part in cells that is called MicroRNA. MicroRNAs are a type of post-transcriptional well organized non-coding RNAs lately discovered in plants and animals. It has been shown that they regulate various biological procedures ranging from the embryotic development to the regularization of neural network model (Xu *et al*., 2009).

MicroRNAs (miRNAs) are 20 to 22 nucleotide RNAs that modulate the operation of eukaryotic mRNAs and have an important role in evolution, virus infection, stress responses, and cancer (Nissan and Parker, 2008). MicroRNAs are single-stranded RNA molecules of about 21 to 23 nucleotides in length, which modulate gene expression (Xu *et al*., 2009). There are some functions of miRNAs such as prevent translation of mRNAs,contributing mRNA and deadenylating progress (Eulalio *et al*., 2008, Filipowicz *et al*., 2008, Jackson and Standart, 2007, Valencia-Sanchez *et al*., 2006).

There are some main functions of MicroRNA where the most important function is related to gene expression regulation. For the first time, they were described in 1993 (Lee *et al*., 1993). In the

* **Corresponding Author:**
Sarbaz H. A. Khoshnaw
E-mail: Sarbaz.hamza@uor.edu.krd
Article History:
Received: 16/07/2018
Accepted: 25/03/2019
Published: 23/04/2019

Victor Ambros lab, and still the term microRNA was only introduced in 2001 (Ruvkun, 2001). As of early 2008, computational analysis by IBM proposed the existence of 50000 dissimilar microRNAs in the typical mammalian cell, each with perhaps a thousand or more possible targets (Glaser, 2008). Accordingly, MicroRNAs are recently well thought out as key regulators of a wide variety of biological pathways, including development, differentiation and on cogenesis.

Currently, remarkable advancement was made in understanding of microRNA functions, biogenesis and mechanisms of action.

The RISC effector complex and mature microRNAs are incorporated, which includes as a key component an Argonaut protein. MicroRNAs affect gene expression by guiding the RISC complex toward particular target mR NAs. It can be seen that there is a big controversial to determine the exact mechanism of this inhibition (Zinovyev *et al*., 2010); see Figure 1.

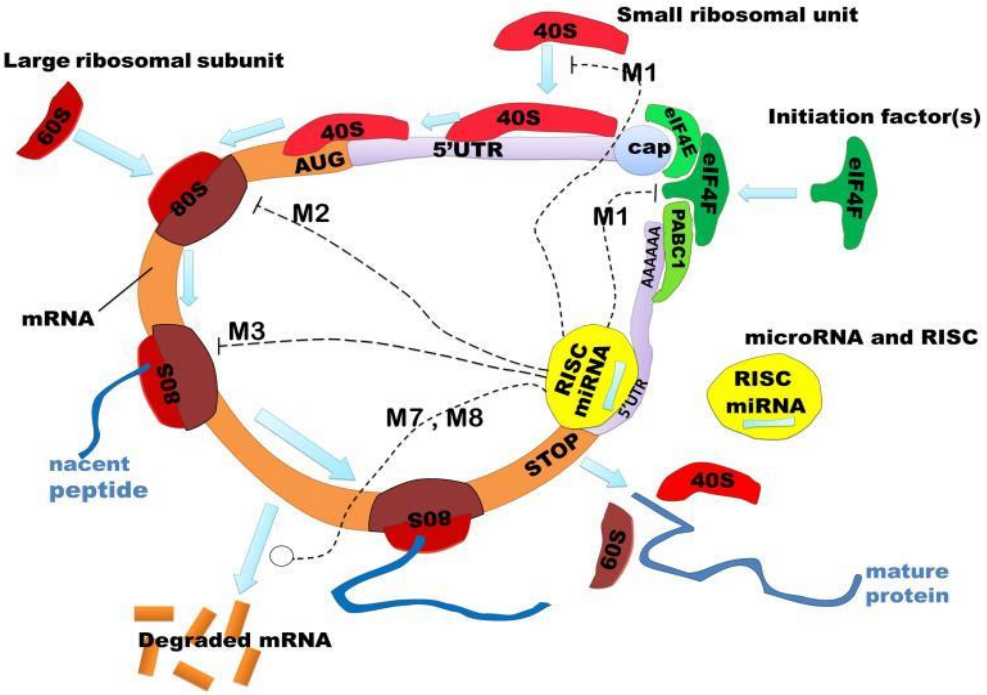

Figure 1: Protein translation process with microRNA mechanisms

In last decades, many possible mechanisms of microRNA have been recognized. The most of all documented mechanisms are negative post - transcriptional regulation of mRNA by mRNA translation inhabitancy and/or mRNA rotting. Whereas, there are some possibilities show that miRNAs might also act at the decomposition stage. There are also some studies in the present literature about to determine and decide which mechanism and in which situations has a control role in living cells. It is clear that some experimental systems handling with the same pairs of miRNA and mRNA. They can provide contentious evidences about which is the actual mechanism of translation subdue noticed in the experiment (Zinovyev et *al.*, 2013).

mRNA translation is an important procedure in cell signaling pathways that can be seen in many systems of biology. In this procedure, the genetic sequences are translated from mRNA to protein by ribosome translocation, after the genetic information included in DNA is transcribed to the mRNA. There are three important components in the mRNA translation process: the mRNA (genetic template), the ribosome (assembly machinery), and the aminoacyl transfer RNAs (aa-tRNAs).

mRNA protein translation is theoretically divided into three levels: initiation, elongation and termination. At the initiation stage, the ribosome first attaches to the mRNA then reads the mRNA codon by codon (from the 5' end of the mRNA to the 3' end). At the elongation stage, it recruits the

appropriate aa-tRNA and unites the latest amino acid into the nascent muster chain, releases the discharged tRNA. At the last stage of protein translation, the completed protein from the mRNA when the ribosome reaches the end of the mRNA eventually are released (Lewin, 2007).

There is a long history of mathematical modeling of mRNA. Models for mRNA then have been developed in recent years with the evolution of systems and synthetic biology. The various constructs of models for mRNA translation are introduced at various levels of abstraction (Zhao and Krishnan, 2014).

In this study, we give a detailed description for mathematical modelling of miRNA that describing the process of protein translation. We simply reviewed the previous study of miRNA protein translation given in (Zinovyev *et al.*, 2013). Then, we use quasi steady state approximation to separate equations into slow and fast subsystems and identifying some analytical approximate solutions for state variables. Finally, elasticity and control coefficient are calculated for the model network to identify effect of reaction rates, parameters and state variables on model dynamics.

2. Model Equations of miRNA

To explain the effect of microRNA interference with translation initiation factors, a non-linear version of the translation model was proposed. It explicitly takes into account recycling of initiation factors (eIF4F) and ribosomal subunits (40S and 60S).

The model has six chemical species *40S*, *60S*, *eIF4F*, *F*, *A*, and *R* and four chemical reactions, all considered to be irreversible; see Figure 2.

The model reactions are given below:
1. *40S* + *eIF4F* ⟶ *F*, assembly of the initiation complex (rate k_1).
2. *F* ⟶ *A*, some late and cap-independent initiation steps, such as scanning the 5'UTR for the start codon *A* (rate k_2).
3. *A* ⟶ *R*, assembly of ribosomes and protein translation (rate k_3).
4. 80S ⟶ 60S + 40S, recycling of ribosomal subunits (rate k_4).

We use stoichiometric vectors, reaction rates and mass action law to define the model equations (Khoshnaw, 2015a, Khoshnaw *et al*., 2016, Khoshnaw, 2015b).

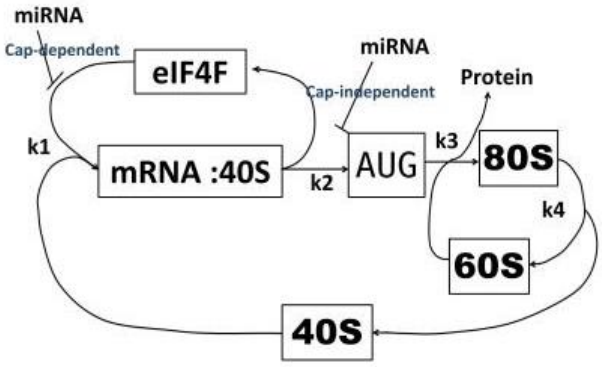

Figure 2: The model pathways for non-linear protein translation.

The model is described by the following system of nonlinear differential equations:

$$\begin{aligned}
\frac{d[40S](t)}{dt} &= -k_1[40S][eIf\,4F] + k_4[R],\\
\frac{d[eIF\,4F]}{dt} &= -k_1[40S][eIf\,4F] + k_2[F],\\
\frac{d[F](t)}{dt} &= k_1[40S][eIf\,4F] - k_2[F],\\
\frac{d[A](t)}{dt} &= k_2[F] - k_3[A][60S], \qquad (1)\\
\frac{d[60S]}{dt} &= -k_3[A][60S] + k_4[R],\\
\frac{d[R]}{dt} &= k_3[A][60S] - k_4[R],\\
Psynth(t) &= k_3[A](t).
\end{aligned}$$

System (1) contains three independent conservations laws:

$$\begin{aligned}
&[F]+[40S]+[A]+[R]=[40S]_0,\\
&[F]+[eIF\,4F]=[eIF\,4F]_0, \qquad (2)\\
&[60S]+[R]=[60S]_0,
\end{aligned}$$

where $[40S]_0$, $[60S]_0$ and $[eIF\,4F]_0$ are total amounts of small, big ribosomal subunits and the

initiation factor respectively. The following assumptions on the model parameters and initial variable states were suggested:

$$k_4 << k_1, k_2, k_3,$$
$$k_3 >> k_1, k_2, \quad (3)$$
$$[eIF4F]_0 << [40S]_0,$$
$$[eIF4F]_0 < [60S]_0 < [40S]_0.$$

More details and descriptions about the model equations and the proposed assumptions can be found in (Zinovyev *et al*., 2013).

3. Fast and Slow Subsystems for miRNA Model

Quasi steady state approximation (QSSA) is an important technique in systems biology. The method can be applied for nonlinear models to classify such systems into fast and slow subsystems and identify some analytical approximate solutions. More details about the QSSA method can be seen in (Khoshnaw, 2015a, Khoshnaw *et* al., 2016, Khoshnaw, 2015b). Based on conservation laws (2), we can remove the following variables:

$$eIF4F = [eIF4F]_0 - F,$$
$$60S = [60S]_0 - R, \quad (4)$$
$$A = [40S]_0 - 40S - F - R.$$

Then, system (1) becomes

$$\frac{d[40S](t)}{dt} = k_1[40S]F - k_1[eIF4F]_0[40S] + k_4R,$$
$$\frac{d[F](t)}{dt} = k_1[eIF4F]_0[40S] - k_1[40S]F - k_2F, \quad (5)$$
$$\frac{d[R](t)}{dt} = k_3[40S]_0[60S]_0 - k_3[60S]_0[40S] - k_3[60S]_0F$$
$$+ k_3[40S]R + k_3FR + k_3R^2 - (k3[60S]_0 + [40S]_0 + k_4)R.$$

By introducing the following new variables

$$x = \frac{[40S]}{[40S]_0}, y = \frac{F}{[eIF4F]_0}, z = \frac{R}{[eIF4F]_0}$$

and $\tau = k_1[eIF4F]_0 t.$ (6)

System (5) takes the form

$$\frac{dx}{d\tau} = x(y-1) + \rho z,$$
$$\varepsilon\frac{dy}{d\tau} = x(1-y) - \alpha_1 y, \quad (7)$$
$$\varepsilon\frac{dz}{d\tau} = \alpha_2(1-x) - \alpha_3 y + \alpha_4 xz + \varepsilon\alpha_4 yz$$
$$+ \varepsilon z^2 - (\alpha_3 + \alpha_4 + \rho)z,$$

where

$$\varepsilon = \frac{[eIF4F]_0}{[40S]_0}, \rho = \frac{k_4}{k_1[40S]_0}, \alpha_1 = \frac{k_2}{k_1[40S]_0},$$
$$\alpha_2 = \frac{k_3[60S]_0}{k_1[eIF4F]_0}, \alpha_3 = \frac{k_3[60S]_0}{k_1[40S]_0} \text{ and } \alpha_4 = \frac{k_3}{k_1}.$$

According to conditions (3),

$\rho = \frac{k_4}{k_1[40S]_0} \to 0$ when $k_4 << k_1$. Then, system (7) is completely on the form of slow and fast subsystems with six parameters. By applying QSSA technique, the system can be simplified when limit $\varepsilon \to 0$, the system takes the form

$$\frac{dx}{d\tau} = x(y-1) + \rho z, \quad (8a)$$
$$0 = x(1-y) - \alpha_1 y, \quad (8b)$$
$$0 = \alpha_2(1-x) - \alpha_3 y + \alpha_4 xz - (\alpha_3 + \alpha_4)z. \quad (8c)$$

We can analytically solve equations (8b) and (8c) for *y* and *z* in terms of *x*,

$$y = \frac{x}{\alpha_1 + x}, \quad (9a)$$
$$z = \frac{\alpha_3 x - \alpha_2(1-x)(\alpha_1 + x)}{(\alpha_4 x - \alpha_4 - \alpha_3)(\alpha_1 + x)}. \quad (9b)$$

Therefore, the approximate solution of system (7) is sufficiently close to the manifold M_0, where M_0 is defined as follows:

$$M_0 = \{(x, y, z) : x \in [0,1], \quad y = \frac{x}{\alpha_1 + x},$$
$$z = \frac{\alpha_3 x - \alpha_2(1-x)(\alpha_1 + x)}{(\alpha_4 x - \alpha_4 - \alpha_3)(\alpha_1 + x)}\}.$$

Thus, we obtain the following reduced differential equation close to the manifold M_0,

$$\frac{dx}{d\tau} = \frac{x^2}{\alpha_1 + x} - x. \qquad (10)$$

The above equation can be solved analytically.

The implicit solution of the separable differential equation takes the form

$$\alpha_1 \ln(x) + x = 1 - \alpha_1 \tau. \qquad (11)$$

$$[40S](t) = 1 + \frac{k_2}{k_1}\ln([40S]_0) - k_2[eIF4F]_0\, t - \frac{k_2}{k_1}\ln([40S](t)),$$

$$F(t) = \frac{[eIF4F]_0[40S](t)}{[40S](t) + \frac{k_2}{k_1}},$$

$$R(t) = \frac{[eIF4F]_0[60S]_0[40S](t) + [60S]_0([40S](t) - [40S]_0)(k_1[40S](t) + k_2)}{([40S](t) + \frac{k_2}{k_1})([40S](t) - [40S]_0 - [60S]_0)},$$

$$[eIF4F](t) = \frac{k_2[eIF4F]_0}{k_1[40S] + k_2},$$

$$[60S](t) = [60S]_0 - \frac{[eIF4F]_0[60S]_0[40S](t) + [60S]_0([40S](t) - [40S]_0)(k_1[40S](t) + k_2)}{([40S](t) + \frac{k_2}{k_1})([40S](t) - [40S]_0 - [60S]_0)},$$

$$A(t) = [40S]_0 - [40S](t) - \frac{[eIF4F]_0[40S](t)}{[40S] + \frac{k_2}{k_1}} - \frac{[eIF4F]_0[60S]_0[40S](t) + [60S]_0([40S](t) - [40S]_0)(k_1[40S](t) + k_2)}{([40S](t) + \frac{k_2}{k_1})([40S](t) - [40S]_0 - [60S]_0)},$$

$$Psynth(t) = k_3([40S]_0 - [40S](t) - \frac{[eIF4F]_0[40S](t)}{[40S] + \frac{k_2}{k_1}} - \frac{[eIF4F]_0[60S]_0[40S](t) + [60S]_0([40S](t) - [40S]_0)(k_1[40S](t) + k_2)}{([40S](t) + \frac{k_2}{k_1})([40S](t) - [40S]_0 - [60S]_0)}).$$

4. Analytical Approximate Solutions

In this section, the analytical solutions for the original model (1) are calculated. This is based on equations (11), (9), (6) and (4). All analytical solutions are given below:

It is obvious that the slow manifold M_0 is normally hyperbolic and stable. We assume that the functions $G_1(y,z)$ is the left side of equation (8b) and $G_2(y,z)$ is the left side of equation (8c). This means

$$G_1(y,z) = x(1-y) - \alpha_1 y, \qquad (12)$$

$$G_2(y,z) = \alpha_2(1-x) - \alpha_3 y + \alpha_4 xz - (\alpha_3 + \alpha_4)z.$$

Then, the Jacobian matrix of G_1 and G_2 is given:

$$J=\begin{pmatrix}\frac{\partial G_1}{\partial y} & \frac{\partial G_1}{\partial z}\\ \frac{\partial G_2}{\partial y} & \frac{\partial G_2}{\partial z}\end{pmatrix}=\begin{pmatrix}-(\alpha_1+x) & 0\\ -\alpha_3 & \alpha_4 x-\alpha_4-\alpha_3\end{pmatrix}.$$

The characteristic equation $\det(J-\lambda I)=0$ can be solved analytically to find the eigenvalues of the Jacobian matrix. We obtained the following eigenvalues:

$$\lambda_1=-(\alpha_1+x),$$
$$\lambda_2=\alpha_4 x-\alpha_4-\alpha_3.$$

It is clear that the first eigenvalue is negative. It means $\lambda_1<0$ since

$x=\frac{[40S]}{[40S]_0}>0$ and $x=\frac{k_2}{k_1[40S]_0}>0$ .The other eigenvalue is also negative $\lambda_2<0$

because $\alpha_3=\frac{k_3[60S]_0}{k_1[40S]_0}$ and $\alpha_4=\frac{k_3}{k_1}, k_3>>k_1,$

and $x\in[0,1]$.

Since eigenvalues have negative real parts $\mathrm{Re}(\lambda_i)<0$, for i = 1, 2 then the slow manifold M_0 is stable. And the approximate solutions of equations (7) for different values of the small parameter ε can be expressed in Figure 3. The approximate solutions are sufficiently close to M_0 when the slow-fast parameter becomes smaller. We have compared the species concentrations of reduced model (10) and the full model (dimensionless form); see Figure 4.

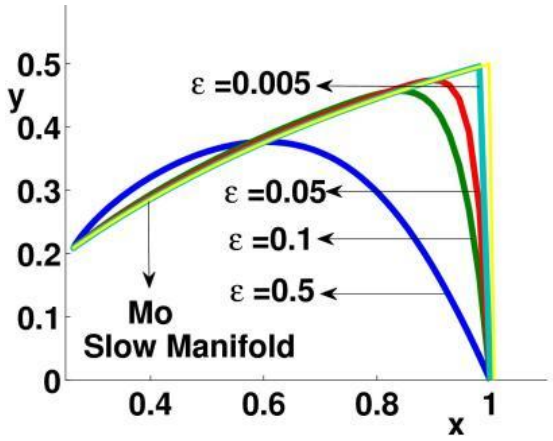

a) $\rho=1,\alpha_1=1,\alpha_2=3,\alpha_3=2$ and $\alpha_4=4$

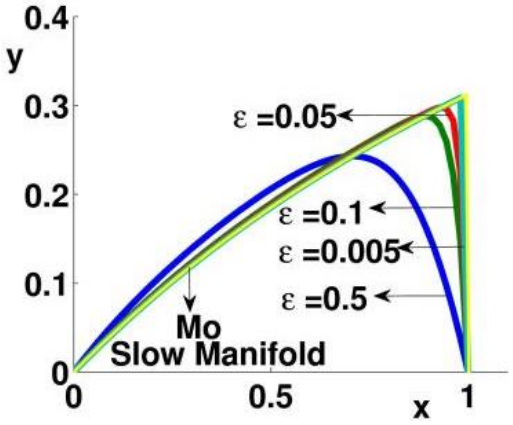

b) $\rho=0.001,\alpha_1=2.2,\alpha_2=3,\alpha_3=2$ and $\alpha_4=4$

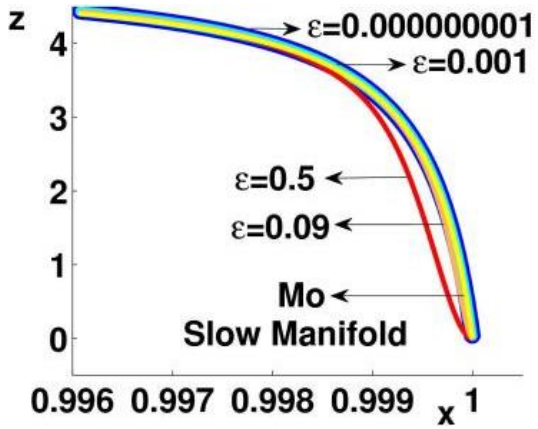

c) $\rho=0.0000000001,\alpha_1=0.0002,\alpha_2=25000000,$ $\alpha_3=0.25$ and $\alpha_4=500$

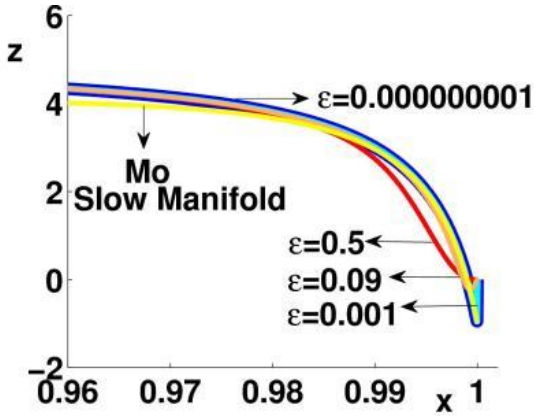

d) $\rho=0.00000001,\alpha_1=0.002,\alpha_2=250,\alpha_3=0.25$

and $\alpha_4=50$

Figure 3: Approximate solutions of equations (7) with slow manifold M_0.

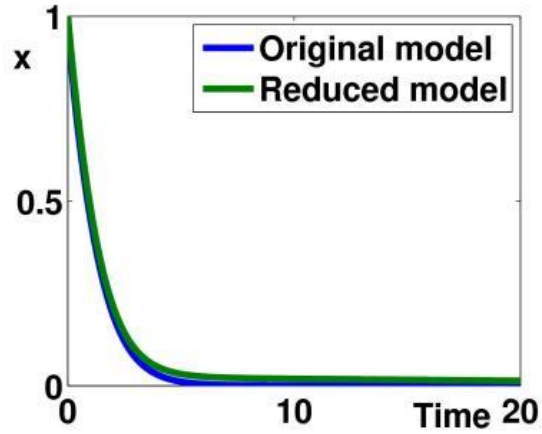

a) $\rho = 0.001, \alpha_1 = 2.2, \alpha_2 = 3, \alpha_3 = 2$ and $\alpha_4 = 4$

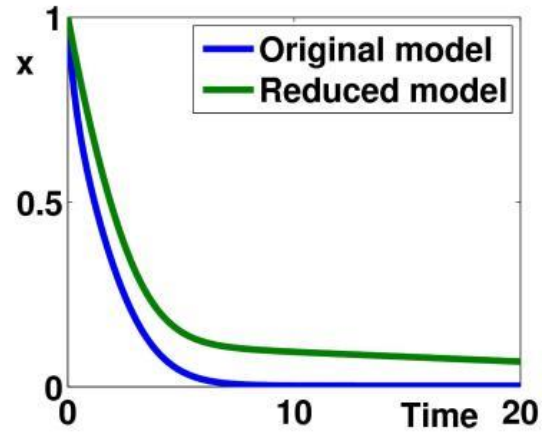

b) $\rho = 0.005, \alpha_1 = 0.5, \alpha_2 = 3, \alpha_3 = 2$ and $\alpha_4 = 4$

Figure 4: Reduced model (10) and the full model (dimensionless form).

5. Elasticity and Control Coefficients for MicroRNA Model

The power to change metabolism states in response to an outer signaling is called metabolic control. It is measurable in terms of influence of the metabolic response to external factors. This is happened without any idea about the purpose /function/mechanism of the response (Newsholme and Start, 1973). The control structure of a metabolic pathway can be quantitatively characterized by metabolic control analysis (MCA). This is a mathematical frame work for describing metabolic, signaling, and genetic pathways. MCA quantifies how variables, such as fluxes and species concentrations, depend on network parameters. In particular, if MCA describes how networks depend on their properties, is called control coefficients. In addition, if MCA depending on its local properties, is called elasticities. By means of control and elasticity coefficients, the control coefficient is the fractional change in metabolic concentration (Puigjaner *et al*., 1997). Metabolic control analysis is an important step forward to determine the complexity of dynamic changes of species in a complex metabolic system (Li *et al*., 2010, Teusink *et al.*, 2000). There are three main types of coefficient analysis. The first one is elasticity coefficients that quantify the sensitivity of a reaction rate to the change of concentration or a parameter. The second type is flux control coefficients that measure the change of a flux along a pathway in response to a change in the reaction rates. The last one is concentration control coefficients that calculate the change of concentration of some metabolite species S_i in response of a change in the rate of a reaction (Newsholme and Start, 1973).

5.1. Elasticity

Elasticity coefficients are used in economics, physics, chemistry, or more generally in mathematics as a definition of point elasticity. The rate of reaction is affected by many different factors, such as pH, temperature, reactant and product concentrations and etc. The elasticity is defined effectively by factors on the reaction rates. Elasticities in biochemistry theory called kinetic orders and describe how sensitive a reaction rate is to changes in reactant, product and effector concentrations (Kacser *et al.*, 1995, Klipp *et al*., 2008, Sauro *et al*., 1987). The elasticity coefficient is the fractional change in the net rate for an individual substrate, with everything else is kept fixed (Puigjaner *et al*., 1997). The main equation of elasticity coefficient given by

$$E_{s_i}^{v_i} = \frac{\partial v}{\partial s}\frac{s}{v},$$

where v_i is reaction rate and s_i is concentration of species. The equation of elasticity measures the change of v_i in response to a change in s_i, while everything else is kept fixed. If we have substrate *S*, inhibition *I* and activation *A* in a pathway then some quantitative amounts can be considered.

There are some typical values for elasticity coefficients that satisfy the following inequalities:

$$E_s^v = \frac{\partial v}{\partial s}\frac{s}{v} > 0, \quad E_p^v = \frac{\partial v}{\partial p}\frac{p}{v} < 0.$$

That means more substrates are required to have fast rates, while more products give slower rates. In addition, if there are given inequalities

$$E_A^v = \frac{\partial v}{\partial A}\frac{A}{v} > 0, \quad E_I^v = \frac{\partial v}{\partial I}\frac{I}{v} < 0.$$

This gives us fast reaction rates required the higher activator concentration, whereas slow reaction rates are depended on the higher inhibitor concentration (Newsholme and Start, 1973).

5.2. Control Coefficients for MicroRNA Model.

A control coefficient quantifies the relative steady state change in a system variable, e.g. metabolite concentration *S* or pathway flux *J*, in response to a relative change in a parameter. We have two main control coefficients, they are concentration control coefficients and flux control coefficients (Kacser *et al*., 1995, Klipp *et al*., 2008, Sauro *et al*., 1987). The equation of flux control coefficients is defined below

$$C_{v_i}^J = \frac{\dfrac{dJ}{dp}\dfrac{p}{J}}{\dfrac{\partial v_i}{\partial p}\dfrac{p}{v_i}} = \frac{d\ln(J)}{d\ln(v_i)} = \frac{dJ}{dv_i}\frac{v_i}{J}.$$

The equation of concentration control coefficients is given by

$$C_{v_i}^s = \frac{\dfrac{ds}{dp}\dfrac{p}{s}}{\dfrac{\partial v_i}{\partial p}\dfrac{p}{v_i}} = \frac{d\ln(s)}{d\ln(v_i)} = \frac{ds}{dv_i}\frac{v_i}{s}.$$

The flux control coefficient $C_{v_i}^s$ gives the relative small change in (a system variable) concentration with small change in pathway flux *J*. The word flux *J* also used to describe the rate of the system. Therefore, changing in the concentration can be fluctuated between increasing and decreasing (Li *et al*., 2010, Teusink *et al*., 2000). Flux coefficients usually vary from 0 to 1. The concentration control coefficient $C_{v_i}^s$ gives the relative change in metabolite concentration *S*. The concentration control coefficients can have large values. They can also vary from negative to positive and small to large value (Li *et al*., 2010, Teusink *et al*., 2000).

Furthermore, there is a relationship between control coefficients and elasticity. The flux control summation theorem was discovered independently by Kacser/Burns group and Heinrich/Rapoport group in the early 1970s and late 1960s respectively. The flux control summation theorem implies that metabolic fluxes are systemic properties and that their control is shared by all reactions in the system. When a single reaction changes its control of the flux this is compensated by changes in the control of the same flux by all other reactions. The two important equations are proposed as follows:

$$\sum_i C_{v_i}^J = 1 \quad \text{and} \quad \sum_i C_{v_i}^s = 0.$$

The connectivity theorems are specific relationships between elasticities and control coefficients. They are useful because they highlight the close relationship between the kinetic properties of individual reactions and the system properties of a pathway. Two basic sets of theorems exist, one for flux and another for concentrations. The concentration connectivity theorems are divided again depending on whether the system species S_n is different from the local species S_m.

$$\sum_i C_{v_i}^J E_s^{v_i} = 0,$$

$$\sum_i C_{v_i}^{S_n} E_{S_m}^{v_i} = 0, \qquad n \neq m$$

$$\sum_i C_{v_i}^{S_n} E_{S_m}^{v_i} = -1 \qquad n = m.$$

5.3. Model Results

For system (1), we have the following reaction rates

$$v_1 = k_1[40S][eIF\,4F], v_2 = k_2 F, v_3 = k_3 A[60S]$$

and $v_4 = k_4 R.$

The following elasticity equations are calculated for system (1):

$$E^{v_1}_{[40S]} = \frac{\partial v_1}{\partial [40S]} \frac{[40S]}{v_1} =$$

$$k_1[eIF\,4F]\frac{[40S]}{k_1[40S][eIF\,4F]} = 1,$$

$$E^{v_2}_{[40S]} = E^{v_3}_{[40S]} = E^{v_4}_{[40S]} = 0,$$

$$E^{v_1}_{[eIF\,4F]} = 1, E^{v_2}_{[eIF\,4F]} = E^{v_3}_{[eIF\,4F]} = E^{v_4}_{[eIF\,4F]} = 0,$$

$$E^{v_1}_{[60S]} = E^{v_2}_{[60S]} = E^{v_4}_{[60S]} = 0, E^{v_3}_{[60S]} = 1, \qquad (13)$$

$$E^{v_1}_{F} = E^{v_3}_{F} = E^{v_4}_{F} = 0, E^{v_2}_{F} = 1,$$

$$E^{v_1}_{A} = E^{v_2}_{A} = E^{v_4}_{A} = 0, E^{v_3}_{A} = 1,$$

$$E^{v_1}_{R} = E^{v_2}_{R} = E^{v_3}_{R} = 0, E^{v_4}_{R} = 1.$$

In general, if an elasticity value is positive then reaction rates are increased. On the other hand, if elasticity value is negative then reaction rates are decreased. For the chemical reaction rates in system (1), we assume that [40S], [eIF4F] and [60S] are fixed boundary species. Therefore, the pathway can reach a steady state. Then, we can calculate the control coefficients for the remaining sates F, A and R. The model has some control coefficient equations based on summation and connectivity theorem as below:

$$C^{J}_{v_1} + C^{J}_{v_2} + C^{J}_{v_3} + C^{J}_{v_4} = 1,$$

$$C^{F}_{v_1} + C^{F}_{v_2} + C^{F}_{v_3} + C^{F}_{v_4} = 0,$$

$$C^{A}_{v_1} + C^{A}_{v_2} + C^{A}_{v_3} + C^{A}_{v_4} = 0,$$

$$C^{R}_{v_1} + C^{R}_{v_2} + C^{R}_{v_3} + C^{R}_{v_4} = 0,$$

$$C^{J}_{v_1}E^{v_1}_{F} + C^{J}_{v_2}E^{v_2}_{F} + C^{J}_{v_3}E^{v_3}_{F} + C^{J}_{v_4}E^{v_4}_{F} = 0,$$

$$C^{J}_{v_1}E^{v_1}_{A} + C^{J}_{v_2}E^{v_2}_{A} + C^{J}_{v_3}E^{v_3}_{A} + C^{J}_{v_4}E^{v_4}_{A} = 0,$$

$$C^{J}_{v_1}E^{v_1}_{R} + C^{J}_{v_2}E^{v_2}_{R} + C^{J}_{v_3}E^{v_3}_{R} + C^{J}_{v_4}E^{v_4}_{R} = 0, \qquad (14)$$

$$C^{F}_{v_1}E^{v_1}_{A} + C^{F}_{v_2}E^{v_2}_{A} + C^{F}_{v_3}E^{v_3}_{A} + C^{F}_{v_4}E^{v_4}_{A} = 0, F \neq A$$

$$C^{F}_{v_1}E^{v_1}_{R} + C^{F}_{v_2}E^{v_2}_{R} + C^{F}_{v_3}E^{v_3}_{R} + C^{F}_{v_4}E^{v_4}_{R} = 0, F \neq R$$

$$C^{A}_{v_1}E^{v_1}_{F} + C^{A}_{v_2}E^{v_2}_{F} + C^{A}_{v_3}E^{v_3}_{F} + C^{A}_{v_4}E^{v_4}_{F} = 0, A \neq F$$

$$C^{A}_{v_1}E^{v_1}_{R} + C^{A}_{v_2}E^{v_2}_{R} + C^{A}_{v_3}E^{v_3}_{R} + C^{A}_{v_4}E^{v_4}_{R} = 0, A \neq R$$

$$C^{R}_{v_1}E^{v_1}_{F} + C^{R}_{v_2}E^{v_2}_{F} + C^{R}_{v_3}E^{v_3}_{F} + C^{R}_{v_4}E^{v_4}_{F} = 0, R \neq F$$

$$C^{R}_{v_1}E^{v_1}_{A} + C^{R}_{v_2}E^{v_2}_{A} + C^{R}_{v_3}E^{v_3}_{A} + C^{R}_{v_4}E^{v_4}_{A} = 0, R \neq A$$

$$C^{F}_{v_1}E^{v_1}_{F} + C^{F}_{v_2}E^{v_2}_{F} + C^{F}_{v_3}E^{v_3}_{F} + C^{F}_{v_4}E^{v_4}_{F} = 0, n = m$$

$$C^{A}_{v_1}E^{v_1}_{A} + C^{A}_{v_2}E^{v_2}_{A} + C^{A}_{v_3}E^{v_3}_{A} + C^{A}_{v_4}E^{v_4}_{A} = 0, n = m$$

$$C^{R}_{v_1}E^{v_1}_{R} + C^{R}_{v_2}E^{v_2}_{R} + C^{R}_{v_3}E^{v_3}_{R} + C^{R}_{v_4}E^{v_4}_{R} = 0, n = m.$$

By substituting the elasticity values in equations (13) into equations (14), the following results are obtained

$$C_{v_1}^J = 1, C_{v_2}^J = C_{v_3}^J = C_{v_4}^J = 0,$$

$$C_{v_1}^F = 1, C_{v_2}^F = -1, C_{v_3}^F = C_{v_4}^F = 0,$$

$$C_{v_1}^A = 1, C_{v_3}^A = -1, C_{v_2}^A = C_{v_4}^A = 0,$$

$$C_{v_1}^R = 1, C_{v_4}^R = -1, C_{v_2}^R = C_{v_3}^R = 0.$$

According to flux control coefficients $C_{v_2}^J = C_{v_3}^J = C_{v_4}^J = 0$, this means that second, third and the last step of reactions have not any effect on model fluxes. On the other hand, the control coefficient $C_{v_1}^J = 1$, this gives us the first reaction rate has a strong effect on the model fluxes. In other words, the model steady state fluxes are controlled by v_1.

Furthermore, concentration control coefficients quantify how variables, such as species concentrations, depend on reaction rates. In this study, it can be more precisely concluded that there is no any relative change in F, A and R regarding to reaction rates v_2, v_3 and v_4. While, there is a significant change in F, A and R with respect to v_1.

6. Conclusions

The non-linear model of miRNA protein translation including seven species and four parameters has been studied. Mass action law and classical chemical kinetics under constant rates are used for modelling the system. We have introduced some new variables to reduce the number of model species and parameters. We proposed QSSA to analyze the fast variables and calculate slow manifolds. As a result, the analytical approximate solutions are sufficiently close to the manifolds when the slow-fast parameter becomes smaller. The analytical approximate solutions give some effective results particularly provided us understanding about global dynamics. It can be also noticed that there is a good agreement between the simplified and the original model dynamics.

Results in this study show some interesting points. The first point is that how variables, such as fluxes and species concentrations, depend on network parameters. Another point is that how reaction rates are sensitive to changes in reactant, product and concentrations. The proposed techniques will be applied to a wide range of complex miRNA mechanisms.

ACKNOWLEDGMENT

We thank the University of Raparin and Koya University for providing its wonderful facilities and for supporting our research.

References

Cooper, G. M. 2000. The cell : a molecular approach / Geoffrey M. Cooper.

Eulalio, A., Huntzinger, E. and Izaurralde, E. 2008. Getting to the root of miRNA-mediated gene silencing. *Cell*, 132**,** 9-14.

Filipowicz, W., Bhattacharyya, S. N. and Sonenberg, N. 2008. Mechanisms of post-transcriptional regulation by microRNAs: are the answers in sight? *Nature reviews genetics*, 9**,** 102.

Glaser, V. 2008. Tapping miRNA-regulated pathways: expression profiling ramps up to support diagnostics and drug discovery. *Genetic Engineering and Biotechnology News*, 28.

Jackson, R. J. and Standart, N. 2007. How do microRNAs regulate gene expression? *Sci. Stke*, 2007**,** re1-re1.

Kacser, H., Burns, J. A. and Fell, D. A. 1995. The control of flux. Portland Press Limited.

Khoshnaw, S. Reduction of a Kinetic Model of Active Export of Importins. AIMS Conference on Dynamical Systems, Differential Equations and Applications, Madrid, 2015a. 7-11.

Khoshnaw, S. H., Mohammad, N. A. and Salih, R. H. 2016. Identifying critical parameters in SIR model for spread of disease. *Open Journal of Modelling and Simulation*, 5**,** 32.

Khoshnaw, S. H. A. 2015b. *Model Reductions in Biochemical Reaction Networks.* Department of Mathematics.

Klipp, E., Herwig, R., Kowald, A., Wierling, C. and Lehrach, H. 2008. *Systems biology in practice: concepts, implementation and application*, John Wiley and Sons.

Lee, R. C., Feinbaum, R. L. and Ambros, V. 1993. The C. elegans heterochronic gene lin-4 encodes small RNAs with antisense complementarity to lin-14. *cell*, 75**,** 843-854.

Lewin, B. 2007. *Cells*, Jones and Bartlett Learning.

Li, C., Donizelli, M., Rodriguez, N., Dharuri, H., Endler, L., Chelliah, V., Li, L., He, E., Henry, A. and Stefan, M. I. 2010. BioModels Database: An enhanced, curated and annotated resource for published quantitative kinetic models. *BMC systems biology*, 4**,** 92.

Newsholme, E. A. and Start, C. 1973. *Regulation in metabolism*.

Nissan, T. and Parker, R. 2008. Computational analysis of miRNA-mediated repression of

translation: implications for models of translation initiation inhibition. *Rna,* 14**,** 1480-1491.

Puigjaner, J., Raïs, B., Burgos, M., Comin, B., Ovádi, J. and Cascante, M. 1997. Comparison of control analysis data using different approaches: modelling and experiments with muscle extract. *FEBS letters,* 418**,** 47-52.

Ruvkun, G. 2001. Glimpses of a tiny RNA world. *Science,* 294**,** 797-799.

Sauro, H. M., Small, J. R. and Fell, D. A. 1987. Metabolic control and its analysis: extensions to the theory and matrix method. *European journal of biochemistry,* 165**,** 215-221.

Teusink, B., Passarge, J., Reijenga, C. A., Esgalhado, E., Van der weijden, C. C., Schepper, M., Walsh, M. C., Bakker, B. M., Van dam, K. and Westerhoff, H. V. 2000. Can yeast glycolysis be understood in terms of in vitro kinetics of the constituent enzymes? Testing biochemistry. *European Journal of Biochemistry,* 267**,** 5313-5329.

Valencia-sanchez, M. A., LIU, J., Hannon, G. J. and Parker, R. 2006. Control of translation and mRNA degradation by miRNAs and siRNAs. *Genes and development,* 20**,** 515-524.

Xu, F., Liu, Z., Shen, J. and Wang, R. 2009. Dynamics of microRNA-mediated motifs. *IET systems biology,* 3**,** 496-504.

Zhao, Y.-B. and Krishnan, J. 2014. mRNA translation and protein synthesis: an analysis of different modelling methodologies and a new PBN based approach. *BMC systems biology,* 8**,** 25.

Zinovyev, A., Morozova, N., Gorban, A. N. and Harel-belan, A. 2013. Mathematical modeling of microRNA–mediated mechanisms of translation repression. *MicroRNA cancer regulation.* Springer.

Zinovyev, A., Morozova, N., Nonne, N., Barillot, E., Harel-bellan, A. and Gorban, A. N. 2010. Dynamical modeling of microRNA action on the protein translation process. *BMC systems biology,* 4**,** 13.

ZANCO Journal of Pure and Applied Sciences
The official scientific journal of Salahaddin University-Erbil
https://zancojournals.su.edu.krd/index.php/JPAS

ISSN (print):2218-0230**, ISSN (online):** 2412-3986**,DOI: http://dx.doi.org/10.21271/zjpas**

RESEARCHPAPER

Numerical Methods for Solving the System of Volterra-Fredholm Integro-Differential Equations.

Adnan A. Jalal[1], Nejmaddin A. Sleman[2], Azad I. Amen[3]

[1]Department of Mathematics, College of Education, Salahaddin University - Erbil, Kurdistan Region, Iraq
[2]Department of Mathematics, College of Education, Salahaddin University - Erbil, Kurdistan Region, Iraq
[3]Department of Mathematics, College of Basic Education, Salahaddin University – Erbil, Kurdistan Region, Iraq

A B S T R A C T:

In this paper, we defined the system of Volterra-Fredholm integro-differential equations of the second kind with the initial conditions. The solution for this equation is introduced by using the modified decomposition method. An algorithm is applied to get that solution. Moreover, we generated some examples and discussed to illustrate the employment of the method.

KEYWORDS: System of integro-differential equations, Linear Volterra-Fredholm, Modified decomposition method.
DOI: http://dx.doi.org/10.21271/ZJPAS.31.2.4
ZJPAS (2019) , 31(2);25-30 .

INTRODUCTION :

In science and engineering, sometimes there are vital problems that can be minimized to a system of integral and integro-differential equations. The latter equation has pulled in much consideration of math scholars to work on and has been a subject of interest for them to solve.

In recent years several researchers have adopted different techniques for solving the systems of Volterra and Fredholm integro-differential equations. The decomposition method has been applied to obtain formal solutions to wide class of problems in many interesting mathematics and physics areas. Recently,

***Corresponding Author:**
Adnan Ali Jalal
E-mail: adnan.jalal@su.edu.krd or adnanali8383@gmail.com
Article History:
Received: 20/01/2019
Accepted: 25/03/2019
Published: 23/04/2019

(Darania and Ivaz, 2008) used Taylor expansion for nonlinear Volterra–Fredholm integro-differential equations, also (Hasan and Suleiman, 2018b) used Trigonometric Functions and Laguerre Polynomials to solve mixed Volterra-Fredholm integral equation. (Fariborzi Araghi and Behzadi, 2011) used Homotopy Analysis Method for the numerical solution of nonlinear Volterra-Fredholm integro-differential equations. (Hasan and Suleiman, 2018a) shows numerical solution of Mixed Volterra-Fredholm integral equations by using Linear Programming Problem, and (Hassan T.I., Sulaiman N.A., 2017) studied Aitken method to solve Volterra-Fredholm integral equations of the second kind with Homotopy perturbation method. (Akyüz-Daşcioğlu and Sezer, 2005) used Chebyshev collocation method to solve the systems of higher-order linear Fredholm–Volterra integro-differential equations.

If we focus on the Adomian decomposition method (ADM), (Wazwaz, 2006, 2011) used Modified ADM for solving nonlinear Fredholm

and Volterra integral equations of the second kind. (Rabbani and Zarali, 2012) used MADM to solve the system of linear Fredholm integro-differential equations. (Bakodah, 2012) used some modifications of Adomian decomposition method apply for solving the system of nonlinear Fredholm integral equations of the second kind, also (Bakodah, H O, Al-Mazmumy, M Almuhalbedi, 2017), He presented an efficient modification of ADM for solving the system of nonlinear Volterra and Fredholm integro-differential equations.

In this paper we introduce a solution of the system of linear Volterra-Fredholm integro-differential equations of the second kind of the following form:

$$\begin{cases} y_1^{(n)}(x) = f_1(x) + \int_a^x k_{11}(x,t)y_1(t)dt + \int_a^b k_{12}(x,t)y_2(t)dt \\ y_2^{(n)}(x) = f_2(x) + \int_a^x k_{21}(x,t)y_1(t)dt + \int_a^b k_{22}(x,t)y_2(t)dt \end{cases} \quad (1)$$

With initial conditions

$$y_1^{(0)}(x_0), y_1^{(1)}(x_0), \dots, y_1^{(n-1)}(x_0) \text{ and}$$

$$y_2^{(0)}(x_0), y_2^{(1)}(x_0), \dots, y_2^{(n-1)}(x_0)$$

The unknown functions $y_1(x)$, and $y_2(x)$ that will be determined, occur inside the integral sign whereas the derivatives of $y_1(x)$, and $y_2(x)$ appear mostly outside the integral sign. The kernels $k_{ij}(x,t)$, and the function $f_i(x)$ for $i,j = 1,2$ are known real-valued functions.

2. MODIFIED ADOMIAN DECOMPOSITION METHOD

The Adomian decomposition method (Adomian, 1988) is the process of fragmenting the unknown function y(x) of an equation into the summation of an infinite terms of components defined by the decomposition series:

$$y(x) = \sum_{n=0}^{\infty} y_n(x) \quad (2)$$

in which the parts $y_n(x), n \geq 0$, are to be set in a reoccurring way. This method concerns itself with discovering the components $y_0, y_1, y_2, \dots$ separately.

The modified decomposition method (Wazwaz, 2011) depends on dividing the function $f(x)$ into two parts, so it can't be used if the function $f(x)$ consists of only one term.

To give a whole description of the method consider a general functional equation

$$Ly + Ry + Ny = f(x), \quad (3)$$

Where $y(x)$ is the unknown function, and the linear terms are decomposed into $L + R$ and Ny denote the nonlinear terms. Since L is easily invertible and R is the remainder of the nonlinear operator and $f(x)$ is the source term. From Eq. (3)

$$Ly = f(x) - Ry - Ny, \quad (4)$$

Applying L^{-1} on the both sides of the above equation and using the given conditions, we get

$$y(x) = g(x) - L^{-1}(Ry) - L^{-1}(Ny), \quad (5)$$

Where

$$L^{-1}(f(x)) = g(x)$$

.

applying the Adomian method the series solution $y(x)$ as defined in Eq. (2)

$$y(x) = \sum_{n=0}^{\infty} y_n(x)$$

The components $y_0, y_1, y_2, \dots$ can easily be determine recursively from the following relations:

$y_0(x) = g(x)$,

$$y_{n+1}(x) = -L^{-1}(Ry_n) - L^{-1}(Ny_n), \; n \geq 0 \quad (6)$$

typically the decomposition method assign the zeroth components $y_0(x)$ as the function g(x). But modified decomposition method propose that the function g(x) defined above in Eq. (5) can be decomposed into two parts namely,$g_0(x)$ and $g_1(x)$,i.e.,

$$g(x) = g_0(x) + g_1(x) \quad (7)$$

In the above equation proper choice of $g_0(x)$ and $g_1(x)$ is essential and depends mainly on the trail basis. Thus the following recursive relations

for the modified decomposition method are formed as:

$$\begin{cases} y_0(x) = g_0(x) \\ y_1(x) = g_1(x) - L^{-1}(Ry_0) - L^{-1}(Ny_0) \\ y_{n+1}(x) = -L^{-1}(Ry_n) - L^{-1}(Ny_n) \end{cases} \quad (8)$$

3. APPLYING MODIFIED (ADM) FOR SOLVING SYSTEM OF LINEAR VOLTERRA-FREDHOLM INTEGRO-DIFFERENTIAL EQUATIONS OF THE SECOND KIND

The Adomian decomposition method gives the solution in an infinite series of components that can be repetitively specified. The acquired series may give the exact solution if such a solution exists. Otherwise, the series gives a parataxis for the solution that gives high accuracy level.

Recall system (1) of linear Volterra-Fredholm integro-differential equations of the second kind:

$$\begin{cases} y_1^{(n)}(x) = f_1(x) + \int_a^x k_{11}(x,t)y_1(t)dt + \int_a^b k_{12}(x,t)y_2(t)dt \\ y_2^{(n)}(x) = f_2(x) + \int_a^x k_{21}(x,t)y_1(t)dt + \int_a^b k_{22}(x,t)y_2(t)dt \end{cases}$$

With initial conditions

$$y_1^{(0)}(x), y_1^{(1)}(x), \dots, y_1^{(n-1)}(x) \text{ and}$$

$$y_2^{(0)}(x), y_2^{(1)}(x), \dots, y_2^{(n-1)}(x)$$

Integrating both sides of (1) from 0 to x n times leads to

$$\begin{cases} y_1(x) = g_1(x) + L^{-1}\int_a^x k_{11}(x,t)y_1(t)dt + \\ \qquad L^{-1}\int_a^b k_{12}(x,t)y_2(t)dt \\ y_2(x) = g_2(x) + L^{-1}\int_a^x k_{21}(x,t)y_1(t)dt + \\ \qquad L^{-1}\int_a^b k_{22}(x,t)y_2(t)dt \end{cases} \quad (9)$$

Where $g_i(x)$ includes $L^{-1}(f_i(x))$; $i = 1,2$ and the initial conditions, and L^{-1} is an n-fold integral operator.

Now decomposing the unknown functions $y_i(x), i = 1,2$ of any equation into a sum of an infinite number of terms defined by the decomposition series as

$$\begin{cases} y_1(x) = \sum_{n=0}^{\infty} y_{1n}(x) \\ y_2(x) = \sum_{n=0}^{\infty} y_{2n}(x) \end{cases} \quad (10)$$

Substituting (10) in (9), we get

$$\begin{cases} \sum_{n=0}^{\infty} y_{1n}(x) = g_1(x) + L^{-1}\int_a^x k_{11}(x,t)\sum_{n=0}^{\infty} y_{1n}(t)\,dt + \\ \qquad L^{-1}\int_a^b k_{12}(x,t)\sum_{n=0}^{\infty} y_{2n}(t)\,dt \\ \sum_{n=0}^{\infty} y_{2n}(x) = g_2(x) + L^{-1}\int_a^x k_{21}(x,t)\sum_{n=0}^{\infty} y_{1n}(t)\,dt + \\ \qquad L^{-1}\int_a^b k_{22}(x,t)\sum_{n=0}^{\infty} y_{2n}(t)\,dt \end{cases}$$

By using the modified decomposition method, we decompose the function $g_i(x)$ as follows:

$$g_i(x) = g_{i0}(x) + g_{i1}(x)$$

We set

$$y_{i0}(x) = g_{i0}(x)$$

and

$$\begin{cases} y_{11}(x) = g_{11}(x) + L^{-1}\int_a^x k_{11}(x,t)y_{10}(t)dt + \\ \qquad L^{-1}\int_a^b k_{12}(x,t)y_{20}(t)dt \\ y_{21}(x) = g_{21}(x) + L^{-1}\int_a^x k_{21}(x,t)y_{10}(t)dt + \\ \qquad L^{-1}\int_a^b k_{22}(x,t)y_{20}(t)dt \end{cases} \quad (11)$$

And also we take

$$\begin{cases} y_{1,j+1}(x) = L^{-1}\int_a^x k_{11}(x,t)y_{1,j}(t)dt + \\ L^{-1}\int_a^b k_{12}(x,t)y_{2,j}(t)dt \\ y_{2,j+1}(x) = L^{-1}\int_a^x k_{21}(x,t)y_{1,j}(t)dt + \\ L^{-1}\int_a^b k_{22}(x,t)y_{2,j}(t)dt \end{cases} \quad (12)$$

$$j = 1,2,\dots$$

Algorithm:

Step (1): Integrate both sides the system n times.
Step (2): We set the function $g_i(x) = g_{i0}(x) + g_{i1}(x)$ for i= 1,2 .
Step (3): assigned to the zeroth component $y_{i0}(x) = g_{i0}(x)$ for i= 1,2 .
Step (4): substitute $y_{i0}(x) = g_{i0}(x)$ for i= 1,2 in equation (11) to get $y_{i1}(x)$.
Step (5): substitute $y_{i1}(x)$ for i= 1,2 in equation (12) to get $y_{i1}(x)$.

4. NUMERICAL EXAMPLES

Example 1. Consider the linear system of Volterra-Fredholm integro differential equations

$$\begin{cases} y_1^{(2)}(x) = x - 2cosx - \int_0^x (x-t)y_1(t)dt - \\ \int_0^{\frac{\pi}{2}} (x-t)y_2(t)dt \\ y_2^{(2)}(x) = sinx - x - 1 + \int_0^x (x-t)^2 y_1(t)dt - \\ \int_0^{\frac{\pi}{2}} (x-t)y_2(t)dt \end{cases}$$

With initial conditions $y_1(0) = y_2'(0) = 1$ and $y_2(0) = y_1'(0) = 0$
The above equations in an operator form equations become

$$\begin{cases} Ly_1 = x - 2cosx - \int_0^x (x-t)y_1(t)dt - \\ \int_0^{\frac{\pi}{2}} (x-t)y_2(t)dt \\ Ly_2 = sinx - x - 1 + \int_0^x (x-t)^2 y_1(t)dt - \\ \int_0^{\frac{\pi}{2}} (x-t)y_2(t)dt \end{cases}$$

Applying L^{-1} , a two-fold integral operator, on both sides we have

$$\begin{cases} y_1(x) = \frac{x^3}{6} - 1 + 2cosx - \\ L^{-1}\int_0^x (x-t)y_1(t)dt - L^{-1}\int_0^{\frac{\pi}{2}} (x-t)y_2(t)dt \\ y_2(x) = 2x - \frac{x^2}{2} - \frac{x^3}{3} - sinx + \\ L^{-1}\int_0^x (x-t)^2 y_1(t)dt - L^{-1}\int_0^{\frac{\pi}{2}} (x-t)y_2(t)dt \end{cases}$$

Where $g_1(x) = \frac{x^3}{6} - 1 + 2cosx$, and
$g_2(x) = 2x - \frac{x^2}{2} - \frac{x^3}{3} - sinx$
Now splitting $g_1(x)$ into two parts
$g_{10}(x) = cosx$, $g_{11}(x) = cosx - 1 + \frac{x^3}{6}$ and also splitting $g_2(x)$ into two parts
$g_{20}(x) = sinx$, $g_{21}(x) = 2x - \frac{x^2}{2} - \frac{x^3}{3} - 2sinx$

$$\begin{cases} y_{10}(x) = cosx \\ y_{20}(x) = sinx \end{cases}$$

And,

$$\begin{cases} y_{11}(x) = \frac{x^3}{6} - 1 + cosx - L^{-1}\int_0^x (x-t)y_{10}(t)dt \\ -L^{-1}\int_0^{\frac{\pi}{2}} (x-t)y_{20}(t)dt = 0 \\ y_{21}(x) = 2x - \frac{x^2}{2} - \frac{x^3}{3} - 2sinx + L^{-1}\int_0^x (x-t)^2 y_{10}(t)dt \\ -L^{-1}\int_0^{\frac{\pi}{2}} (x-t)y_{20}(t)dt = 0 \end{cases}$$

Also we take

$$\begin{cases} y_{1,n+1}(x) = 0, \\ y_{2,n+1}(x) = 0, \end{cases} \quad n \geq 1.$$

Thus

$$\begin{cases} y_1(x) = cosx \\ y_2(x) = sinx \end{cases}$$

which is the exact solution.

Example 2. Consider the linear system of Volterra-Fredholm integro differential equations

$$\begin{cases} y_1^{(2)}(x) = 6x - \frac{3x^2}{4} - \frac{x^6}{5} + \int_0^x xt\, y_1(t)dt \\ \qquad + \int_0^1 x^2 t\, y_2(t)dt \\ y_2^{(2)}(x) = 2 - \frac{x^5}{5} - \frac{3}{2}x + \int_0^x t\, y_1(t)dt \\ \qquad + \int_0^1 2xt\, y_2(t)dt \end{cases}$$

With initial conditions $y_1(0) = y_1'(0) = y_2'(0) = 0$ and $y_2(0) = 1$

The above equations in an operator form equations become

$$\begin{cases} Ly_1 = 6x - \frac{3x^2}{4} - \frac{x^6}{5} + \int_0^x xt\, y_1(t)dt\ + \\ \qquad \int_0^1 x^2 t\, y_2(t)dt \\ Ly_2 = 2 - \frac{x^5}{5} - \frac{3}{2}x + \int_0^x t\, y_1(t)dt\ + \\ \qquad \int_0^1 2xt\, y_2(t)dt \end{cases}$$

Applying L^{-1} , a two-fold integral operator, on both sides we have

$$\begin{cases} y_1(x) = x^3 - \frac{x^8}{280} - \frac{x^4}{16} + L^{-1}\int_0^x xt\, y_1(t)dt \\ \qquad + L^{-1}\int_0^1 x^2 t\, y_2(t)dt \\ y_2(x) = x^2 - \frac{x^7}{210} - \frac{x^3}{4} + 1 + L^{-1}\int_0^x t\, y_1(t)dt \\ \qquad + L^{-1}\int_0^1 2xt\, y_2(t)dt \end{cases}$$

Where $g_1(x) = x^3 - \frac{x^8}{280} - \frac{x^4}{16}$, and

$$g_2(x) = x^2 - \frac{x^7}{210} - \frac{x^3}{4} + 1$$

Now splitting $g_1(x)$ into two parts, $g_{10}(x) = x^3$, $g_{11}(x) = -\frac{x^8}{280} - \frac{x^4}{16}$ and also splitting $g_2(x)$ into two parts, $g_{20}(x) = x^2 + 1$, $g_{21}(x) = -\frac{x^7}{210} - \frac{x^3}{4}$

$$\begin{cases} y_{10}(x) = x^3 \\ y_{20}(x) = x^2 + 1 \end{cases}$$

and,

$$\begin{cases} y_{11}(x) = -\frac{x^8}{280} - \frac{x^4}{16} + L^{-1}\int_0^x xty_{10}(t)dt \\ \qquad + L^{-1}\int_0^{\frac{\pi}{2}} x^2 t y_{20}(t)dt = 0 \\ y_{21}(x) = -\frac{x^7}{210} - \frac{x^3}{4} + L^{-1}\int_0^x t\, y_{10}(t)dt \\ \qquad - L^{-1}\int_0^{\frac{\pi}{2}} 2xt\, y_{20}(t)dt = 0 \end{cases}$$

Also we take

$$\begin{cases} y_{1,n+1}(x) = 0, \\ y_{2,n+1}(x) = 0, \end{cases} \quad n \geq 1.$$

Thus

$$\begin{cases} y_1(x) = x^3 \\ y_2(x) = x^2 + 1 \end{cases}$$

which is the exact solution.

5. CONCLUSIONS

In this paper, the modified decomposition method is used to solve the system of Volterra-Fredholm integro differential equations. This method is more proficient than its traditional one as it is less complicated, needs less time to get to the solution and most importantly the exact solution is achieved in two iterations.

The essential condition for that to succeed is that the zeroth component should include the exact solution.

References

Adomian, G. (1988) 'A review of the decomposition method in applied mathematics', *Journal of Mathematical Analysis and Applications*, 135(2), pp. 501–544. doi: 10.1016/0022-247X(88)90170-9.

Akyüz-Daşcioğlu, A. and Sezer, M. (2005) 'Chebyshev polynomial solutions of systems of higher-order linear Fredholm-Volterra integro-differential equations', *Journal of the Franklin Institute*, 342(6), pp. 688–701. doi: 10.1016/j.jfranklin.2005.04.001.

Bakodah, H O, Al-Mazmumy, M Almuhalbedi, S. O. (2017) 'An Efficient Modification of the Adomian decomposition Method for Solving Integro-Differential Equations', *Mathematical Sciences Letters*, 21(1), pp. 15–21.

Bakodah, H. O. (2012) 'Some Modifications of Adomian Decomposition Method Applied to Nonlinear System of Fredholm Integral Equations of the Second Kind', *Int. J. Contemp. Math. Sciences*, 7(19), pp. 929–942..

Darania, P. and Ivaz, K. (2008) 'Numerical solution of nonlinear Volterra-Fredholm integro-differential equations', *Computers and Mathematics with Applications*, 56(9), pp. 2197–2209. doi: 10.1016/j.camwa.2008.03.045.

Fariborzi Araghi, M. A. and Behzadi, S. S. (2011) 'Numerical solution of nonlinear Volterra-Fredholm integro-differential equations using Homotopy Analysis Method', *Journal of Applied Mathematics and Computing*, 37(1–2), pp. 1–12. doi: 10.1007/s12190-010-0417-4.

Hasan, P. M. and Suleiman, N. A. (2018a) 'Numerical Solution of Mixed Volterra-Fredholm Integral Equations Using Linear Programming Problem', *Applied Mathematics*, 8(3),pp.42–45.doi: 10.5923/j.am.20180803.02.

Hasan, P. M. and Suleiman, N. A. (2018b) 'Numerical Treatment of Mixed Volterra-Fredholm Integral Equations Using Trigonometric Functions and Laguerre Polynomials', *ZANCO Journal of Pure and Applied Sciences*, 30, pp. 97–106.

Hassan T.I., Sulaiman N.A., S. S. (2017) 'Using Aitken method to solve Volterra-Fredholm integral equations of the second kind with Homotopy perturbation method', *ZANCO Journal of Pure and Applied Sciences*, 29(4), pp. 257–264.

Rabbani, M. and Zarali, B. (2012) 'Solution of Fredholm Integro-Differential Equations System by Modified Decomposition Method', *The Journal of Mathematics and Computer Science*, 4(4), pp. 258–264.

Wazwaz, A. M. (2006) 'The modified decomposition method for analytic treatment of differential equations',*Applied Mathematics and Computation*, 173(1), pp. 165–176. doi: 10.1016/j.amc.2005.02.048.

Wazwaz, A. M. (2011) *Linear and Nonlinear Integral Equations:Methods and Applications*. Springer Heidlberg Dordrecht London New York: Springer. doi: 10.1007/978-3-642-21449-3.

.

ZANCO Journal of Pure and Applied Sciences
The official scientific journal of Salahaddin University-Erbil
https://zancojournals.su.edu.krd/index.php/JPAS

SN (print):2218-0230**, ISSN (online):** 2412-3986**,DOI:** http://dx.doi.org/10.21271/zjpas

RESEARCH PAPER

Risk Assessments in Construction of Water Supply Projects in Kurdistan Region-Iraq

Khalil I.Wali[1] and Bnar N. Hamadameen[2]

[1]Department of Civil, College of Engineering, Salahaddin University – Erbil, Kurdistan Region, Iraq
[2]Department of Civil, College of Engineering, Salahaddin University - Erbil, Kurdistan Region, Iraq

A B S T R A C T:
Water distribution systems play a critical role in supplying sufficient water to users with acceptable quantity, pressure, and quality. These infrastructures are usually designed to fulfill base demands with additional capacity for emergency conditions. To evaluate the reliability of water supply systems under threatening conditions, risk assessment has been recognized as a useful tool to identify the hazard, analyses vulnerabilities, and risks, and select proper mitigation measures. A questionnaire has been deigned including 51 factors that create risk events that can occur during construction works implementation. The Probability /impact risk rating matrix were used as basis for quantitative risk analysis to determine the most critical risks which were a great impact on project and also to indicate moderate risks that must be taken into consideration. The findings of the questionnaire indicated that the most crucial risk related to design and contract of water supply projects were improper estimate quantity and quality of water needed for each individual of customer, inaccurate selection the standard and specifications of materials, change of design because of improper understanding of customer needs, inadequate estimation of available flow and pressure of water, improper design documentation and drawings. In construction and management phase, the most significant risk factors were poor quality performance, improper quality control, inadequate safety requirements on site, and delay payment on contract. While war, military operation, terrorism attack, and inadequacy of insurance became a maximum critical risk factor as a political issue. Also force majors such as earthquake, flood and water pollution from pipes corrosion summarized as serious environment risk factors. Furthermore lack of labor skill or qualified plumper became the most critical risk must be considered during resource managing.

KEY WORDS: Risk management, Risk assessment, Water supply system
DOI: http://dx.doi.org/10.21271/ZJPAS.31.2.5
ZJPAS (2019) , 31(2);31-40 .

1. INTRODUCTION

Risk management has become a necessary requirement for construction projects. Risk management consists of risk identification, risk assessment and risk control. Risk assessed by the qualitative method and quantitative method. Risk management is the organized process of identifying, analyzing, and responding to project risk and it contains maximizing the probability and consequences of positive attitude and minimizing the probability and consequences of attitude adverse to project goals, project risk is indeterminate event or condition that if happens has a positive or negative influence on project aims (Li, 2007).

Risk management is a systematic method of looking at risk and consciously determining how each should best be treated for identifying purposes of risk and uncertainty, determining their impacts and developing appropriate management risk plan and responses. Assessment of the impact of risks is a complex problem, which must be approached systematically by breaking down the task into four stages that are risk classification, risk identification, risk Analysis and risk response. (Abd, 2015).

* **Corresponding Author:**
Bnar Naaman Hamadameen
E-mail: Bnar.hamadameen@su.edu.krd
Article History:
Received: 07/08/2018
Accepted: 27/03/2019
Published: 23/04/2019

As the result of their complexity and uniqueness, all construction projects are vulnerable to a high risk. The condition for this risk reduction is an identification of risk events and valuation of their occurrence probability and impact (Rybka et al., 2016a)

Providing good and safe drinking water is considered a basic political issue for public health protection and must be the main objective of water supply systems. Drinking water systems are vulnerable and subject to wide range of risks. The safety of drinking water depends on a number of factors, including quality of source water, the effectiveness of treatment and integrity of the distribution system. System-tailored hazard identification and risk assessment must be considered as a starting point for system management (Vieira, 2005).

To be effective in providing safe drinking water supply system, risk management must involve the entire system from catchment to the client. If the risks unacceptable, risk mitigation measures should be applied, and replacement for risk mitigation evaluated. (Bergion et al., 2017).

Efficient risk management is of the principal importance to water utilities. Three attributes are crucial to water users which that must be adequate quantities of water on demand, must be delivered at sufficient pressure and it must be safe to use. Access to a reliable supply of drinking water and safe water quality are basic requirements of human health and economic development .In the third edition of the guidelines for drinking-water quality published by the World Health Organization (WHO), it is pointed out that a comprehensive risk management approach is the most effective way to ensure the safety of drinking water supply (WHO, 2004).

Water distribution system must satisfy all consumers' needs but are vulnerable to a range of failure types that can occur during an intentional extreme event and compromise their normal functions. It is important for the utility managers to assess the composition of the water distribution system in order to manage the threat. Normally, one would want to minimize the risk of undesirable consequences. In most cases, it is not possible to completely eliminate risk; however, one can mitigate it. (Ataoui and Ermini, 2017).

Blokker et al. (2017) studied on risk assessment during repair of drinking water distribution system; quantitative microbial risk assessment model was established to evaluate the risk due to fecal contamination results after maintenance of drinking water mains.

Rybka et al. (2016b) investigated the adverse events happening throughout the implementation of water supply and sewerage systems construction.

Ameyaw and Chan (2015) indicated most significant risk factors in Public Private Partnership (PPP) projects such as: inadequate contract design, water valuing and tax review uncertainty ,political restriction, public resistance to PPP ,construction time and cost overrun, non-payment of bills, absence of PPP experience ,financing risk, imperfect demand forecasting.

Zhang et al. (2014) studied on risk assessment of long-distance water supply system and stated that the maximum serious risk internal reason of water supply system was water hammer, and to eliminate the potential risks of a pipe burst, water hammer was computed under different conditions.

Chan et al. (2014) identified and evaluated typical risks related to Public Private Partnership projects in the Chinese water supply sector. The discovers displayed that completion risk, inflation, and price change risk have a higher impact on Chinese water public-private partnership projects.

Roozbahani et al. (2013) studied on risk assessment from tap to source of urban water supply systems that was usually subjected to a multiplicity of undefined threatening hazards. These threats differed to three main groups of natural, human-made, and operational hazards, which influence water quantity or water quality.

Tchórzewska-Cieślak (2011) applied a fuzzy logic based method for risk assessment of drinking water system by defining the fuzzy rules between likelihood of pipe failures, consequence of failure, and sensitivity of water mains, drinking water technical system is an essential element of urban infrastructure.

Wibowo and Mohamed (2010) investigated of risk critically and allocation in privatized water supply projects in Indonesia and discussed the perception of regulator and operator in the term of project risk critically and allocation and both regarded to the principal concerned which was non-availability of raw water.

Zeng et al. (2008) studied risk factors in build-operate-transfer BOT water supply projects in China, because of increasing population had pressure on existing infrastructure facilities, the

lack of which would down economic development and social growth, in order to encouraged infrastructure supplies from the private sector the Chinese government had discovered the system BOT model operating the analytic hierarchy process (AHP) technique, constructs a three-level hierarchy for determining the critical risk factors for water supply projects.

Sadiq et al. (2007) studied on the evaluation the risk of water quality failures in a distribution network, each basic risk item in a hierarchical framework were stated by a triangular fuzzy number, which was originated from the composition of the likelihood of a failure event and the associated failure consequence.

In order to evaluate the reliability of water supply systems under threatening conditions, risk assessment recognized as a useful tool to identify the hazard, analyses vulnerabilities, and risks. Therefore, the present paper aims to indicate most critical and significant risk factors that have a great influence on water supply projects. In addition, it aims to identify and assess of risks during the implementation of water supply projects by determining the probability of occurrences and their impact of factors.

2. RESEARCH METHODOLOGY

In order to achieve main objective of this paper a review of the literature was conducted to investigate risk and identify the risk factors and sources in water supply system of construction project. Risk assessed by qualitative risk management (RM) and one method of qualitative (RM) is questionnaires. The questionnaire used as a simple and effective way for purpose of data collection, it was consisted of two sections, first section solicited general information about respondents such as year experience and profession , and second section carried a total of 51 risk factors associated to construction of water supply system and asked respondents to indicate the probability of occurrences of these risk factors and impact on construction of water supply system .These risk factors were sourced from a wide range of literature including journal paper and books worldwide as well as those specially focused on construction of water supply system. The 51 risk factors were categorized into five groups with ten risk factors related to design and contract phase, twenty one related to construction and management phase, three related to financial risks, five associated to political risk, five linked to environment risk, and seven connected to resources and procurement risk. The likert scale used for assessing probability and impact were from 1 to 5 where: 1 = very low, 2 = low, 3 = moderate, 4 = high, 5 = very high. About 50 forms of questionnaires created and distributed in water supply projects located in Erbil city area. A total of 42 usable responds returned with acceptable percentage respondents was (84%), all the respondents carried out in water supply projects in Erbil city .The answers listed in the returned questionnaires were collated and qualitatively analyzed using the Statistical Package for Social Sciences (SPSS) version 22 and Microsoft excel 2010.

Risk score computed as the probability multiplied by impact. The range of risk score, the rating and color are assigned to indicate the importance of each risk (Westland, 2007).

0.8	0.080	0.240	0.400	0.560	0.720
0.4	0.040	0.120	0.200	0.280	0.360
0.2	0.020	0.060	0.100	0.140	0.180
0.1	0.010	0.030	0.050	0.070	0.09
0.05	0.005	0.015	0.025	0.035	0.045
Impact ↑ Probability →	0.1	0.3	0.5	0.7	0.9

Table (1) Risk Matrix (PMI, 2017)

As shown in Table 1 Risks marked in the right upper corner with red color are the risks with the greatest negative impact on the project performance. On the other hand, risks marked in the left bottom corner with yellow color are categorized with low influence and minor effect on the project performance .The remaining risks in the middle of the matrix with orange color are classified as a moderate level where the risks should be concerned, but not as extreme as the most negative risks. From this matrix, it is easy to reflect over which action to take against an evaluated risk. All risks will be ranked which facilitates to alert the most critical (Gajewska and Ropel, 2011).

3. STUDY AREA AND DATA ANALYSIS

3.1 Study Area

The study area covered the city of Erbil which is the capital of both Erbil Governorate and Kurdistan Regional Governorate; the area of Erbil Governorate is about 15074km2 , with the population of 1542421 capita and geographically distributed of 24% rural, and 76% urban (WFP VAM,2009).

3.2 Data Analysis

From Table 2 as shown below the percentage and frequency of respondents according to degree of education the same percentage of B.Sc. and Ph.D. participate in questionnaires, which was (40.5%), and M.Sc. with (19%). As indicated in Table 3 most of respondents according to role in construction project was consultant and site engineer with (47.6%) and (45.2%) respectively .Regarding to professions of respondents as shown in Table 4 also consist of the same percentage of professions in civil and water resources of respondents with (42.9%). Table 5 related to year of experience of respondents (38.1%) of respondents was year experience between 6 to 15 year and (31%) of respondents was year experience between 16 to 25 year and the same amount (31) of respondents was year experience greater than 26 year .As shown in table 6 , (59.5%) of respondents related to number of project executed in civil projects which was between 6 to 35 project and (31%) of respondents which was 5 and less than 5 project executed in civil project. Result in table 7 indicated that (42.9%) of respondents considering by number of project executed in water supply projects which was between 5 to 20 project, and (35.7%) of respondents related to less than 5 project executed in water supply project.

Table (2) Degree of Education of Respondents.

Category	Frequency	Percentage%
BSc	17	40.5
MSc	8	19.0
PhD	17	40.5
Total	42	100.0

Table (3) Role of Respondents in Construction Projects.

Category	Frequency	Percentage %
Contractor	3	7.1
Consultant	20	47.6
Site engineer	19	45.2
Total	42	100.0

Table (4) Professions or Qualification of Respondents

Category	Frequency	Percentage%
Civil	18	42.9
Mechanical	2	4.8
Electrical	3	7.1
Water resource	18	42.9
Architect	1	2.4
Total	42	100.0

Table (5) Year of Experience of Respondents

Category	Frequency	Percentage%
6 - 15 year	16	38.1
16 - 25year	13	31.0
26 year and more	13	31.0
Total	42	100.0

Table (6) Number of Civil Projects Executed by Respondent

Category	Number	Percentage%
5 and less than	13	31.0
6 - 35	25	59.5
36- 65	2	4.8
66 and more	2	4.8
Total	42	100.0

Table (7) Number of Water Supply Project Executed by Respondents

Category	Number	Percentage%
Less than 5	15	35.7
5-20	18	42.9
20-35	5	9.5
More than 35	4	9.5
Total	42	100

4. RESULT AND DISCUSSION

The results were combined in a Table 8 based on a matrix above after computing mean of probability and mean of impact for each risk factor according to equation (1) (Xu et al., 2010).

$$M = \frac{\sum(f*s)}{N} \quad (1)$$

Where:

M = Mean of Probability and Mean of Impact

s=Score give to each risk factors by respondents ranging from 1 to 5.

f= Frequency of each rating (1-5) for each risk factor.

N=Total number of respondents.

Also risk score obtained by multiplying probability and impact according to equation (2) (Gajewska and Ropel, 2011).

*Risk Score=Probability *Impact (2)*

Such as for risk factor D1 (0.461*0.319) equal to (0.147).

For risks marked with red color, are those with the biggest negative influence on the project risk marked with orange color are those categorized with moderate level, risk indicated with yellow color are those arranged with low effect on project performance.

The most critical risk factor which had a great effect on projects according to risk rate is inappropriate estimate quantity and quality of water needed for each individual of customer and it was became a higher location as a critical risk in design stage, whereas inaccurate selection the standard and specifications of materials became the second crucial risk factors. The third most significant risk was change of design because of improper understanding of customer needs. Additionally, inadequate estimation of available flow and pressure of water and improper design documentation and drawings were indicated as a serious risk factor. All other factors were in moderate level of impact on projects.

The considerable risk factors summarizes in construction stage were poor quality performance, improper quality control, afterward inadequate safety requirements on site and delay payment on contract, also there were two risk factor with low influence in project which were weakness of disputes arbitration system and inadequate of excavation work due to lack of equipment efficiency. While war, military operation, terrorism attack, and inadequacy of insurance became a maximum critical risk factor as a political issue, also force majors such as earthquake and flood, pollution of pipes from fecal animals or humans, corrosion of pipes that causes of water pollution summarized as a serious environment risk factors .Furthermore, lack of labor skill or qualified plumber became the most critical risk that must be considered throughout resources managing.

Table (8) Probability, Impact and Risk score of Risk Factors.

	RISK FACTORS	**Probability**	**Impact**	**Risk Score**
	1-Design and Contract Risk factors.			
D1	Poor project definition, and inadequate of project scope.	0.461	0.319	0.147
D2	Improper design documentation and drawings.	0.49	0.410	0.203
D3	Change of design as a result of inappropriate identification of customer requirements,	0.671	0.505	0.34
D4	Inadequate design check by consultant concerning the level of risks of whole project.	0.562	0.343	0.193
D5	Inaccurate cost and time estimation.	0.514	0.357	0.184
D6	Inadequate soil investigations and site survey to determine the profile of the location or site field.	0.529	0.336	0.177
D7	Inadequate estimation of available flow and pressure of water.	0.676	0.443	0.30
D8	Improper calculate quantity and quality of water necessary for each single of customer.	0.667	0.545	0.363
D9	Inaccurate selection the standard and specifications of materials (pipes, pumps ….etc.)	0.636	0.552	0.351
D10	Inappropriate form or type of the contract	0.476	0.279	0.133
	2-Construction and Management Risk factors			
C1	Construction time and cost overrun.	0.495	0.250	0.124
C2	Delays due to lack of availability of utilities.	0.452	0.202	0.092
C3	Occurrences of variations.	0.505	0.269	0.136
C4	Poor quality performance. Improper quality control	0.514	0.526	0.271
C5	Inadequate safety requirements on site.	0.481	0.424	0.204
C6	Inaccurate estimation the quantity of work in the bill of quantities.	0.495	0.248	0.123
C7	Unprofessional construction supervision.	0.476	0.190	0.091
C8	Insufficient managing of human resources by contractor or subcontractor	0.405	0.240	0.097
C9	Increases of remedial action due to absence of quality required.	0.390	0.186	0.073
C10	Inadequate of excavations works due to lack of equipment efficiency or capacity.	0.300	0.143	0.043
C11	Pipe line failures due to Inadequate welding of connections.	0.405	0.271	0.110
C12	Water leakage during distribution of pipe networks.	0.348	0.269	0.094
C13	Poor relation and disputes with partner.	0.362	0.183	0.066
C14	Weakness of disputes arbitration system.	0.343	0.145	0.050

C15	Poor coordination between head office and site offices.	0.362	0.186	0.067
C16	Change of top management.	0.419	0.169	0.071
C17	Internal management problem.	0.414	0.186	0.077
C18	Inadequate time management as a result of making change from management strategies of the project or change of project manager.	0.424	0.200	0.085
C19	Improper using available site information to provide calculated basis for risks.	0.448	0.207	0.093
C20	Poor communication and willingness to discuss risk and mitigation strategies.	0.449	0.202	0.091
C21	Delay of payment on contract	0.629	0.321	0.202
	3-Financial Risk factors			
F1	Increase in price as a result of raw materials price increase, or fluctuation in prices.	0.552	0.264	0.146
F2	Improper project planning and budgeting.	0.457	0.264	0.121
F3	Lack of skill in cost management of the project	0.429	0.157	0.067
	4-Political Risk factors			
P1	Changes in laws and regulations and permits	0.419	0.217	0.091
P2	Imperfect laws and supervision system	0.457	0.240	0.110
P3	Change in government and political opposition	0.467	0.298	0.139
P4	War, military operation, terrorism attack	0.629	0.562	0.353
P5	Inadequacy of insurance	0.614	0.364	0.224
	5-Environmental Risk factors			
E1	Skill deficiency of project managers in environmental protection.	0.429	0.231	0.099
E2	force majeure such as Earthquake, flood	0.405	0.583	0.236
E3	Corrosion of the pipes causes water pollution.	0.462	0.433	0.200
E4	Adverse weather condition or geotechnical condition	0.424	0.290	0.123
E5	Pollution of pipes from faecal of animals or human	0.486	0.417	0.202
	6- Resource and Procurement Risk factors			
R1	Purchased the Materials (pipes ,pumps, valves ,taps, connections) that don't comply with standard specifications	0.448	0.279	0.125

R2	Improper certificate of tests required for materials (pipes, pumps….etc.)	0.457	0.240	0.110
R3	The effects of defective equipment and machine quality	0.438	0.236	0.103
R4	Improper procurement plan to provide materials to site.	0.371	0.190	0.071
R5	Defect or damage of pipes during transportation, handling, fixing	0.467	0.245	0.114
R6	Labor accident.	0.471	0.357	0.168
R7	Lack of labor skill level or plumber qualification.	0.619	0.424	0.262

Impact						
0.8						
0.4			C5,D2,E5,C4 E3,E2	D7,R7,D3,D8, P4,P5,D9		
0.2		C12 R4 C15,C13,C9	E4,R1,R2,R3,R5, R6,C11,C6,C3,F1,F2 ,D1,C8,P1,P2, P3,C1,D6 C2,C18,C19,C20, D10,D5 C7,E1, C17 C16,F3	D4 C21		
0.1		C10,C14				

0.05					
	0.1	0.3	0.5	0.7	0.9

Figure1: Risk Map Matrix for Risk Factors

5. CONCLUSIONS

Risk assessment in water supply system has been recognized as a very important process, in order to achieve the most significant risks which have great impact on project. It is concluded from findings of this study the most critical risk factor which had a great impact on projects according to risk rate is improper estimate quantity and quality of water needed for each individual of customer and it was became a higher position as a critical risk in design stage, whereas inaccurate selection the standard and specifications of materials became the second crucial risk factors. The third most considerable risk was change of design because of improper understanding of customer needs. Furthermore, inadequate estimation of available flow and pressure of water and improper design documentation and drawings were pointed as a serious risk factor. All other factors were in moderate level of impact on projects.

The result of risk factors in construction stage summarizes that the most significant risk factors were poor quality performance, improper quality control, afterward inadequate safety requirements on site and delay payment on contract turn into considerable risk factors, also there were two risk factor with low influence in project which were weakness of disputes arbitration system and inadequate of excavation work due to lack of equipment efficiency.

While war, military operation, terrorism attack, and inadequacy of insurance became a maximum critical risk factor as a political issue, also force majors such as earthquake and flood, pollution of pipes from fecal animals or humans, corrosion of pipes that causes of water pollution summarized as a serious environment risk factors .Furthermore, lack of labor skill or qualified plumber became the most critical risk that must be considered throughout resources managing.

REFRENCES

ABD, A. 2015. *BUILDING PROJECTS RISKS SOURCES: CONCEPTUAL FUZZY ASSESSMENT APPROACH*.

AMEYAW, E. E. & CHAN, A. P. 2015. Risk ranking and analysis in PPP water supply infrastructure projects: an international survey of industry experts. *Facilities*, 33**,** 428-453.

ATAOUI, R. & ERMINI, R. 2017. Risk Assessment of Water Distribution Service. *Procedia Engineering*, 186**,** 514-521.

BERGION, V., LINDHE, A., SOKOLOVA, E. & ROSÉN, L. 2017. Risk-based cost-benefit analysis for evaluating microbial risk mitigation in a drinking water system. *Water research*.

BLOKKER, M., SMEETS, P. & MEDEMA, G. 2017. Quantitative Microbial Risk Assessment of Repairs of the Drinking Water Distribution System. *Microbial Risk Analysis*.

CHAN, A. P., LAM, P. T., WEN, Y., AMEYAW, E. E., WANG, S. & KE, Y. 2014. Cross-sectional analysis of critical risk factors for PPP water projects in China. *Journal of Infrastructure Systems*, 21**,** 04014031.

GAJEWSKA, E. & ROPEL, M. 2011. Risk Management Practices in a Construction Project–a case study. *Swedia, Chalmers University Of Technology*.

LI, H. 2007. *Hierarchical risk assessment of water supply systems.*

ROOZBAHANI, A., ZAHRAIE, B. & TABESH, M. 2013. Integrated risk assessment of urban water supply systems from source to tap. *Stochastic environmental research and risk assessment*, 27**,** 923-944.

RYBKA, I., BONDAR-NOWAKOWSKA, E. & POLONSKI, M. 2016a. Cost risk in water and sewerage systems construction projects. *Procedia engineering*, 161**,** 163-167.

RYBKA, I., BONDAR-NOWAKOWSKA, E. & POŁOŃSKI, M. 2016b. Causes and effects of adverse events during water supply and sewerage system constructions. *Archives of Civil Engineering*, 62**,** 173-184.

SADIQ, R., KLEINER, Y. & RAJANI, B. 2007. Water quality failures in distribution networks—risk analysis using fuzzy logic and evidential reasoning. *Risk Analysis*, 27**,** 1381-1394.

TCHÓRZEWSKA-CIEŚLAK, B. 2011. Fuzzy failure risk analysis in drinking water technical system. *Reliability: Theory & Applications*, 6.

VIEIRA, J. 2005. Water safety plans: methodologies for risk assessment and risk management in drinking-water systems.

WESTLAND, J. 2007. *The Project Management Life Cycle: A Complete Step-By-Step Methodology for Initiating, Planning, Executing & Closing a Project Successf*, Kogan Page Publishers.

WFP VAM 2009. the Information Analysis Unit, OCHA-United Nations Office for the Coordination of Humanitarian Affairs. *www.iauiraq.org/report.GP-Erbil.pdf*

WHO 2004. *Word Health Organization Guidelines for drinking-water quality: recommendations*, World Health Organization.

WIBOWO, A. & MOHAMED, S. 2010. Risk criticality and allocation in privatised water supply projects in Indonesia. *International Journal of Project Management*, 28**,** 504-513.

XU, Y., YEUNG, J. F., CHAN, A. P., CHAN, D. W., WANG, S. Q. & KE, Y. 2010. Developing a risk assessment model for PPP projects in China—A fuzzy synthetic evaluation approach. *Automation in Construction*, 19**,** 929-943.

ZENG, S., WAN, T., TAM, C. M. & LIU, D. Identifying risk factors of BOT for water supply projects. Proceedings of the Institution of Civil Engineers-Water Management, 2008. Thomas Telford Ltd, 73-81.

ZHANG, J., GAO, J., DIAO, M., WU, W., WANG, T. & QI, S. 2014. A case study on risk assessment of long distance water supply system. *Procedia Engineering*, 70**,** 1762-1771.

ZANCO Journal of Pure and Applied Sciences
The official scientific journal of Salahaddin University-Erbil
https://zancojournals.su.edu.krd/index.php/JPAS

ISSN (print):2218-0230**, ISSN (online):** 2412-3986**, DOI: http://dx.doi.org/10.21271/zjpas**

RESEARCH PAPER

Comparison between Theim and Theis Equations in Analysis of Pumping Tests

Dana Khider Mawlood

Department of Civil Engineering, College of Engineering, Salahaddin University - Erbil, Kurdistan Region, Iraq.

A B S T R A C T:
The presented study is tried to analyze the main difference between the application of Theim (1906) and Thies (1935) equations for steady and non- steady conditions to determine the property of layer such as (Transmissivity , Specific yield and storativity). Thies and Theim methods can be applied for pumping test, using a single well testing lead to well losses and aquifer losses, the results of property layer need further adjustment therefore, advisable to have observation well in order to avoid losses (such as well losses and aquifer losses), however, by applying Theim equation, the property of layer was restricted just for Transmissivity since the application is for equilibrium condition. The benefit is performed to evaluate the capacity of an aquifer to meet municipal or industrial water requirement and hydraulic characteristics reflect the potential of an aquifer for water development.

KEY WORDS: Steady-state condition, transient flow condition, equilibrium, non-equilibrium equation.
DOI: http://dx.doi.org/10.21271/ZJPAS.31.2.6.
ZJPAS (2019) , 31(2);41-47 .

INTRODUCTION :

Globally groundwater is the main source of water supply because most of the countries depend on the groundwater for their purposes such as irrigation, drinking water, and industrial. One of the main purposes of the pumping test is to predict the specific capacity of the well, it is the proportion of pumping rate to drawdown in the well, also, it is the associated with the hydraulic flow properties, the specific capacity of the well is precious number that can be utilized to estimate the volume of water abstracted in the well, and it has a major function for design of well and estimating radius of influence.

* **Corresponding Author:**
Dana Khider Mawlood
E-mail: dana.mawlood@su.edu.krd
Article History:
Received: 12/11/2018
Accepted: 02/04/2019
Published: 23/04/2019

Appropriate management of ground-water resources imposes an accurate evaluation of the parameters (hydraulic properties) that governor the movement and storage of water. Aquifer tests, implemented by pumping a well at aconstant rate and monitoring the resulting variations in hydraulic head in the aquifer, it was the most normally used method for determination of aquifer hydraulic properties (Moench et al., 2000).

The test data were analyzed through many methods according to the situation of each locations. The first scientist was Theim in 1906 that developed a method for both confined and unconfined aquifer according to the Dupuit assumptions in 1863, who governed the equation for flow in water table aquifer for steady state (equilibrium conditions). It is evident from the Thiem equation that the drawdown varies with the logarithm of the distance from the pumping well. Thiem equation can be used to compute constant pumping rate (Q), steady drawdown (s_1 or s_2) or distance of the point of observation from the

pumping well (r_1 or r_2) if the aquifer parameter T and other variables are known. Additionally, this equation can also be used to calculate aquifer parameter T (or, K if the aquifer thickness is given) if other variables are known. Later, Theis (1935) based on heat transfer derived a method for transient groundwater flow in confined aquifer, then Jacob (1946) simplified Theis solution for long time of pumping test and small radial distance, both previous equations are applicable for unconfined aquifer type, if the drawdown is very small compared to the saturated thickness of the aquifer, after that Hantush M S (1960) find a solution for leaky (semi-confined) aquifer, then Neuman S P in 1975 developed a solution for unconfined aquifer type unsteady-state conditions, the application of all the previous methods are derived based on the particular assumptions.

2. METHOLOGY

2.1 Theim (1906) Solutions.

In (1906) Theim was first modified Dupuit (1863) equation and on this basis developed the solution for both confined and unconfined aquifer types. The cone of depression surrounding a pumping well is stabilized (i.e drawdown and radius of influence are static) the Thiem equation is used to determine the hydraulic conductivity for the aquifer (note: the storage coefficient cannot be found under steady state condition).

2.1.1 Theim Confined Aquifer Equations

For a well located in fully penetrate confined aquifer, Fig.1, two piezometric head or more required rather than pumping well to monitoring drawdown at time of pumping test (K.Subramanya et al.,1999).

The following assumptions should be taken into account during governing the equation:

1. The aquifer is confined.
2. The aquifer has an infinite areal extent.
3. The aquifer is homogeneous, isotropic and of uniform thickness over the area influenced by the test.
4. Prior to pumping, the piezometric surface is horizontal over the area that will be influenced by the test.
5. The aquifer is pumped at a constant discharge rate.
6. The well is screened over the entire thickness of the aquifer ensuring entirely horizontal flow.
7. The hydraulic gradient between the pumping well and monitoring wells is at steady-state.
8. The water removed from storage is discharged instantaneously with decline of head.
9. Storage in the well can be neglected (the diameter of the well is small).

The two-dimensional radial flow to well for confined aquifer under steady-state condition is as follows:

$$\frac{1}{r}\frac{\partial h}{\partial r} + \frac{\partial^2 h}{\partial r^2} = 0 \qquad (1)$$

Darcy's Law

$$q = -K\frac{\partial h}{\partial r} \qquad (2)$$

Continuity

$Q=-2\pi rbq$
(3)

Eliminating q gives

$$Q=-2\pi rbq\frac{\partial h}{\partial r} \qquad (4)$$

Rearranging and integration

$$\frac{Q}{2\pi Kb}\int_{r1}^{r2}\frac{1}{r}dr = \int_{h1}^{h2} dh \qquad (5)$$

Which gives,

$\frac{Q}{2\pi Kb}\ln\frac{r_2}{r_1}=h_2 - h_1$
(6)

In terms of draw down (which is the measurement made in the field)

$\frac{Q}{2\pi Kb}\ln\frac{r_2}{r_1}=s_1 - s_2$
(7)

This is called the Thiem Equation and can be used to estimate the transmissivity.

At least two piezometers should be used whenever possible (using the drawdown at just one piezometer and at the abstraction well leads to errors due to well losses at the abstraction well).

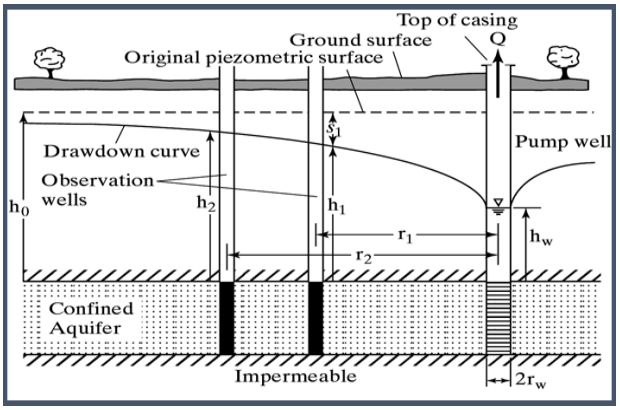

Figure (1): Fully penetrated confined aquifer

2.1.2. Theim Unconfined Aquifer Equations

Theim in (1906) developed a method based on Dupuit (1863) solution for groundwater flow in unconfined aquifer with the saturated thickness of H (G.P. Kruseman et al.,1991), the flow reaches to steady-state condition after long duration of test, and the solution required two observation wells, to measuring groundwater table during the test, which is depicted in Fig.2.

The following assumptions should be taken into account during governing the equation (Phileepe et al.,2005):

1. The aquifer is unconfined
2. The aquifer has infinite aerial extent
3. The aquifer is homogeneous, isotropic, uniform thickness.
4. The groundwater table is horizontal prior to pumping
5. The aquifer is fully penetrated through the entire thickness.
6. The aquifer is pumped at constant rate.

The two-dimensional radial flow equation for water-table aquifer is as follow:

$$\frac{\partial^2 h^2}{\partial r^2} + \frac{1}{r}\frac{\partial h^2}{\partial r} = 0 \qquad (8)$$

The above equation is Theim -equilibrium equation, it can be written in another form, which is called of Dupuit-Theim equation, who applied the boundary conditions between pumping well and radius of influence;

@r=r_w ,h=hw

@r=R ,h=H

$$(H^2 - hw^2) = \frac{Q}{\pi K}\ln\left|\frac{R}{rw}\right| \qquad (9)$$

Sometimes unconfined aquifer behaves as the confined aquifers, especially when the saturated thickness of the aquifer is much higher than the drawdown. In such case the adjustment of drawdown required during data analysis.

$$(H^2 - hw^2) = \frac{Q}{\pi K}\ln\left|\frac{R}{rw}\right| \qquad (10)$$

This is the same equation of the confined aquifer.

There is also another equation form, when the drawdown is adjusted:

$$s' = s - \frac{s^2}{2H} \qquad (11)$$

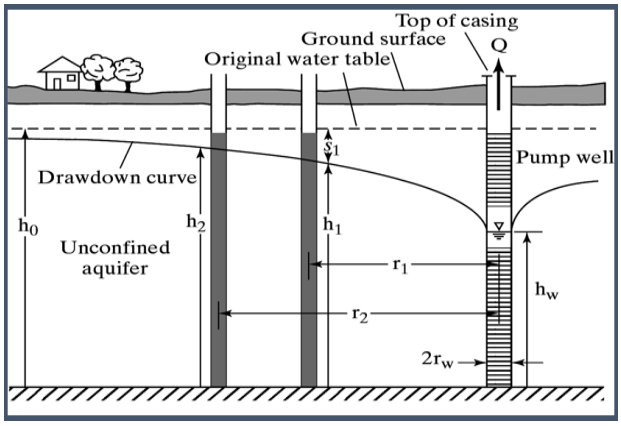

Figure (2): Fully penetrated unconfined aquifer

2.2 Theis (1935) Non-equilibrium Well Pumping Equation.

Charles Vernon Theis (1900-1987) was the first hydrologist to develop a rigorous mathematical model of transient flow of water to a pumping well by recognizing the physical analogy between heat flow in solids and groundwater flow in porous media. The Theis (1935) solution (or Theis non-equilibrium method) introduced a groundbreaking tool for determining the hydraulic properties. Analysis involves matching the type curve for confined aquifers to field drawdown data as a function of time collected during a pumping test, his solution based on direct analogy between heat transfer and groundwater flow to a well in a well with one additional observation well, the geometry of the well and water flow condition during Theis research in the field. Using a model describing the flow of heat from a heat

source, Theis(1935)derived a mathematical equation for the transient flow of groundwater to a well. The equation was originally developed for a fully penetrating well in a confined aquifer, but may also be used for unconfined aquifers if the drawdown is considerably smaller than the saturated thickness. Theis developed a standard type curve which relates the theoretical response of an aquifer to pumping. The type curve is obtained by plotting W(u)(the well function vs.1/u.

The following assumptions should be taken into account during the governing equation.

The procedure is to plot drawdown versus time on logarithmic paper and match with Theis type curve, Figure 3. The matches involve that using one transparent sheet and slide the two curves along, horizontally and vertically, until the theoretical curve matches or fits the data.

2.2.1 Governing Theis Equation

When a well penetrating an extensive confine aquifer is pumped at a constant rate, the influence of the discharge extends outward with time. The rate of decline of head times the storage coefficient summed over the area of influence equals the discharge. Because the water must come from a reduction of storage within the aquifer, the head will continue to decline as long as the aquifer is effectively infinite; therefore, unsteady, or transient, flow exists. The rate of decline, however, decreases continuously as the area of influence expands.

$$\frac{\partial^2 h}{\partial r^2}+\frac{1}{r}\frac{\partial h}{\partial r}=\frac{S}{T}\frac{\partial h}{\partial t} \qquad (12)$$

Where:

h: is head (m)

r: is radial distance from the pumped well. (m)

S: is the storage coefficient.

T: is transmissivity, which is equal to Kb, (m2/s)or (m2/min).

K: is hydraulic conductivity (m/s) or (m/min).

b: is the thickness of the confined aquifer (m).

t: is the time since beginning of pumping . (min or sec)

Theis (1935) obtained a solution for equation (6) based on the analogy between groundwater flow and head condition by

$$s=\frac{Q}{4\pi T}\int_u^\infty \frac{e^{-u}}{u}du=\frac{Q}{4\pi T}W(u)$$
$$=\frac{Q}{4\pi T}\left[-0.5772-ln(u)+u-\frac{u^2}{2.2!}+\frac{u^3}{3.3!}-\frac{u^4}{4.4.!}+\cdots\right] \qquad (13)$$

Is obtained, where

S: is drawdown (m).

Q: is constant well discharge (m^3/s) or (m^3/min).

$$u=\frac{r^2 S}{4Tt} \qquad (14)$$

Equation (13) is known as the nonequilibrium ,or Thies , equation. The integral is a function of the lower limit u is known as an exponential integral. It can be expanded as a convergent series as shown in Equation (13) and is termed the well function, W (u).

Alternatively, using U.S customary units (gallon-day – foot system) where S is in ft, Q is in gpm , T is in gpd/ft, u is in ft, and t is in days, we have

$$s=\frac{114.6Q}{T}W(u) \qquad (15a)$$

$$u=\frac{1.87r^2S}{Tt} \quad (\text{t in days}) \qquad (15b)$$

$$u=\frac{2693r^2S}{Tt} \quad (\text{t in minutes}) \qquad (15c)$$

The non-equilibrium equation permits determination of the formation constant S and T by means of pumping tests of wells. The equation is widely applied in practice and preferred over the equilibrium equation because (1) a value for S can be determined, (2) only one observation well is required, (3) a shorter period of pumping is generally necessary, and (4) no assumption of steady –state flow conditions is required.

The assumption includes:

1. The aquifer is homogenous, isotropic, of uniform thickness, and of infinite areal extent.
2. Before pumping, the piezometric surface is horizontal.
3. The well is pumped at a constant discharge rate.
4. The pumped well penetrates the entire aquifer, and flow is everywhere horizontal within the aquifer to the well.
5. The well diameter is infinitesimal so that storage within the well can be neglected.
6. Water removed from storage is discharge instantaneously with decline of head.

The influence of a constant pumping rate. Because of the mathematical difficulties encountered in applying Equation (13), or its equivalent, Equation (15), several investigators have developed simpler approximate solutions that can be readily applied for field purposes.

2.2.2 Theis Method of Solution

$$s = \frac{Q}{4T\pi} W(u) \quad (16)$$

Where:

W (u), termed the well function

Rewriting Equation (8)

$$\frac{r^2}{t} = \frac{4T}{S} u \quad (17)$$

Step 1. Plot the time- drawdown data on log-log graph paper. The drawdown is plotted on the vertical axis and the time since pumping started on the horizontal axis (not shown).

Step 2. Superimpose this plot on the type curve sheet of the same size scale as the time-drawdown plot, so that the plotted points match the type curve. The axes of both graphs must be kept parallel.

Step 3. Select a match point, which can be any point in the overlap area of the curve sheet. It is usually most convenient to select a match point where the coordinates on the curve are known in advance.

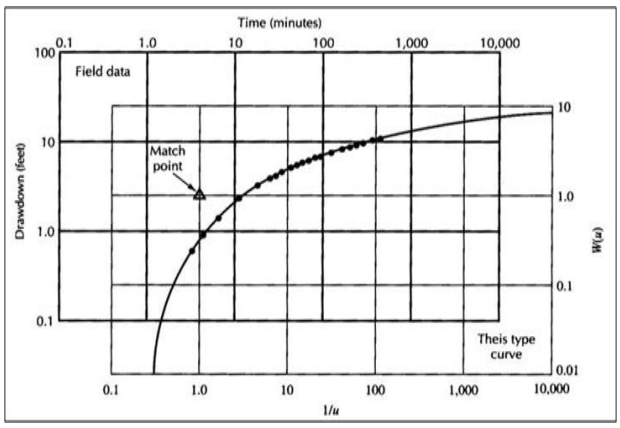

Figure (3): Theis Graphical solution and matching point

3. APPLICATION OF THE STEADY STATE EQUATIONS

Study Area

This data was collected from a well test in (Qushtapa camp), which is located at a distance of about 26 km from the center of Erbil city with coordinate of (26.001469, 44.07336).Figure 4 is illustrated the location of Qushtapa sub-basins.

Figure 4 : Qushtapa Erbil's sub-basins

Table 1 Pumping test data results from Directorate of Erbil Groundwater

Project Name: bdele well / kushtapa camp				
Well Name No. :3		**Date of Test : 2018/11/4**		
Static water level :124.6m		**Well Depth :431m**		
Machine type	**SP30-39**	**Pipe dia.**	**3 inch**	
Length of pipe	**250 m**			
No.	**Time**	**Depth to water level (m)**	**Drawdown (m)**	**Discharge (gal/min)**
1	0	124.6	0	0
2	0.5	137	12.4	145
3	1	141	16.4	145
4	1.5	146	21.4	145
5	2	150.6	26	145
6	3	156.6	32	145
7	4	161	36.4	145
8	5	165	40.4	139
9	6	166.5	41.9	139
10	7	168	43.4	139
11	8	169.2	44.6	139
12	9	170.5	45.9	139
13	10	171.2	46.6	139
14	15	172	47.4	139
15	20	172	47.4	139
16	25	172	47.4	139
17	30	172	47.4	139
18	40	172	47.4	139

3.1 Theis (1935) Equation

Solution:

By hand calculation:

1/u =7 => u = 0.1428, t=2 Minute=0.001389 day/

S= 26 m

r_w= 0.11 m because no observation well is used, so we use radius of well

By using theis equation (10) we can find T

$$T=\frac{Q}{4\pi s} * W(u) = \frac{900.72}{4\pi * 26} * 1.4 = 3.86 \ \frac{m^2}{day}$$

By using theis equation (8) we can find S

$$u=\frac{r^2 S}{4Tt} \qquad S = \frac{4Ttu}{r^2} =$$

$$\frac{4*3.2466\frac{m^2}{day}*0.001389day*0.1428}{0.11^2} = 0.2531$$

Figure (8): Graphical solution of pumping test data by theis (1935) method by using (AQTESOLVE) Program. ohical solution of pumping test data by theis (1935) method by using (AQTESOLVE, AQUIFER TEST and AQUIFER WIN 32) Programs.

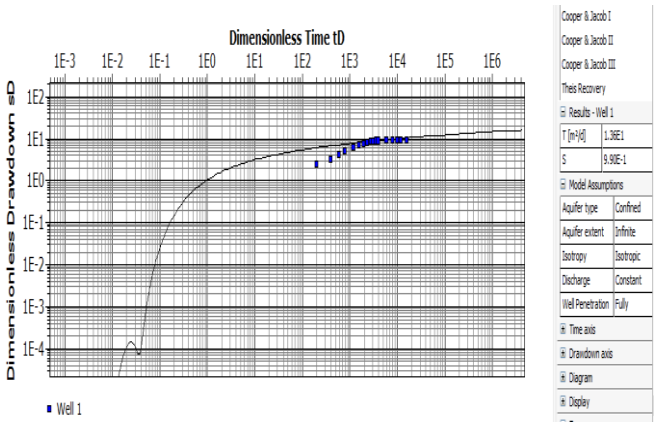

Figure (5): Graphical solution of pumping test by Thies (1935) method by using Aquifer test program.

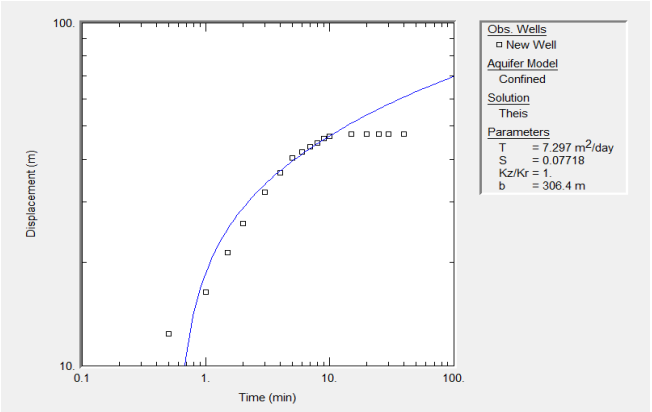

Figure (6):

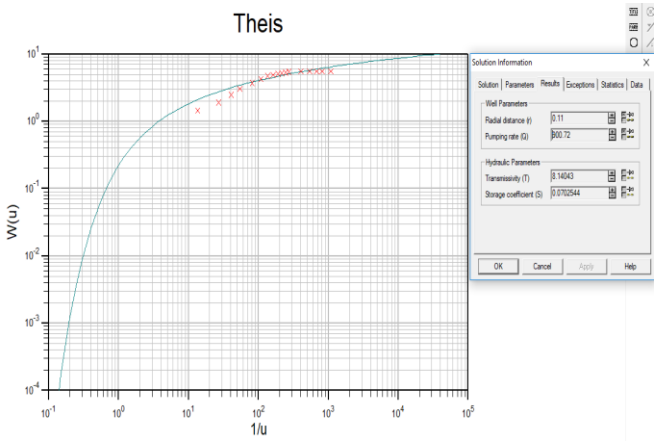

Figure (7): Graphical solution of Thies (1935) equation by using Aquifer Win32 program.

3.2 Theim (1906) Equation for Confined Aquifer

Solution:

Table 2 Distance Drawdown Data.

well No.	Distance(m)	Drawdown(m)
2	200	0.9
3	250	0.3

$$T = \frac{Q}{2\pi (S_1 - S_2)} \ln \frac{r_2}{r_1}$$

$$T = \frac{900.72}{2\pi (0.9 - 0.3)} \ln \frac{250}{200} = 53.314 \ m^2/day$$

4. RESULT AND DISCUSSION

The data generated from aquifer tests can be calculate T and/or S by means of mathematical models describing groundwater flow towards the well. These models (flow equations) are derived using a mass balance approach and may therefore apply to equilibrium or non-equilibrium fow conditions. Table 3 presents aquifer parameters results from Qushtapa area by Theis and Theim method. During the comparison between the calculated and standard range of Transmissivity, The calculated value of Transmissivity of Qushtapa well which can be classified according to (Table 4) from intermediate to low.

Table 3 Result of Transmissivity and Storativity by Theis and Theim.

	Transmissivity (T) m^2/day	Storativity (S)
Theis by (hand calculation)	3.86	0.2531
Theis by (aquifer test program)	13.6	0.99
Theis by (AQTISOLVE program)	7.297	0.07718
Theis by (aquifer win 32 program)	8.14	0.0702
Theim steady state	53.314	–

Table 4: Transmissivity classification (Jirikrasny et al., 1993).

Coefficient of Transmissivity (m^2/day)	class of Transmissivity magnitude	Designation of Transmissivity magnitude
>1000	I	very high
100 to 1000	II	High
10 to 100	III	Intermediate
1 to 10	V	Low
0.1 to 1	IV	Very low
<0.1	VI	Imperceptible

CONCLUSION

Drawdowns are observed during an abandoned pump test, which might otherwise be considered inappropriate for estimation of aquifer parameters, Theim equation can be used in equilibrium conditions for estimating the values of Transmissivity, by using observation well for unconfined aquifer or piezometric well for confined aquifer. Theis equation has been represented in terms of two new parameters. Simple expressions in terms of these parameters have been derived to evaluate the transmissivity and storage coefficient of a confined aquifer in unequilibrium condition.

REFERENCES

COOPER H H, JACOB C E. 1946. A generalized graphical method for evaluating formation constants and summarizing well field history. Eos, Transactions American Geophysical Union, 27(4): 526–534.

DARCY, H. 1856. Les fontaines publiques de la ville de Dijon: exposition et application, Victor Dalmont.

DAVID BANKS, (2012), From Fourier To Darcy, From Carslaw To Theis: the analogies between the subsurface behavior of water and heat, Indian Journal Of Groundwater, DOI 10.7343/As-013-12-0025.

G.P. KRUSEMAN, AND N .A.DE RIDDER, (1991), Analysis and evaluation of pumping test data, 2nd edition, International institute for land reclamation and Improvement/ILRI, No.11, 2000.

HANTUSH M S. 1960. Modification of the theory of leaky aquifers. Journal of Geophysical Research, 65(11): 3713–3725.

JACK BRUIN AND H. E HUDSON JR.(1961), Selected Methods For Pumping Test Analysis, State of Illinois, No.25.

JIRI KRASNY. (1993).Classification of Transmissivity Magnitude and Variation.Vol.31,No2.

K. SUBRAMANYA, (1999), Engineering Hydrology, 2nd. Edition, Tata McGraw-Hill.

MOENCH, A. F., GARABEDIAN, S. P. & LEBLANC, D. R. 2000. Estimation of hydraulic parameters from an unconfined aquifer test conducted in a glacial outwash deposit, Cape Cod, Massachusetts. GERON CORP MENLO PARK CA.

NEUMAN S P. 1975. Analysis of pumping test data from anisotropic unconfined aquifers considering delayed gravity response. Water Resources Research, 11(2): 329–342.

THEIS C V. 1935. The relation between the lowering of the piezometric surface and the rate and duration of discharge of a well using groundwater storage. Eos, Transactions American Geophysical Union, 16(2): 519– 524.

VEDAT BATU,(1998), Aquifer Hydraulics, John Wiley And Sons. Inc.

PHILEEPE RENARD, (2005), Hydraulics Of Wells And Well Testing, John Wiley and sons, Neuch at el, Switzerland.

MICHAEL KASENOW, (2006), Aquifer Test Data: Analysis And Evaluation, Water resources publications.

.

ZANCO Journal of Pure and Applied Sciences
The official scientific journal of Salahaddin University-Erbil
https://zancojournals.su.edu.krd/index.php/JPAS

ISSN (print):2218-0230**, ISSN (online):** 2412-3986**, DOI: http://dx.doi.org/10.21271/zjpas**

RESEARCH PAPER

Characterization of Microsatellite Loci in different Fig (Ficus carica L.) Landraces in Duhok and Erbil Provinces in Kurdistan Region-Iraq.

Shaymaa H. Ali

Scientific Research Center, College of Science, University of Duhok, Duhok, Kurdistan Region, Iraq.

A B S T R A C T:

Fig (*Ficus carica* L.) is one of the underused fruit crops cultivated in Mediterranean countries, which is considered as an important resource for commercial cultivation and breeding. In the current study, simple sequence repeats (SSR) markers were implemented to investigate genetic polymorphism and to assess the phylogenetic relationships among 14 fig landraces in Kurdistan Region-Iraq. Results revealed that, twenty SSR loci produced 73 alleles across all 14 studied samples. The expected heterozygosity was ranged from 0.071 to 0.796. The observed heterozygosity was ranged between 0.071 and 1.0000. Polymorphic information content, *Fis* and *p*-value were ranged from 0.067-0.735, 0.0020-1.0000 and 0.0020-1.0000 respectively. The genetic distances among the studied genotypes were ranged between 0.0145 and 0.2372. The UPGMA clustering analysis discriminated all these 14 fig genotypes and classified them completely into seven major genetic clusters namely; C1, C2, C3, C4, C5, C6 and C7 in the phylogenetic tree. Overall, it can be concluded that there were significant genetic diversities among these local fig landraces. The selected SSR markers allowed an unambiguous differentiation between studied fig landraces and proved the reliability of these markers in fingerprinting of fig genotypes. Also, it is noteworthy to mention that the study findings will aid the management of fig genotypes and might help the selection of these landraces for future breeding program in this region.

KEY WORDS: Fig (*Ficus carica* L.), PCR, SSR, Genetic diversity.
DOI: http://dx.doi.org/10.21271/ZJPAS.31.2.7
ZJPAS (2019), 31(2); 48-56 .

1. INTRODUCTION:

A diploid species (2n = 26) fig tree (*Ficus carica* L.), which belongs to the family *Moraceae*, is considered as one of the oldest traditional fruit that distributed along the Mediterranean basin, east and western Asia (Almajali *et al*., 2012). This tree, is comprehensively characterized by the presence of latex in all its parts, it is naturally well adapted to dry and harsh climate with hot summer. This is due to developing of large root system, many meters away from the trunk, to obtain water from soil.

Thus, it can be grown in areas with hot and dry environments and the hot resistant feature may make this tree more adaptable to the climate changes and global warming consequences (Sugiura *et al*., 2007; Perez- Jiménez *et al*., 2012). A gynodioecious fig plant is present in two sexual forms in nature, the pollinator or male tree (caprifig) and the female tree (domesticated fig), which is the producer of the edible fruit (Chatti *et al*., 2010; Ikegami *et al*., 2013). Therefore, the pollinators like wasps (*Blastophaga psenes*) play significant roles in the biological cycle of *Ficus carica* (Chatti *et al*., 2010). This tree is traditionally considered as a medicinal plant, as its organic extracts are well known to have many

* **Corresponding Author:**
Dr. Shaymaa Hadi Ali
E-mail: shaymaa@uod.ac
Article History:
Received: 22/12/2018
Accepted: 12/02/2019
Published: 23/04/2019

antibacterial, antiviral as well as antioxidant activities (Trichopoulou *et al*., 2006; Lansky *et al*., 2008; Lazreg-Aref *et al*., 2012; Ganopoulos *et al*., 2015).

The preservation of the genetic diversity of traditional varieties and promoting the conservation of the agro diversity and the genetic resources through international initiatives may have definitely very significant and positive consequences on food production and security (Esselman *et al*., 2000). Although, fig tree populations exhibit a rich genetic biodiversity, it has not yet been subjected to intensive plant breeding programs, as it needs to be properly identified, fully exploited and classified (Giraldo *et al*., 2010). In general, the classical identification of cultivars relies mainly on the morphological traits including flesh color, skin color, floral characteristics, parthenocarpy and pollination requirement (Caliskan *et al*., 2018). These morphometric classifications lead to miss assessing the genetic relatedness among cultivars. As, these phenotypic features might vary through years and geographical regions and might greatly be affected by the interactions between genotype and environment (Chatti *et al*., 2010). Therefore, discrimination of the morphologically similar cultivars at the molecular level is crucial to assess fig tree biodiversity and genetic resources. As such, molecular techniques provide a precise identification and reliable information for the genetic characterization of germplasm (Caliskan *et al*., 2012; Ganopoulos *et al*., 2015).

To date, many DNA-based molecular markers have been developed and being long used for germplasm characterization such as restriction fragment length polymorphism (RFLP), amplified fragment length polymorphism (AFLP), random amplified polymorphic DNA (RAPD) and simple sequence repeat (SSR) or microsatellites markers (Stafne *et al*., 2005) Among these, SSR markers, which are short variable number tandem repeats of nucleotide sequences, have received valuable attentions, and become a marker of choice in most plant species for genetic diversity analysis, and fingerprinting. This is due to its reproducibility, co-dominant, and high level of polymorphism, as well as simplicity of detection through PCR based assays, and its reliability (Gupta *et al*., 2000; Giraldo *et al*., 2010).

In the present study, SSR markers were employed to characterize local fig landraces from Duhok and Erbil provinces in Kurdistan region of Iraq. Also, to estimate the genetic diversity and phylogenetic relationships among fig landraces to provide a reliable molecular database for future fig breeding program in this region.

2. MATERIALS AND METHODS

2.1. Sample Collection

In the current study, fresh and young leaves of 14 fig landraces including; rohani bahari, zard payazi, mamezi rash, shoshi gawra, kongi doshawi, taqtaq, zard chawsor, zard gawra, zard bahari, mamezi shen, rash, shenik, arzani and rohani, were collected from different locations at Duhok (Malta, Bagera and Balata) and Erbil (Shaqlawa, Hiran and TaqTaq) provinces.

2.2. Genomic DNA Extraction

The genomic DNA was extracted according to the method previously described by Weigand *et al*., (1993). Briefly, 3g of fresh leave tissues were used from each sample. The tissue was ground to a fine powder using liquid nitrogen. Then the powder was dissolved in pre-heated (60°C) extraction buffer (CTAB) (2gm CTAB (cetyl trimethyl ammonium bromide), 28 ml of 5 M NaCL, 10ml of 1M Tris-HCL, 4 ml of 0.5 M EDTA, the volume was adjust to 100 ml by distilled water) and incubated at 60°C in shaking water bath for 30 min. The mixture was then treated with an equal volume of chloroform/isoamyl alcohol (24:1, v/v) and then centrifuged at 4000g for 30mins. The aqueous phase was transferred to a clean tube and precipitated with 0.66 volume of isopropanol. Precipitated nucleic acid was then hooked out and dissolved in 500-750µl of Tris-EDTA (TE)-buffer (1ml of 1Mtris-HCl (Ph8.0) 0.2ml of 0.5M EDTA to 100ml with dH2O.

2.3. Purification of Extracted Genomic DNA

The extracted DNA sample from previous step was transferred to sterile Eppendorf tube, mixed with an equal volume of phenol/chloroform isoamyl (25:24:1, v/v) and centrifuged at 12000g for 15min. The aqueous layer was transferred to a new sterile Eppendorf tube, 0.1 volume of sodium acetate and 2 volumes of absolute ethanol were added, mixed gently and centrifuged for 5min at 12000g. The supernatant was removed and the pellet dried out for 5mins at room temperature. The pellet was then re-suspended in 350-500µl (depending on pellet size) of TE buffer and stored at -20°C for further downstream applications.

2.4. PCR Amplification of SSR Markers

A total of 20 SSR primers, which were previously developed by Khadari *et al*., (2004), Zavodna *et al*., (2005), and Vignes *et al*., (2006), were used for PCR amplifications and genetic variabilities of respective trees. The PCR amplification was performed in 25µl reaction volume containing 12.5µl of 1X one *Taq* quick-load master mix, 1µl of each primer including forward and reverse (6pmol/µl), 7.5µl of nuclease free water and 2µl of (25-50ng) genomic DNA. Reaction tubes were placed in a thermal cycler (Applied Biosystems-2720) to carry out DNA amplification. The PCR cycle parameters were as follows; initial denaturation at 94°C/45s for 1 cycle, denaturation at 94°C/45s, annealing 50°C - 56°C/45s, extension at 72°C/2-3min for 30 cycles and final extension at 72°C /10 min for 1 cycle. The PCR products were confirmed by electrophoresis on agarose gel 2% (w/v), 100bp ladder were used to verify the product size, stained with ethidium bromide and visualized by UV transilluminator.

2.5. Data scorning and analysis

Gel electrophoresis images were used to score and analyze SSR-data. Number of alleles per locus, observed (Ho) and expected heterozygosity (He), polymorphic information content (PIC), *Fis*, *P*-value, Fixation index genetic distances and phylogenetic tree, all were statistically analyzed by using Power marker V3.0 and Fig Tree V1.3.1 software programs (Rambaut, 2009).

3. RESULTS AND DISCUSSION

The results revealed that 73 alleles were produced across all studied genotypes (Table 1). The number of alleles (richness of primer) was varied from one primer to another. The highest number of alleles was 7 detected at FinsQ6HEX-L locus, while the lowest number of alleles was 2 which were found with primers (FinsK9HEX-L, MFC1, FinsQ5FAM-L, FinsI12FAM-L and MFC7). Major allele frequencies ranged between 0.3571 and 0.9643 detected at MFC5 and FinsQ5FAM-L loci, respectively with a mean of 0.5946. The number of alleles obtained in the present investigation was lower than that obtained by Achtak *et al*., (2009) who used microsatellite markers as reliable tools for Fig cultivar identification, whereas it was higher than those detected by Ikegami *et al*., (2009) and Chatti *et al*., (2010). The total number of alleles obtained in this study was slightly lower than that obtained by Perez-JiMénez *et al*., (2012). The high number of alleles might be due to increasing of heterozygosity levels in modern cultivars during selection program (Khadari *et al*., 2004). However, type and number of genotypes should also be taken into consideration in any comparison.

In addition, the observed heterozygosity was ranged between 0.071 and 1.0000. The highest observed heterozygosity was detected with primer FinsU9NED-L and the lowest observed heterozygosity was obtained with primer FinsQ5FAM-L. The lowest observed heterozygosity was lower than that reported by Ikegami *et al*., (2009), while the highest observed heterozygosity was found to be higher than that obtained by Ikegami *et al*., (2009). Also, the values were higher than those detected by Saddoud *et al*., (2007), Saddoud *et al*., (2011), and Perez-JiMénez *et al*., (2012), whereas they were comparable with those reported by Saddoud *et al*., (2005). Additionally, the expected heterozygosity was ranged from 0.071 (FinsQ5FAM-L) to 0.796 (MFC4). Higher values of expected heterozygosity were reported by Ikegami *et al*., (2009). In contrast, lower values were obtained by Khadar *et al*., (2004) and Perez-JiMénez *et al*., (2012). Also, values were slightly higher than those detected by Essid *et al*., (2015).

Furthermore, the mean of expected heterozygosity, obtained in the present study, was higher than observed heterozygosity. This might be due to the much more diverse genetic background within these genotypes (Liang *et al*., 2015). Gene diversity is a parameter which assumed as the fundamental genetic variability of a species or a population which act as a tool for stability of natural communities or ecosystem as well as increase productivity and invasion resistance (Urrestarazu *et al*., 2012 and Takahashi *et al*., 2018).

The highest polymorphic information content was 0.735 obtained with MFC4 locus while the lowest information content was 0.067 found at FinsQ5FAM-L locus. Both, the highest and lowest PIC were lower than PIC obtained by Baraket *et al*., (2011) and Saddoud *et al*., (2011). Further, the lowest *Fis* value was -0.8571(FinsI12FAM-L), while the highest *F*is was 1.0000 (FinsM5HEX-L, FinsP8NED-L, FinsJ10NED-L, FinsH5HEX-L, FinsA1NED-L, MFC3, MFC7, MFC6 and MFC8). The negative values of *F*is might refer to the similar distribution of migration and mutation to genetic variation in the material. It is also noteworthy that the presence of null alleles (F) in such kind of investigations, leads to higher *F*is values (Urrestarazu *et al*., 2012). In addition the negative *Fis* and *F* produced as a result of excess heterozygosity. The lowest and highest *P*-values were ranged between 0.0020 and 1.0000, respectively.

Additionally, 11 out of 20 SSR primers had *PIC* values higher than 0.5. PIC value depicts the richness of the SSR markers and their capability in detection of variability among genotypes depending on their genetic relationships (Kumari *et al*., 2018). The PIC values in the current study might indicate that these loci have a high polymorphism and could be exploited in genetic diversity analysis. Contrastingly, PIC values less than 0.5 indicate low polymorphism of the locus (Botstein *et al*., 1980). The presence of high polymorphism in SSR markers due to the unique mechanism responsible for generating SSR allelic diversity by replication slippage (Baraket *et al*., 2011). Fixation index values were ranged between -0.3022 (FinsI12FAM-L) and 1.000 (FinsH5HEX-L, MFC8, MFC5 and MFC3). Negative fixation index has been shown with seven SSR loci and positive fixation index found with 13 SSR markers. The presence of positive F value indicates an excess of observed homozygotes while the negative F value depicts an excess of observed heterozygotes (Ganopoulos *et al*., 2015).

Differences between studies might be due to the differences in sample size, differences in the type of genotypes, number of SSR loci used in each study as well as the differences in genetic diversity present within genotypes (Kumari *et al*., 2018).

The obtained SSR data where further analyzed to construct genetic distances among the selected genotypes. The lowest genetic distance was 0.0145 between rash, zard bahari, shoshi gawra and zard chawsor (Table2). This is indicate that they are genetically similar, have similar alleles and share the same common ancestor (Esselman *et al*., 2000). Thus, these genotypes might have some common morphological characters as well such as, leaf shape, fruit color, and fruit shape. In contrast, the highest genetic distance (0.2372) was found between rash and zard payazi, suggesting less similarity and have different alleles. Genetic distance information is useful for evaluation of the diversity at genetic level among genotypes which could aid and simplify the selection process in breeding program, preservation and introducing of new accessions before elimination of the redundant genotypes (Govindaraj *et al*., 2015).

The genetic distance results were further analyzed and used to construct phylogenetic relationships between the studied fig landraces implementing the NTSYS programme and UPGMA clustering method (Nei, 1972) as shown in (Figure 1). The results revealed that all 14 local varieties were clustered into seven main genetic clades namely; C1, C2, C3, C4, C5, C6 and C7. Within the fourth main genetic group two sub-clusters could be found, the first sub-cluster represented zard gawra, while the second sub-group represented rash and zard bahari genotypes. Grouping of genotypes in separate clusters usually relies on their evolutionary paths and their geographical distribution. Furthermore, such kind of classification and phylogeny, which depend

totally on the genetic background of the genotypes through stable genetic markers, are crucial to eliminate blind selection for the purpose of breeding program and/or preservation of types (Gregory, 2008).

4. CONCLUSIONS

In conclusion, it can be stated that SSR markers were successfully used for genotyping and for investigating a collection of local fig genotypes in this region. Also, the SSR markers were found to be reproducible, as well as to be very informative, useful and reliable tool to distinguish and discriminate between phenotypically and genetically related landraces.

Lastly, the estimation of genetic diversity and genetic relationships of landraces might assist to understand the genetic differentiation of these traditional genotypes in the region and to draw a smart delineation of these specific gene pools (genotypes).

Acknowledgements

This work was supported and funded by the Kurdistan Regional Government, Ministry of Higher Education and Scientific Research, University of Duhok, College of Science.

The author would like to thank Dr. Bestoon A. Gozeh and his family for their cooperation in collecting the studied samples.

Conflict of Interest

The author has no conflicts of interest to disclose.

Table (1) Results of SSR analysis, name of primer, number of alleles, major allele frequency, observed heterozygosity (Ho), expected heterozygosity (He), polymorphic information content (PIC), P-value, inbreeding coefficient (Fis) and fixation index (F).

locus	Sequence(5'-3')	Range of allele size(bp)	No. of alleles	Major. Allele Frequency	Ho	He	*PIC*	*p-value*	*Fis*	*F*(Null)
FinsK9HEX-L	F:ACGCACTTAACCCTTTCAG R:TTCGAGTCAACGAAACAAA	350-400	2	0.7857	0.429	0.349	0.280	1.0000	-0.238095	-0.1189
MFC2	F:GCTTCCGATGCTGCTCTTA R:TCGGAGACTTTTGTTCAAT	200-320	6	0.5357	0.357	0.685	0.629	0.0020	0.488189	0.3055
MFC1	F:ACTAGACTGAAAAAACATTG R:TGAGATTGAAAGGAAACGAG	250-420	2	0.7500	0.500	0.389	0.305	0.5010	-0.300000	-0.1423
FinsQ5FAM-L	F:CATGTCAGGAGGTGTCTAGG R:CTCCAAATGGGTATGTCAAG	200-350	2	0.9643	0.071	0.071	0.067	1.0000	-0.000000	-0.0094
MFC4	F:CCAAACTTTTAGATACAACTT R:TTTCTCAACATATTAACAGG	180-400	6	0.3571	0.714	0.796	0.735	ND	0.106529	-0.0169
FinsQ6HEX-L	F:TTCTCCAATTAAACCTCCAA R:CATGAAATCACCTTCCTCAT	110-400	7	0.5357	0.929	0.685	0.629	0.7310	-0.373984	-0.2331
FinsI12FAM-L	F:AGGTGGAATGAGGAGAGAGT R:AAACATCCTTTCTGGACTTG	190-280	2	0.5357	0.929	0.516	0.374	0.0070	-0.857143	-0.3022
FinsM5HEX-L	F:ATGAATGGTGAAATCCTGAA R:CATGGCCTCAACTTAGAAAC	185-200	3	0.5714	0.000	0.593	0.501	ND	1.000000	0.9999
FinsP8NED-L	F:TGAAGAAAACGGAGCTTG R:CTAAATCTGACGGTTCAAAA	160-190	4	0.5714	0.000	0.624	0.553	ND	1.000000	0.9999
FinsJ10NED-L	F:GAACCTTCAACCTCAATCAA R:CTCCCCTTTCCTAGTCCTTA	170-180	3	0.7143	0.000	0.466	0.406	ND	1.000000	0.9984
FinsT7HEX-L	F:GAATCTGGAGGTGGAATAAAC R:AAAGATCGCTCGTCAACC	180-400	3	0.5000	0.500	0.553	0.424	0.7840	0.099010	0.0343
FinsH5HEX-L	F:GACCGTATAGATGATTTGGG R:CATCCTGTGAACGACACTT	300-340	3	0.4286	0.000	0.667	0.567	ND	1.000000	1.0000
FinsA1NED-L	F:AATCCCCGTACTTCACTT R:AGAACTTATTGCACGGACAG	280-295	3	0.7143	0.000	0.466	0.406	ND	1.000000	0.9984
FinsN1HEX-L	F:AGGGCTGAGATAGGTTGATT R:TAAGTTGGTGTGTGGCATC	190-400	3	0.5000	1.000	0.638	0.541	0.0020	-0.603524	-0.2727
MFC3	F:GATATTTTCATGTTTAGTTTG R:GAGGATAGACCAACAACAAC	150-400	5	0.5000	0.571	0.675	0.598	0.0320	0.157895	0.0739
MFC7	F:CACAATCAAAATAGTTACCG R:AGCGAAGACAGTTACAAAGC	190-230	6	0.5714	0.000	0.656	0.605	ND	1.000000	1.0000
MFC6	F:AGGCTACTTCAGTGCTACA R:GCCATAAGTAATAAAAACC	340-345	2	0.7857	0.000	0.349	0.280	ND	1.000000	0.9901
MFC8	F:GTGGCGTCGTCTCTAATAAT R:TATTCTATGCTGTCTTATGTCA	230-250	4	0.7857	0.000	0.381	0.348	0.0020	1.000000	0.9933

MFC5	F:ACCAATCCTAATAATAATCC R:ACACGCTTACTAGAATTACC	150-190	3	0.4286	0.000	0.667	0.567	ND	1.000000	1.0000
FinsN3FAM-L	F:AAAACTTCTCCTCTGCTATTT R:TTTGCTTCTTCTCTGTTTGAC	150-190	4	0.3571	0.000	0.751	0.674	ND	1.000000	1.0000
Mean			3.65	0.5946	0.3	0.548	0.502			

Table (2) Genetic distance value obtained with SSR markers through selected samples for this study.

Sample	1	2	3	4	5	6	7	8	9	10	11	12	13	14
1	0.0000	0.0299	0.0774	0.0149	0.0443	0.0299	0.2002	0.0149	0.0443	0.0606	0.0299	0.0299	0.0451	0.1537
2	0.0299	0.0000	0.0774	0.0457	0.1069	0.0299	0.2002	0.0149	0.0443	0.0924	0.0924	0.0606	0.1086	0.1210
3	0.0774	0.0774	0.0000	0.0953	0.0919	0.0774	0.1489	0.0625	0.0919	0.1102	0.0774	0.0774	0.0937	0.1060
4	0.0149	0.0457	0.0953	0.0000	0.0602	0.0457	0.2230	0.0308	0.0602	0.0774	0.0457	0.0457	0.0614	0.1727
5	0.0443	0.1069	0.0919	0.0602	0.0000	0.0751	0.2147	0.0602	0.0896	0.0751	0.0145	0.0443	0.0293	0.2372
6	0.0299	0.0299	0.0774	0.0457	0.0751	0.0000	0.2002	0.0149	0.0443	0.0299	0.0606	0.0299	0.0606	0.1210
7	0.2002	0.2002	0.1489	0.2230	0.2147	0.2002	0.0000	0.1853	0.2147	0.2002	0.2002	0.2002	0.2189	0.1924
8	0.0149	0.0149	0.0625	0.0308	0.0602	0.0149	0.1853	0.0000	0.0602	0.0457	0.0457	0.0457	0.0614	0.1388
9	0.0443	0.0443	0.0919	0.0602	0.0896	0.0443	0.2147	0.0602	0.0000	0.1069	0.0751	0.0145	0.0751	0.1354
10	0.0606	0.0924	0.1102	0.0774	0.0751	0.0299	0.2002	0.0457	0.1069	0.0000	0.0606	0.0606	0.0606	0.1876
11	0.0299	0.0924	0.0774	0.0457	0.0145	0.0606	0.2002	0.0457	0.0751	0.0606	0.0000	0.0299	0.0148	0.2227
12	0.0299	0.0606	0.0774	0.0457	0.0443	0.0299	0.2002	0.0457	0.0145	0.0606	0.0299	0.0000	0.0299	0.1537
13	0.0451	0.1086	0.0937	0.0614	0.0293	0.0606	0.2189	0.0614	0.0751	0.0606	0.0148	0.0299	0.0000	0.2227
14	0.1537	0.1210	0.1060	0.1727	0.2372	0.1210	0.1924	0.1388	0.1354	0.1876	0.2227	0.1537	0.2227	0.0000

1= arzani, 2= Kongi doshawi, 3= Mamezi rash, 4= Mamezi shen, 5= rash, 6= rohani, 7= Rohani bahari, 8= shenk, 9= Shoshi qawra, 10= Taq taq, 11= Zard bahari, 12= Zard chawsor, 13= Zard gawra, 14= Zard payazi.

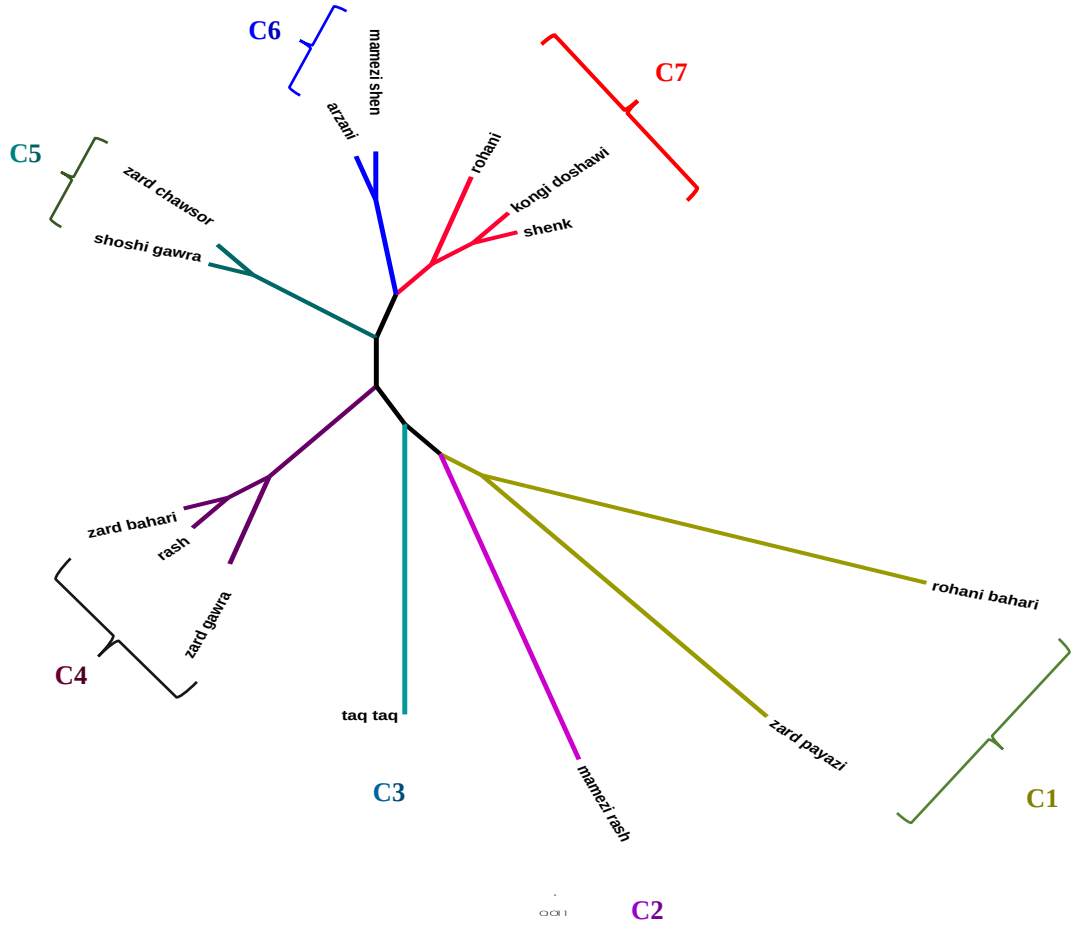

Figure (1) Phylogenetic relationships among 14 Fig genotypes based on SSR marker, using Power Marker V3.0, Fig Tree v.1.3.1, proportion of shared alleles and UPGMA clustering.

References

ACHTAK, H. O. A., ATER M., SANTONI S., KJELLBERG F. & KHADARI B. (2009). Microsatellite markers as reliable tools for fig cultivar identification. *American Journal of Horticulture Science*, 134, 624-631.

ALMAJALI D., ABDEL-GHANI A. & MIGDADI H. (2012). Evaluation of genetic diversity among Jordanian fig germplasm accessions by morphological traits and ISSR markers. *Scientia Horticulturae*, 147, 8-19.

BARAKET G., CHATTI K., SADDOUD O., ABDELKARIM A., MARS M., TRIFI M. & HANNACHI A. (2011). Comparative assessment of SSR and AFLP markers for evaluation of genetic diversity and conservation of fig (*Ficus carica* L.) genetic resources in Tunisia. *Plant Moleclar Biology Rep*orter, 29, 171-184.

BOTSTEIN D., WHITE R. L., SKOLNICK M. H. & DAVIS R.W. (1980). Construction of a genetic map in man using restriction fragment length polymorphisms. *American Journal of Human Geneti*, 32, 314-331.

CALISKAN O. A. A., POLAT P. C. & BAKIR M. (2012). Molecular characterization of autochthonous Turkish fig accessions. *Spanish Journal of Agricultural Research*, 10(1), 130-140.

CALISKAN O., BAYAZIT S., ILGIN M., KARATAS N. & ERGUL A. (2018). Genetic diversity and population structure in caprifigs (*Ficus carica* Var. caprificus) using SSR-markers. *Spanish Journal of Agricultural Research*, 16(3), 1-12.

CHATTI K. G. B. A. A., SADDOUD O., MARS M., TRIFI M. & SALHI HANNACHI A. (2010). Development of molecular toolls for characterization and genetic diversity analysis in

Tunisian fig (*Ficus carica*) cultivars. *Biochemical Genetics*, 48(9-10), 789-806.

ESSELMAN E. J., CRAWFORD D. J., BRAUNER S., STUESSY T. F., Anderson G. J. & SILVA O. M. (2000). RAPD marker diversity within and divergence among species of *Dendroseris* (*Asteraceae: Lactuceae*). *American Journal of Botany*, 87, 591–596.

ESSID A., ALJANE F., Ferchichi A. & HORMAZA J. I. (2015). Analysis of genetic diversity of Tunisian caprifig (*Ficus carica* L.) accessions using simple sequence repeat (SSR) markers. *Hereditas*, 152(1), 1-7.

GANOPOULOS I. A., XANTHOPULOU A., MOLASSIOTIS E., KARAGIANNIS T., MOYSIADIS P., KATSARIS F., ARAVANOPOULOS A., TSAFTARIS A., KALIVAS A. & MADESIS P. (2015). Mediterranean basin (*Ficus carica* L.) from genetic diversity and structure to authentication of protected designation of origion cultivar using microsatellite markers. *Trees*, 29(6), 1959-1971.

GIRALDO E. LOPEZ-CORRALES M. & JOSE IGNACIO HORMAZA J. I. (2010). Optimization of the management of an ex-situ germplasm bank in common fig with SSR. *American Journal of Horticulture Science*, 133, 69-77.

GUPTA P. K. & VARSHNEY K. (2000). The development and use of microsatellite markers for genetic analysis and plant breeding with the emphasis on bread wheat. *Euphytica*, 113, 163-185.

GREGORY T. R. (2008). Understanding Evolutionary Trees. Evo Edu Outreach. 1(2), 121-137.

IKEGAMI H. H., NOGATA K., HIRASHIMA M., AWAMURA & NAKAHARA T. (2008). Analysis of genetic diversity among European and Asian fig varieties (*Ficus carica* L.) using ISSR, RAPD and SSR markers. *Genetic Resources and Crop Evolution*, 56(2), 201-209.

IKEGAMI H., NOGATA H., HIRASHIMA K., MITSUO AWAMURA M. & NAKAHARA T. (2009). Analysis of genetic diversity among European and Asian fig varieties (*Ficus carica* L.) using ISSR, RAPD, and SSR markers. *Genetic Resources and Crop Evolution*, 56, 201-209.

IKEGAMI H., HABU T., MORI K., NOGATA H., HIRATA C., HIRASHIMA K., TASHIRO K. & KUHARA S. (2013). De novo sequencing and comparative analysis of expressed sequence tags from gynodioecious fig (*Ficus carica* L.) fruits: caprifig and common fig. *Tree Genetics and Genomes*, 9, 1075-1088.

KHADARI B., ATER M., MAMOUNI A., ROGER J. P. & KJELLBERG F. (2004). Molecular characterization of Moroccan fig germplasm using inter simple sequence repeat and simple sequence repeat markers to establish a reference collection. *Horticulture Science*, 40(1), 29-32.

LANSKY E. P., PAAVILAINEN H. M., PAWLUS A. D. & NEWMAN R. A. (2008). *Ficus spp*. (fig): ethnobotany and potential as anticancer and anti-inflammatory agents. *Journal of Ethnopharmacol*, 119, 195-213.

LAZREG-AREF H., Mars M., Fekih A., AOUNI M., SAID K. (2012). Chemical composition and antibacterial activity of a hexane extract of Tunisian caprifig latex from the unripe fruit of *Ficus carica*. *Pharmaceutical Biology*, 50, 407-412.

LIANG W., DONDINI L., FRANCESCHI P. D., PARIS R., SANSAVINI S. & TARTARIN S. (2015). Genetic diversity, population structure and construction of a core collection of apple cultivars from Italian germpalsm. *Plant Molecular Biology Reporter*, 33(3), 458-473.

NEI M. (1972). Genetic distance between populations. American National. 106, 283-292.

PEREZ- JIMENEZ M. L. B., DORADOo G., PUJADAS-SALVA A., GUZMAN G. & HERNANDEZ P. (2012). Analysis of genetic diversity of southern Spain fig tree (*Ficus carica* L.) and reference materials as a tool for breeding and conservation. *Hereditas*, (149(3), 108-113.

RAMBAUT A. FigTree v1.3.1: (2009). Tree figure drawing tool, available from http://treebiodauk/software/figtree/. Accessed 2012 March 23.

SADDOUD O., SALHI-HANNACHI A., CHATTIK-RHOUMA A., MARS M., MARRAKCHI M. & TRIFI M. (2005). Tunisian fig (*Ficus carica* L.) genetic diversity and cultivars identification mediated by microsatellites markers. *Fruits*, (60(2), 143-153.

SADDOUD O., CHATTI K., SALHI-HANNACHI A., MARS M., RHOUMA A., MARRAKCHI M. & TRIFI M. (2007). Genetic diversity of Tunisian figs (*Ficus carica* L.) as revealed by nuclear microsatellite. *Hereditas*, 144, 149-157.

SADDOUD O., BARKET G., CHATTI K., TRIFI M. MARRAKCHI M., MARS M. & SALHI-

HANNACHI A. (2011). Using morphological characters and simple sequence repeat (SSR) markers to characterize Tunisian fig (*Ficua carica* L.) cultivars. *Acta Biologica Cracoviensia Series Botanica*, 53, 7-14.

SUGIURA T., KUURODA H. & SUGIURA H. (2007). Influence of the current state of global warming on fruit tree growth in Japan. *Horticulture Research*, 6, 257-263.

TRICHOPOULOU A., VASILOPOULOU E., GEORGA K., SOUKARA S. & DILIS V. (2006). Traditional foods: why and how to sustain them. *Trends Food Science Technology*, 17, 498-504.

URRESTARAZU J., MIRANDA C., SANTESTEBAN L. G. & ROYO J. B. (2012). Genetic diversity and structure of local apple cultivars from northeastern Spain assessed by microsatellite markers. *Tree Genetics and Genomes*, 8, 1163- 1180.

VIGENS H., HOSSA M., BEAUNE D., FEVRE D., ANSTETT M. C., BORGES R. M., KJELLBERG F. & CHEVALLIER M. H. (2006). Development and characterization of microsatellite markers for a monoecious *Ficus species*, *Ficus insipida*, and cross-species amplification among different sections of Ficus. Molecular Ecology Notes, 6, 792-795.

WEIGAND F., BAUM M. and UDUPA S. (1993). DNA molecular marker technigues. ICARDA, Aleppo, Syria, 51, 1-10.

ZAVODNA M., ARENS P., VAN P. J. & VOSMAN B. (2005). Development and characterization of microsatellite markers for two dioecious *Ficus species*. *Molecular Ecology Notes*, 5, 355-357.

STAFINE E. T., CLARK J. R., WEBER C. A., GRAHAM J. & LEWERS K. S. (2005). Simple sequence repeat (SSR) markers for genetic mapping of raspberry and blackberry. *American Society for Horticulture Science*, 130(5), 1-7.

GOVINDARAIJ M., VETRIVENTHAN M. & SRINIVASAN M. (2015). Importance of genetic diversity assessment in crop plants and its recent advances: an overview of its analytical perspectives. *Genetics Research Internationa*, 2015, 1-14. Article ID 431487.

KUMARI A., SINHA S., RASHMI K., MANDAL S. S. & SAHAY S. (2018). Genetic diversity analysis in maize (*Zea mays* L.) using SSR markers. *Pharmacognosy and Phytochemistry* S PP. 1116-1120. E- ISSN: 2278-4136 P-ISSN: 2349-8234.

TAKAHASHI Y., TANAKA R., YAMAMOTO D., NORIYUKI S. & KAWATA M. (2018). Balanced genetic diversity improves population fitness. Proceeding Royal Society B. 285, 1-17. http://dx.doi.org/10.1098/rspb.2017.2045.

ZANCO Journal of Pure and Applied Sciences
The official scientific journal of Salahaddin University-Erbil
https://zancojournals.su.edu.krd/index.php/JPAS

ISSN (print):2218-0230**, ISSN (online):** 2412-3986**, DOI: http://dx.doi.org/10.21271/zjpas**

RESEARCH PAPER

Algae as indicator to assess trophic status in Dokan Lake, Kurdistan region of Iraq.

Janan Jabbar Toma

Department of Environmental science, College of Science, Salahaddin University - Erbil, Iraq., Malaysia

A B S T R A C T:

This survey was related to study the algal status of Dokan Lake to evaluate the trophic status of lake productivity. Data for application of phytoplankton compound quotient (PCQ) equations and dominant genus scores were collected from previous studies for Dokan lake periods during 1980, 2000 and 2016. A total of 101,61and 135 respectively algal taxa which have into 6 taxonomic groups were determined. From phytoplankton content in this survey, it seems that among diatom species ***Cyclotella ocellata***, ***Stephanodiscus astrea***, ***Nitzschia* spp** and ***Navicula* spp** were the most common taxa in this survey. On the other side, non-diatom species in this search were to be dominanated by Pyrophyta in especially in warm months such as ***Ceratium hirundinella*** and ***Peridium cinctum***. Ecological status of the Dokan Lake was mesotrophic in 1980 and 2000 while in 2016 was hypertrophic according to phytoplankton compound quotient (PCQ=4.5, 2.8 and 8.0) respectively. As a result of dominant genus scores (3.8, 4.2 and 6.5), the lake has a mesotrophic character according to trophic level in 1980 and 2000, and was meso-eutrophic in 2016. In addition, the water quality of Dokan Lake was moderate in 1980 and 2000 and moderate polluted in 2016.

KEY WORDS: Algae, Trophic, Status, Dokan, Lake.
DOI: http://dx.doi.org/10.21271/ZJPAS.31.2.8
ZJPAS (2019) , 31(2);57-64 .

INTRODUCTION:

Algae play an important role for assess quality of water system. Algae are significant indicators of water environment since they response to both qualitative and quantitative composition of species in a wide range of water situations due to change in chemistry of water such as increases contamination depend on different wastes and affect the content of genus that are able to tolerate these condition(Bergström, 2010).

Algal abundance in a water system reflects the main ecological condition and, then, it may be used as an indicator of quality of water system (Saha et al. 2000). Pressure of population, urbanization, industrialization and increased activity of agriculture have importantly contribution to the contamination of aquatic systems. Continuous monitoring of the quality of aquatic ecosystems is one of the best protect method, using organisms for monitoring of water environmental is the most popular topic for the scientific community (Tokatli, 2013).

* **Corresponding Author:**
Janan Jabbar Toma E-mail:
janan.toma@su.edu.krd
Article History:
Received:14/11/2018
Accepted:26/02/2019
Published: 23/04/2019

The trophic status means to the value of productivity in a Lakes as calculated by phosphorus, algal composition, and the distance light penetration in depth of lakes. Trophic status in clean standing water depend on amount of biological productivity happing in the water (Chandrashekar *et al*., 2014). Increase primary productivity is not necessary means of poor condition as it is natural for Lakes to change from low to high trophic states but this is a slow process (Sullivan and Reynolds, 2004). Early recognition of various in the quantity and quality of phytoplankton in lakes play role to determine the origin of the trophic status of lake classification. The trophic system has continued to evolve and at the same time, there have been developments in the recognition of plankton types. These have been mainly concerned with the phytoplankton and include the use of a different of indices and quotients. This field has been developed mainly by European workers with, as yet, little application to the waters of North America (Chandrashekar et al., 2014). The objectives of this investigation were to evaluate the trophic status of Dokan Lake at different period and to determine the productivity of lakes by comparing the results of PCQ and dominant genius.

2. MATERIALS AND METHODS

2.1 Data collection

Application algae for phytoplankton compound quotient (PCQ) equations and dominant genus scores were collected from previous published studies for Dokan Lake (Shaban, 1980; Toma, 2000 and Farkha & Fatah, 2016).

2.2 Study area

The Dokan Dam constructed in Dokan district in the Lesser Zab River for concrete arch dam in Sulaymaniyah Governorate, Iraq (latitude: 35º 57′ 15″ N; longitude: 44º 57′ 10″ E). The dam was built from 1954 to 1959 as a multi-purpose dam for storage of water, irrigation and electricity production. It is 116.5m height and can withhold 6,970,000,000 m3 of water. The catchment area is 11,690 km2 and surface area is about 270 km2 (Goran, 2014) (Figure 1). This survey explains the content of phytoplankton as well as determining the environmental status of the lake .Ecological status of the lake depending to the phytoplankton compound quotient (PCQ) was calculated in the manner as proposed by (Nygaard G.1949) and (Ott and Laugaste, 1996) and arranged by Nygaard. PCQ gives quite good determination to lake trophic state, although algal groups in formula may contain species with various preferences to trophic conditions. Moreover, (Ott and Laugaste, 1996), added to the original formula 2 extra division: Cryptophyta to numerator and Chrysophyceae to denominator.

PCQ=Cyanophyta*+Chlorophyceae*+ Centrales*+Euglenophyceae*+Cryptophyta* +1/ Desmidiales*+Chrysophyceae*+1

Where * is the number of different species.

Ecological status of the Dokan Lake estimated depending on planktonic algae content and the phytoplankton compound quotient (PCQ). PCQ was used to determine the ecological status of the lake (Table 1). Many researchers suggested the idea that the proportion of number of species of the groups existing in the phytoplankton with one another (Nygaard, 1949; Thunmark, 1945 and Hutchinson, 1967) indicates the efficiency of the lake. Among those proportions the coefficient proposed by (Nygaard, 1949) was applied more frequently. This index is one that is best useful for explaining the trophic degree of a lake. Nygaard's compound index was modified by (Ott and Laugaste, 1996).The trophic status and PCQ values of the lakes have been indicated in Table (1).

Table 1. Ecological status of the Dokan Lake according to the phytoplankton compound quotient (PCQ) (Ott and Laugaste, 1996)

Lake status	PCQ	Lake status	PCQ
Oligotrophic	< 2	Eutrophic	5-7
Mesotrophic	2-5	Hypertrophic	>7

Species composition of the phytoplankton community is a good bioindicators for water quality (Peerapornpisal *et al*, 2007). In this study, the diversion of phytoplankton was studied and the water quality was determined based on the physical and chemical properties.

In Table (2), list of dominant genus and in Table (3) the ranges in determining the trophic structure of the lake and water quality according to dominant genus have been given.
In determining the trophic status, several criteria are used in terms of nutrient concentration, species combination of phytoplankton, fauna and flora quantity and quality. And the differences that may arise in determining the trophy levels of the lakes among them are analyzed looking through several parameters. Trophic status brings a new approach to trophic restriction of lakes. PCQ (Ott and Laugaste, 1996) and dominant genus (Peerapornpisal *et al*, 2007) were used in order to determine trophy.

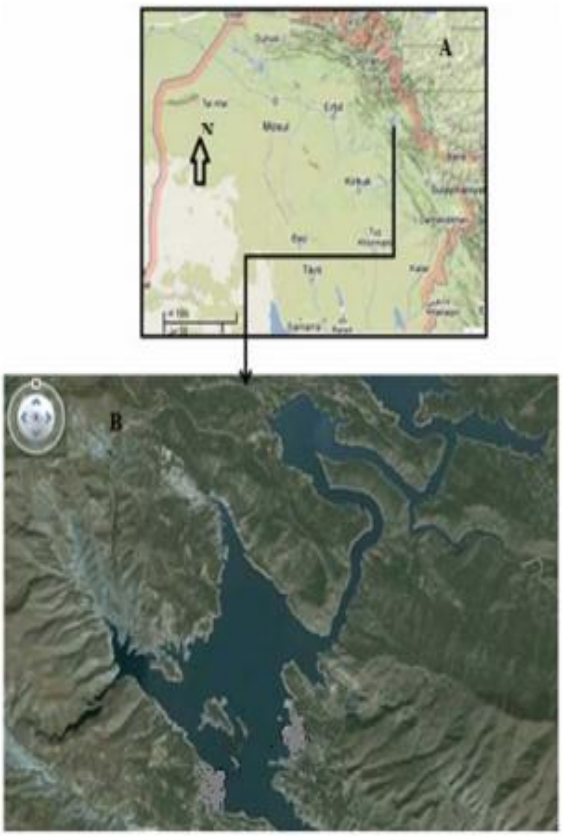

Figure (1):- A- Map of Northern Iraq show Dokan Lake. B- Map of Dokan Lake

Table 2. List of dominant genus scores of Dokan Lake according to (Peerapornpisal *et al*, 2007)

Genus	Score	Genus	Score
Actinastrum	5	Gymnodinium	**6**
Acanthoceras	5	Gyrosigma	**7**
Amphora	6	Isthmochloron	**5**
Anabaena	8	Kirchneriella	**5**
Ankistrodesmus	7	Melosiera	**5**
Aphanocapsa	5	Merismopedia	**9**
Aphanothece	5	Micractinium	**7**
Aulacoseira	6	Micrasterias	**2**
Bacillaria	7	Microcystis	**8**
Botryococcus	4	Monoraphidium	**7**
Centritractus	4	Navicula	**5**
Ceratium	4	Nephrocytium	**5**
Chlamydomonas	6	Nitzschia	9
Chlorella	6	Oocystis	6
Chroococcus	6	Oscillatoria	9
Closterium	6	Pandorina	6
Cocconeis	6	Pediastrum	7
Coelastrum	7	Peridiniopsis	6
Cosmarium	2	Peridinium	6
Crucigenia	7	Phacus	8
Crucigeniella	7	Phormidium	9
Cryptomonas	8	Pinnularia	5
Cyclotella	2	Planktolyngbya	7
Cylindrospermopsis	7	Pseudanabaena	7
Cymbella	5	Rhizosolenia	6
Dictyosphaerium	7	Rhodomonas	8
Dimorphococcus	7	Rhopalodia	5
Dinobryon	1	Scenedesmus	8
Encyonema	6	Staurastrum	3
Epithemia	6	Staurodesmus	3
Euastrum	3	Stauroneis	5
Eudorina	6	Strombomonas	8
Euglena	10	Surirella	6
Eunotia	2	Synedra	6
Fragilaria	5	Tetraedron	6
Golenkinia	5	Trachelomonas	8
Gomphonema	6	Volvox	6
Gonium	6		

Table 3. Water quality scores followed trophic level and general water quality of Dokan Lake (Peerapornpisal *et al*, 2007)

Score	Water quality by trophic level	General water quality
1.0 – 2.0	Oligotrophic status	Clean
2.1 – 3.5	Oligo-mesotrophic status	Clean-moderate
3.6 – 5.5	Mesotrophic status	Moderate
5.6 – 7.5	Meso-eutrophic status	Moderate-polluted
7.6 – 9.0	Eutrophic	Polluted
9.1 – 10	Hypereutrophic status	Very polluted

3. RESULTS AND DISCUSSION

The phytoplankton composition of Dokan Lake in previous studied during 1980, 2000 and 2016,. A total of 101, 61 and 135 algal taxa which have into 6 taxonomic groups were determined respectively. The range of taxonomic groups from the most rich in species to less species, were Bacillariophyta were dominant ranged from (55-68%), Chlorophyta varied by (14-23%), While Cyanophyta ranged between (8-14%) then, Chrysophyta and Pyrophyta changed from (1-5%), finally Euglenophyta fluctuated from(1 to 3%) respectively of Dokan Lake are given in figure 2, 3 and 4 .

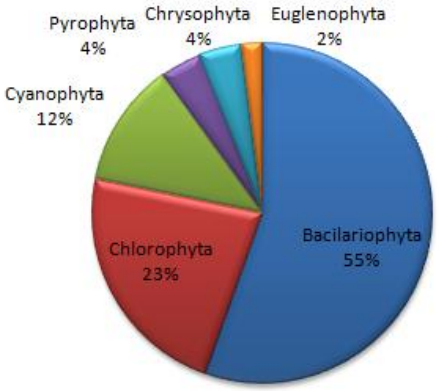

Fig. 2:- Distribution of the phytoplankton species for each division collected from Dokan in 1980 (Shaban, 1980)

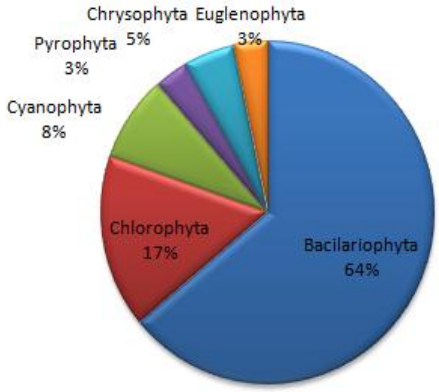

Fig. 3:- Distribution of the phytoplankton species for each division collected from Dokan Lake in 2000 (Toma, 2000)

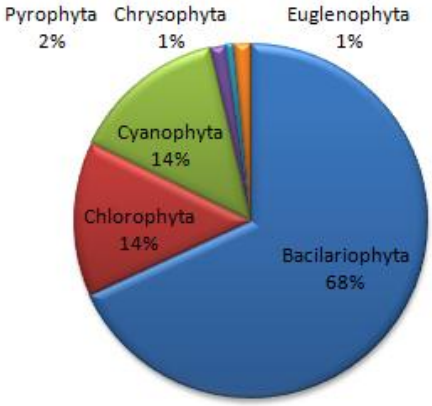

Fig. 4:- Distribution of the phytoplankton species for each division collected from Dokan Lake in 2016 (Farkha & Fatah, 2016)

The list of planktonic Algae dominant seasonally in Dokan Lake is given in Table 4. Looking the species frequently present in mesotrophic and Eutrophic character lakes have been recorded in previous studies of Dokan Lake (1980, 2000 and 2016).

Table 4:- Dominant genius recorded at different seasons in Dokan Lake (Shaban, 1980; Toma, 2000 and Farkha & Fatah, 2016)

Dokan(1980)	Dokan(2000)	Dokan(2016)
Cyclotella	Cyclotella	Oscillatoria

Stephanodiscus	Stephanodiscus	Navicula
Synedra sp	Pediastrum	Nitzschia
Ceratium	Ceratium	Fragilaria
Peridinium	Peridinium	Cymbella
		Gomphonema

Algal species are good indicators of water quality and any changes in environment (Patrick, 1977 and Dixit *et al*, 1992). The content of phytoplankton is uses to determine the trophic status, productivity rate, nutrient level, quality of water and rate of pollution in lakes (Reynolds, 1998). ***Ceratium hirundinella***, ***Dinobryon divergens***, ***Cosmarium* spp**, ***Pediastrum* spp**. examples of the algae are among the algal bio-indicators recorded in summer months observed in Dokan Lake from previous studies (Reynolds, 1990). ***Ceratium hirundinella*** and ***Peridinium cinctum*** among Pyrophyta are the algae dominant in hot season in Dokan Lake (Shaban, 1980 and Toma, 2000). ***C. hirundinella*** is the estimated of mesotrophic waters and they are usually common in the summer in oligotrophic and mesotrophic lakes (Eloranta, 1995 and Reynolds et al, 2002), the mass occurrence of this species has been noted in spring (Noges, 1998) and in summer in a mesotrophic lake (Huszar *et al*, 2003) and a shallow eutrophic lake (Gligora, et *al*, 2003). Another Pyrophyta, such as ***Peridinium cinctum*** has been recorded intensely in the hot months, also this species exists in mesotrophic lakes as well (Reynolds et al, 2002). Among Chrysophyta, ***Dinobryon divergens*** and ***D. sertularia*** are identified in Dokan Lake by (Shaban, 1980; Toma, 2000 and Farkha & Fatah, 2016). One or more than one studies in the same year by the same authors by (Kristiansen, 2005) had appeared that the presence of a few species such as **Dinobryon** may indicate oligotrophic, but high Chrysophyta species variance at lower overall biomass is more indicate of eutrophic conditions. The large biomass of **Dinobryon** was noted in spring in a mesotrophic lake (Laugaste et al, 1996) and in November in a Meso-eutrophic lake (Naselli-Flores and Barone, 2000). Among the Pyrophyta, ***C. hirundinella*** and golden-green algae **Dinobryon sp**. was recorded as dominant in Meso-eutrophic Lake Dokan in summer months (Zębek, 2009). Species of ***Cyclotella ocellata*** and ***Stephanodiscus astrea*** identified in Dokan lake and they are more dominant than species the others (Shaban, 1980; Toma, 2000 and Farkha & Fatah, 2016). (Reynolds, 1993) stated that some species were affected by ecological factors specially temperature, therefore species that come into prominence in winter and spring seasons was **Cyclotella** species. **Cyclotella** and **Stephanodiscus** species are recognized by many of the researchers as typical components of mesotrophic lakes (Trifonova, 1998 and Moss, 1998). According to (Round, 1956), **Cyclotella** and **Stephanodiscus** species are bio-monitor species in transition to eutrophic. (Reynolds (1990) stated that in midsummer ***Cyclotella ocellata***, ***Stephanodiscus astrea***, ***Ceratium hirundinella***, ***Dinobryon divergens*** were mesotrophic species Cyanophyta, especially ***Oscillatoria* sp** was found to be most frequent algae in many sites in Dokan lake by (Farkha & Fatah, 2016). (Fattah, 2010; Wu and Suen, 1985) concluded that ***Oscillatoria* sp**. was found in organic polluted water. Most of algal taxa disappear during rainy season may be due to high water turbidity and suspended solids (Fattah, 2010; Wu and Suen, 1985). Similar conclusion was made in Dokan Lake (Farkha & Fatah, 2016). A total of 92 diatoms were identified by (Farkha & Fatah, 2016) they belong to 24 genus in Dokan Lake; Pinnate diatoms make up almost all of the main bulk of Bacillariophyta. In most aquatic ecosystems bacillariophyceae species community, diatoms density, diversity and their association with environmental variables used as biological indicators for the assessment of water quality (Singh, et al, 2010). Many local and global survey concluded that lake phytoplankton were dominated by Bacillariophyta species (Soylu, and Gonulol, 2003; Al-Nakshabandi, 2002 and Fattah, 2010) this dominancy is related to that diatoms tolerate broad range of light, temperature and other ecological factors. The most common and diverse genera that identified by (Farkha & Fatah, 2016) in Dokan lake were **Nitzschia**, **Navicula**,

Gomphonema, Fragilaria, Cymbella these genera considered calcareous and were rich in studied water bodies due to the geological nature of the studied area and high CaCO3 content, these results were in agreement with the result obtained by (Fattah, 2010; Celekli and Kulkoyluoglu, 2007). **Nitzschia and Navicula** were the most represented genera at all studied sites in Dokan lake because of their wide environmental condition tolerance range (Fattah, 2010).

Ecological status of the Dokan Lake during 1980, 2000 and 2016 according to the phytoplankton compound quotient (PCQ) (Ott and Laugaste 1996. PCQ value was calculated as 4.5, 2.8 and 8 respectively. According to this trophic status of Dokan Lake is mesotrophic 1980 and 2000, while was Hypereutrophic in 2016. Algal species are excellent indicators of water quality and environmental change (Patrick, 1948 and Dixit *et al,*1992). Algae as indicators are used for assessment quality of water and trophic level of water. In this investigation, the important species among Dokan Lake planktonic algae which are recorded as dominant were given in (Table 5). The water quality and trophic level of Dokan Lake were determined depending to dominant genus scores (Peerapornpisal, *et al*, 2007) . The dominant genus score and phytoplankton compound quotient (PCQ) obtained was 3.8, 4.2 and 6.5 and 4.5, 2.8 and 8 in Dokan lake during years 1980, 2000 and 2016 respectively which exist widespread in mesotrophic lakes were the dominant taxon through this study. Ecological status of the Dokan Lake was Mesotrophic in years 1980 and 2000 while changed to Hypereutrophic according to the phytoplankton compound quotient and trophic (Table 6). Since this value is included in the range of 3.6–5.5, trophic level of Dokan Lake is "mesotrophic" and moderate water quality in 1980 and 2000 and Hypereutrophic and moderate polluted in 2016 depending ontable (3).

Table 5:- Dominant genera and scores in the Dokan Lake during 1980, 2000 and 2016

Genus	Score	Genus	Score
Cyclotella	2	Peridinium	6
Stephanodiscus	1	Oscillatoria	9
Synedra sp	6	Navicula	5
Ceratium	4	Nitzschia	9
Fragilaria	5	Cymbella	5
Gomphonema	6		

Table 6:- phytoplankton compound quotient (PCQ) and dominant genus score in Dokan Lake during 1980, 2000 and 2016

Dokan lake	PCQ	Dokan lake	dominant genus score
1980	4.5	1980	3.8
2000	2.8	2000	4.2
2016	8	2016	6.5

4. CONCLUSIONS:

The trophic structure of Dokan Lake varied depending on the structure of phytoplankton community and species dominancy as well as others environmental factors. ***Ceratium hirundinella*** and ***Peridium cinctum*** that belong to Pyrophyta, and ***Dinobryon divergens*** and ***D. sertularia*** that belong to Chrysophyceae

level of Dokan Lake is "mesotrophic" and moderate water quality in 1980 and 2000, Hypereutrophic and moderate polluted in 2016 depending according to PCQ and dominant genus scores.

REFERENCES

Al-Nakshabandi, I.Y.R.2002. "A Phycolimnological study on Duhok impoundment and its main watershed". Ph.D. Thesis, University of Duhok.

Bergström, A.K. The 2010. Use of TNDZTP and DINDZTP ratios as indicators for phytoplankton nutrient limitation in oligotrophic lakes affected by N deposition. *J of Aquatic Sciences*. 27:277-281.

Celekli, A. and Kulkoyluoglu, O.2007. "On the Relationship between Ecology and Phytoplankton Composition in a Karstic Spring (Cepni, Bolu)". *Ecological Indicators.* Vol. (7), pp. 497-503.

Chandrashekar, C., K.V. Lokesh, H. Pushpa and G. Ranganna. 2014. Studies on the assessment of

trophic status of Lakes. *Inter. J. of Current Microbio. and. Appl. Sci.* 3(6): 245-254.

Dixit S.S; Smol. J.P; Kingston, J.C and Charles, D.F.1992. Diatoms-Powerful indicators of environmental change. *Environ Sci Tech*. 26:22−33.

Eloranta, P.1995. Phytoplankton of the national park lakes in central and southern Finland. Ann Bot. Fenn .32:193−209.

Farkha, T.K& Fatah, A. O. 2016. A Phytoplankton Distribution study of Dukan basin in Sulaimani district -Kurdistan Region of Iraq. *Journal of Zanco Sulaimani*. 18-2: 1-10.

Fattah, A.O.2010. "Phycolimnological study on Khabour River". M.Sc. Thesis. University of Duhok-Duhok, Iraq.

Gligora, M; Plenkovic-Moraj, A and Ternjej I.2003. Seasonal distribution and morphological changes of Ceratium hirundinella in two Mediterranean shallow lakes. Hydrobiology .506-509:213−220

Goran, S. M. A. 2014. Ecological study on Dukan Lake with particular reference to bioaccumulation of some heavy metals and PAHs in fish and Gull tissues. Ph.D. Dissertation. Salahaddin University, Erbil- Iraq.

Huszar, V; Kruk, C and Caracao, N.2003. Steady-state assemblages at phytoplankton in four temperate lakes (NE USA). *Hydrobiologia* .502:97−109.

Hutchinson, G.E. A.1967. Treatise on limnology, 2nd ed., Introduction to lake biology and the limn plankton, New York.

Kristiansen, J.2005. Golden algae: A biology of Chrysophytes, Koeltz Scientific Books, Germany.

Laugaste, R; Jastremskij, VV and Ott I. 1996. Phytoplankton of Lake Peipsi-Pihkva: species composition, biomass and seasonal Dynamics. *Hydrobiology* .338:49−62.

Moss B.1998. Ecology of freshwater: man and medium, past to future. Blackwell Science Ltd, Oxford.

Naselli-Flores, L and Barone, R. 2000.Phytoplankton dynamics and structure: a comparative analysis in natural and man-made water bodies of different trophic state. *Hydrobiology* .438:65−74.

Noges, P.1998.Laugaste R. Seasonal and long-term changes in phytoplankton of Lake Vortsjarv, Limnologica .28:21−28.

Nygaard G.1949. Hydrobiological studies on some Danish ponds and lakes. Part 2. The quotient hypothesis and some new or little known phytoplankton organisms. Det Kong Danske Vidensk Selskab, *Biol Skr* 1949; 7:1−293.

Ott, I and Laugaste, R. 1996.Futoplanktoni koondindeks (FKI). Uldistus Eesti väikejärvede kohta, Eesti Keskkonnaministeeriumi Infoleht nr. 3, 1996. [The phytoplankton compound quotient (PCQ), generalisation about Estonian small lakes. In Estonian].

Palmer, C.M. 1969.A Composite rating of algae tolerating organic pollution. *J Phycol* .5:78−82.

Patrick R. 1948.Factors effecting the distribution of diatoms. Bot. Rev.14:473−524.

Patrick R.1977. Ecology of freshwater diatoms and diatom communities, In: Dietrich Werner (Ed.), the biology of diatoms, University of California Press, Berkeley, 284–332.

Peerapornpisal, Y; Pekkoh, J; Powangprasit, D; Tonkhamdee, T; Hongsirichat, A and Kunpradid T.2007. Assessment of water quality in standing water by using dominant phytoplankton (AARL-PP Score). *J Fish Technol Resh* 2007; 1:71−81

Reynolds C.S; Huszar, V; Kruk, C; Naselli-Flores, L and Melo, S.2002. Review towards a functional classification of the freshwater phytoplankton. *J Plankton Res* .24:417−428.

Reynolds CS. 1998. What factors influence the species composition of phytoplankton in lakes of different trophic status. *Hydrobiol*; 369:11−26.

Reynolds CS.1990. Temporal scales of variability in pelagic environments and the response of phytoplankton. *Freshwater Biol* .23:25−53.

Reynolds, C.S. 1993.Scales of disturbance and their role in plankton ecology. *Hydrobiol* .249:157−171

Round, F.E. 1956.The phytoplankton of three water supply reservoirs in Central Wales. Arc F *Hydrobiology* 1956; 52:457−469.

Saha, S.B, Bhattacharya, S.B, Chaudhary, A., 2000, Diversity of phytoplankton of sewage pollution brackish water Tidal ecosystems. **Environ. Biol**., 21, 9-14.

Shaban, A.A.G. (1980)An ecological study on phytoplankton in Dokan lake. M.Sc. Thesis, Univ. of Sulaimaniyah.

Singh, M.; Lodha, P and Singh, G. P. 2010. "Seasonal diatom variations with reference to physico-chemical properties of water Mansagar lake of Jaipur, Rajisthan". *Research Journal of Agriculture Science*. Vol. (1), No. 4, pp. 451-457.

Soylu, E. N. and Gonulol, A. 2003."Phytoplanktons and Seasonal Variations of the River Yesilrmark, Amasya, Turkey". *Turkish Journal of Fisheries and Aquatic Sciences*. Vol. (3), pp. 17-24.

Sullivan, P. E. and C. S. Reynolds. 2004. The Lakes handbook: Limnology and limnetic ecology. Blackwell Publishing Company. 699pp.

Thunmark, S. 1945. Zur sociologic des susswasser planktons. Eine methodologisch-okologische studied. Folia Limnologica Scandinavica, 3.

Tokatli, C., 2013, Evaulation of Water Quality By Using Trophic Diatom Index: Example of Porsuk Dam Lake. *Journal Applied Biological Sciences*, 7 (1), 01-04.

Toma, J. J. 2000. "Limnological study of Dokan Lake, Kurdistan region, Iraq".M.Scs. Thesis, University of Salahaddin – Erbil.

Trifonova, I.S.1998. Phytoplankton composition and biomass structure in relation to trophic gradient in some temperate and subarctic lakes of north-western Russia and the Prebaltic. *Hydrobiology* .369/370:99−108.

Wu, J. T. and Suen, W. C.1985. "Change of Algal Association in Relation to Water Pollution". *Botanical Bulletin Academia Sinica*. Vol. 26, pp. 203-212.

Zębek, E.2009. Seasonal changes in net phytoplankton in two lakes with differing morphometry and trophic status (northeast Poland). *Arch. Pol. Fish* 2009; 17:267−278.

ZANCO Journal of Pure and Applied Sciences
The official scientific journal of Salahaddin University-Erbil
https://zancojournals.su.edu.krd/index.php/JPAS

ISSN (print):2218-0230**, ISSN (online):** 2412-3986**, DOI: http://dx.doi.org/10.21271/zjpas**

RESEARCH PAPER

Phytotoxicity of sewagewater and leachate of solid waste on seed germination and seedling growth of *Vicia faba* L. (Faba bean).

*Yahya A. Shakha, Pakhshan M. Maulood[1], Zhyan A. Sadraddin, Madina H. Khalifa
Department of Environmental Sciences, College of Science, Salahaddin University - Erbil, Iraq.
[1]Department of Biology, College of Science, Salahaddin University - Erbil, Kurdistan Region, Erbil- Iraq

A B S T R A C T:
The present study was conducted in greenhouse of Science College during January to April 2017 in order to evaluate the effect of sewagewater and solid waste leachate used for irrigation on some vegetative growth and seed germination of Faba bean (*Vicia faba* L.) plant. The results showed that pH values of sewagewater was near neutrality while leachate was in acid side of neutrality. Electrical conductivity (EC) of leachate pass 8000 µS.cm^{-1}. In most vegetative growth characters of Faba bean plant (Plant height, root dry weight, numbers of flowers, legumes and nodules) the sewagewater treatment record the high values in compared to control treatment. On the other hand, leachate treatments had very harmful effect on plant vegetative growths with lowest value in most variables (except chlorophyll content) with significant differences ($P \leq 0.05$) between it, especially at the last months of growth the bean plant of leachate treatment exposed to wilting and dead with zero values recorded for many studied variables (root dry weight and numbers of legumes and nodules). Same results were obtain for seed germination assay irrigated by leachate with lowest germination rate and highest inhibition of germination.

KEY WORDS: Phytotoxicity , seed germination , sewagewater, leachate, faba bean.
DOI: http://dx.doi.org/10.21271/ZJPAS.31.2.9
ZJPAS (2019) , 31(2);65-70 .

INTRODUCTION :

Legumes, or pulses, are flowering plants in the Leguminosae family (also known as Fabaceae [Taiz and Zeiger, 2006; Morris, 2003]. Legumes are popular in agriculture for their characteristics in enriching the soil, requiring little fertilizer nitrogen [Caldwell and Grant, 1968]. Faba bean (*Vicia faba* L.) is an important winter pulse crop and green manure legume [Hirich *et al*., 2014; Hirich *et al*., 2012; Ismaiel *et al*., 2014]. The nutritional content make it a good source of protein (more than 25% in dried seed), starch, cellulose, minerals and vitamin C [Duc, 1997].

* **Corresponding Author:**
Yahya A. Shekha
E-mail: yahya.shekha@su.edu.krd or yahyanian@gmail.com
Article History:
Received: 10/04/2018
Accepted: 06/03/2019
Published: 23/04/2019

materials and plant nutrient (N, Ca, Cu, Mn and Zn) are finding agricultural use as a cheap way of disposal, especially in arid and semi-arid areas that originally suffer from shortage of freshwater resources [Taiz and Zeiger, 2006]. Use of domestic wastewater in irrigation of crops and vegetables as a valuable water resource and alternative source to chemical fertilizers [FAO, 1992]. In spite of, these advantage many reports referred to using domestic wastewater can cause several environmental problems such as soil sickness, soil and groundwater contamination and phytotoxicity [Caldwell and Grant, 1968].
Sewage adversely affects many crops such as radish during maturity stage and as a result the production decreases substantially [Mapanda *et al*., 2005]. Ahmad *et al*. [2011] observed during their investigation that sewagewater have inhibition effect on chemical soil properties, seed

germination and growth characteristic of different crops.

Accumulated solid wastes create a major source of contamination for environment [Shekha, 2013; Shekha *et al*., 2017]. Management of municipal solid waste (MSW) in non-engineered landfills can't prevent toxic constituents extracted from leachate to causes potential health hazard to living organisms as a result of surface and groundwater pollution [Turki and Bouzid, 2017; Li *et al*., 2017]. Leachate is a complex mixture loaded with organic matter, inorganic compounds, heavy metals, and other toxicant generated from physical, chemical, and biological decomposition of MSW [McBean *et al*., 1995]. Phytotoxicity of landfill leachate have been assessed for several tested plants. [Chaingnon and Hissinger, 2003; Srivastava et al., 2005] attention to use seed germination and root elongation for many plants in eco-toxicity assessment. Vishnoi *et al*. [2013] mentioned to increasing toxicity of heavy metals in soil solution intake by cultivated plants in soils polluted by leachate. Li *et al*. [2017] found the inhibitory effects of leachate on both seed germination and seedling growth of some tested plants. Turki and Bouzid [2017] observed better grow of four tested plants irrigated by leachate than those received only water. On the other hand, high doses of leachate causes inhibition growth and reduction of chlorophyll content in *Vicia faba* was recorded during study conducted by [Gupta and Rajamani**,** 2015].

The aim of the present study is to evaluate the effects of both sewagewater and leachate on some growth and seed germination characteristics of *Vicia faba* L. plant.

2.MATERIALS AND METHODS

2. 1. Sample collection and analysis

The study was conducted in the green house of Science College, Salahaddin University-Erbil during December to April 2017. The experiment was design as a completely randomized design with three replicates. The soil was packed in plastic pots (7 kg capacity) at a rate of 5 kg. Seeds of Faba bean (4 seeds) were cultivated for each pots. Soil pots were irrigated with treatments (T1: Distilled water as a control, T2: Tap water, T3: Domestic sewagewater, and T4: Leachate of solid waste).

After more than 70 days from started experiment, plant growth was measured. Chlorophyll *a* content was measured by using (At leaf, V40) in three plant leaves for each replication. The harvested plants were oven dried at 65°C for 48hrs. and immediately dry weight was obtained. Wet digestion with H_2SO_4 and H_2O_2 for dried plant material was performed. Potassium and sodium was measured from digested samples by using flame photometer; phosphorus by colorimetric method, while nitrogen determined by kjeldahl procedure [Ryan *et al*., 2001].

2.2. Seed germination experiment:

Faba bean seeds washed with tap water and presoaked in distilled water for 10hrs. surface sterilization conducted by 10% sodium hypochlorite for ten minutes then washed extensively with sterilized distilled water. Ten seeds with three replication for each treatments were arranged in Petri dish on two filter papers. Ten milliliters of each treatment solutions were added, and incubated at 25°C. for first 5 days germinated seeds were counted and after 15 days PL and RL measurements were recorded [El-Ghamery & Basuoni, 2015].

2.3. Domestic wastewater analysis:

Sewagewater samples were collected from Erbil sewage channel near Sarkars road of Makhmur. While leachate was collected from garbage car in landfill. Sampling and analysis are carried out for each of the different water types used for irrigating the crops during the course of the experiment. Water collected in 2000 ml polythene bottles and transported immediately for laboratory analysis. pH and electrical conductivity (EC) of all water and leachates samples were measured by using pH meter (OAKTON, pH 2100 Series) and EC meter (WTW D 8120) respectively as described by [APHA, 1998].

2.4. Statistical analysis:

One way analysis of variance (ANOVA) was subjected for treatments by using SPSS 22, means were compared using Duncan's multiple range tests [SAS, 2004]**.** Statistical significance was defined at $P \leq 0.05$.

3. RESULTS AND DISCUSSION

Both pH and EC values of tested water (treatments) used for irrigation pots and germination assay are presented in Table (1). It was observed that pH value tend to an alkaline side of neutrality for control (T1) and tap water (T2) treatments, while it decreased to 6.6 in sewagewater (T3) and become in acid side of neutrality 4.6 for leachate. Osuagwa *et al*. [2015] reported that petrification of solid waste which contain various human discarded of its food scrapes enriched with fats, proteins and carbohydrates may produce an acid leachate. On the other hand, high value of EC was found in the leachate, it is beyond permissible level (sever potential risk) for crop irrigation [Ayers & Westcot, 1985]. Similar results were found for pH and EC values measured in leachates of Erbil city by [Shekha *et al*., 2017].

Table (1). pH and EC ($\mu S.cm^{-1}$) values of different water treatments used for irrigation purpose.

Variables	Treatments			
	Control (T1)	Tap water (T2)	Sewagewater (T3)	Solid waste leachate (T4)
pH	7.066± 0.033^{ab}	7.533± 0.033^{b}	6.676± 0.374^{a}	4.706± 0.052^{c}
EC	4.866± 0.185^{a}	260.6± 4.630^{a}	771.0± 43.25^{b}	8130± 210.0^{c}

Note: Values in each columns with different letters are significantly different at P≤0.05. Values in rows with same letters are not significantly different.

Data in Table (2) shows some vegetative growth of Faba bean plant irrigated by different water treatments. Maximum plant height and root dry weight was recorded in sewagewater treatments (34.6 cm and 12.06cm respectively), with significant differences at (P≤0.05) to leachate treatment only (Figure 1). This may be related to the nature of sewagewater composition contain most essential nutrients for plant growths which enhanced plant for better growth and fulfill any deficiency of these nutrients in soil [Fathi *et al*., 2014; Alghobar *et al*., 2014; Mohammad & Ebead, 2012; Akbari *et al*., 2012; Khan *et al*., 2012; Zeid & Abou El-Ghate, 2007]. Generally, in most vegetative growth characteristics for Faba bean plant irrigated with leachate (T4) have lowest growth rate in comparison to other treatments (Figure 2, 3 & 4). This may be attributed to lowest pH and highest EC values of leachate which effect on soil physicochemical properties that reflect on nutrients availability for cultivated plant. In addition to various toxic heavy metals and other organic matter which may inhibited bean growths through effects on metabolic rate and enzymes activities of plant [Adamcová *et al*., 2016; Farombi *et al*., 2011; Sang & Li, 2004].

Table (2). Effect of different types of irrigated water on some vegetative characteristic growth *Vicia faba* L. (bean) plant (data represented as mean± S.E).

Variables	Treatments			
	Control (T1)	Tap water (T2)	Sewagewater (T3)	Solid waste leachate (T4)
Plant height (cm)	32.16± 3.609^{a}	28.66± 0.666^{a}	34.66± 2.403^{a}	7.333± 1.330^{b}
Shoot dry weight (gm)	3.576± 0.409^{ab}	6.186± 0.769^{b}	5.175± 0.356^{b}	1.207± 0.166^{a}
Root dry weight (gm)	7.400± 0.584^{a}	6.694± 1.119^{a}	12.06± 1.512^{a}	0.000± 0.000^{b}
Leaf area (cm^2)	20.77± 3.844^{a}	21.21± 2.962^{a}	14.87± 2.666^{a}	7.282± 1.660^{a}
No. of branches	3.333± 0.333^{a}	3.333± 0.666^{a}	3.333± 0.333^{a}	0.333± 0.003^{b}
No. of leaves	20.66± 2.666^{a}	23.00± 3.725^{a}	15.66± 2.027^{a}	1.666± 0.660^{b}
No. of flowers	12.66± 1.453^{ab}	10.33± 1.174^{ab}	21.33± 3.844^{a}	3.000± 0.300^{b}
No. of legumes	1.666± 0.666^{a}	2.000± 0.577^{a}	4.333± 0.333^{b}	0.000± 0.000^{c}
No. of nodules	219.3± 18.01^{a}	190.0± 27.13^{ab}	393.0± 33.00^{a}	0.000± 0.000^{b}
Chlorophyll a content	52.13± 1.510^{a}	41.70± 0.929^{b}	42.30± 0.953^{b}	42.66± 0.635^{b}

Note: Values in each columns with different letters are significantly different at P≤0.05. Values in rows with same letters are not significantly different.

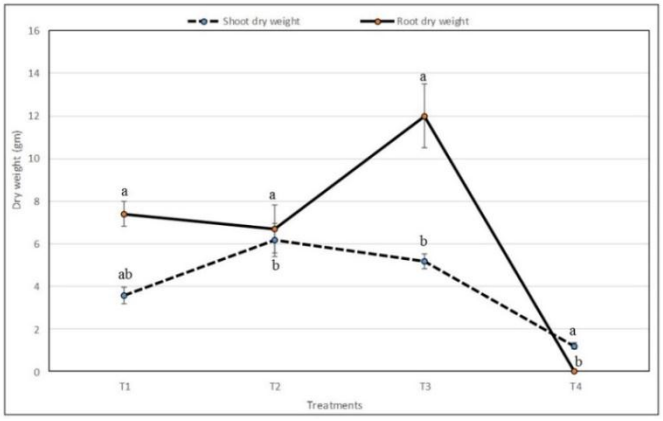

Figure 1: Shoot and root dry weight (gm.) of Faba bean irrigated by different water treatments.

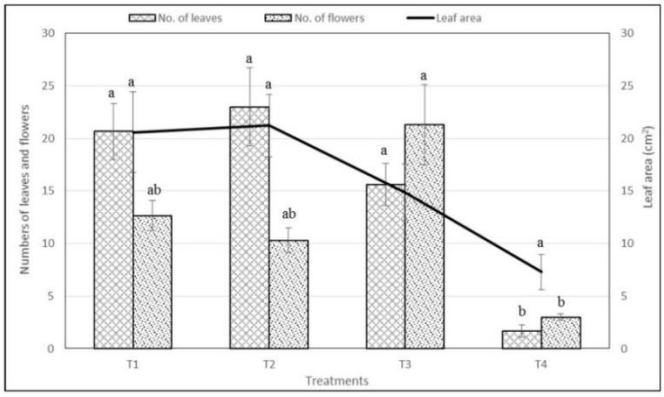

Figure 2: Effect of different water treatments on number of leaves, flowers and leaf area of Faba bean.

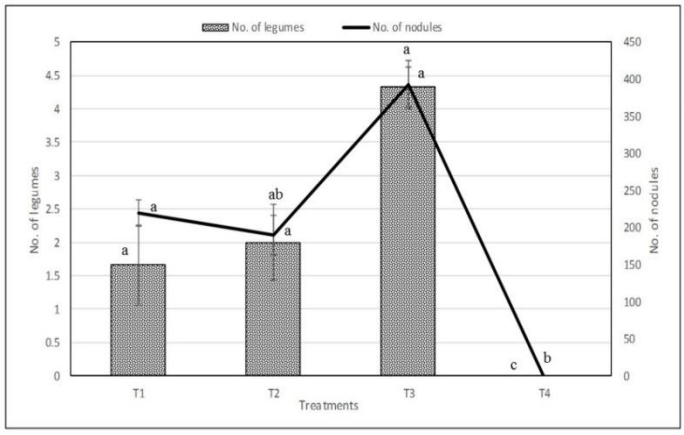

Figure 3: Effect of different water treatments on number of legumes and nodules of Faba bean.

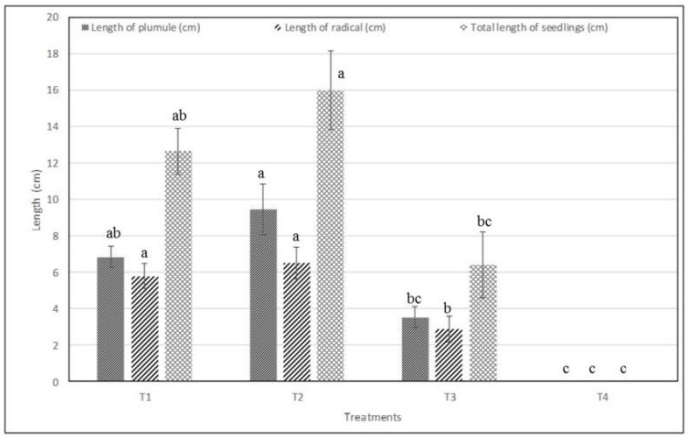

Figure 4: Effect of different water treatments on length of plumule and radical (cm) of Faba bean.

In the late period of growth the bean plant exposed to wilting and dead, that was reflect from results of root dry weight, numbers of legume and nodule, which was zero. That indicated the harmful effect of leachate on soil microorganisms in rhizosphere through several of toxic materials that inhibited and prevent formation of nodules. In contrast highest number nodules and legumes were recorded in bean plant irrigated with sewagewater (Figure 3). This may be related to high nutrients and microorganisms contain in wastewater, which supplied favorable habitat and food availability in rhizosphere zone and enhanced formation of legumes and nodules.

As shown in Table (3), some chemical analysis of bean plant irrigated with different water treatments. It is obvious from results that all analyzed components in bean plant were increased from control treatment to sewagewater treatment with statistically no significant differences at ($P \leq 0.05$). As a result of wilting and drying of bean plant irrigated with leachate no plant was available to assay these components. Results reveals that irrigation with sewagewater lead to accumulation of ions, nutrients and other compounds in plant parts of bean plant [Khan *et al*., 2012].

Table (3): Plant component of *Vicia faba* L. (data represented as mean± S.E) irrigated by different water treatments.

Plants components	Treatments			
	Control (T1)	Tap water (T2)	Sewagewater (T3)	Solid waste leachate (T4)
K^+ mg.gm^{-1}	62.40± 2.400^a	73.42± 7.260^a	92.51± 10.18^a	00.00± 00.00^b
Na^+ mg.gm^{-1}	42.08± 1.278^a	50.94± 5.654^a	53.89± 6.870^a	00.00± 00.00^b
Total phosphorus	1.152± 0.485^a	3.662± 0.717^a	4.362± 2.723^a	00.00± 00.00^a
Kjeldhal nitrogen %	1.136± 0.170^a	1.548± 0.286^a	1.711± 0.091^a	00.00± 00.00^b

Note: Values in each columns with different letters are significantly different at $P \leq 0.05$. Values in rows with same letters are not significantly different.

In the present study the results of germination assay was arranged in Table (4). Results showed a decrease in germination percentage of bean plant from 52.8% and 8.3% for sewagewater and leachate treatments respectively with respect to control treatment (80.8%). Highest inhibition of germination % observed for last two treatments 37.1 and 81.8% respectively. Turki and Bounzi [2017] confirmed toxic inhibitory effects of raw leachate to seed germination percentage and plant growth, they related that to high nitrogen and salinity content of leachate. High content of toxic organic matter and heavy metals in the leachate may resulted in concealed the action of nutrients that caused inhibition of plant growth [Gupta & Rajamni, 2015; Li *et al*., 2008]. The plumule and radical elongation was tend to increase in seed irrigated by tap water (T2) compared to control treatment with no significant differences at ($P \leq 0.05$) between them, while, it reduced for sewagewater treatment (T3). This may be attributed to phytotoxicity of sewagewater containing various toxic heavy metals suppression growth of seeds. Generally, our results revealed that all seeds treated with leachate showed completely inhibition on plant growth as well as other studied parameters (zero value) (Table 4, Figure 4), with significant differences at ($P \leq 0.05$) to other treatments. Li *et al*. [2017] reported that polluting components of leachate have a greater harm on the germination process. Vishnoi *et al*. [2013] mentioned that the reduction in shoot and

root length for *Pisum sativum* irrigated with leachate, to adverse effect of heavy metals and their toxicity to plant growth. Toxicity of heavy metals to plants is represented by leaf chlorosis, stunted growth and disturbed of different metabolic pathways [Yadav, 2010].

Table (4): Effect of different water treatments on seed germination characteristics of *Vicia faba* L. (data represented as mean± S.E).

Germinated seed variables	Treatments			
	Control (T1)	Tap water (T2)	Sewagewater (T3)	Solid waste leachate (T4)
Germination rate %	80.53± 15.45^{a}	77.76± 14.69^{a}	52.83± 10.70^{a}	8.33± 1.83^{b}
Inhibition of germination %	0.00± 0.00^{a}	5.02± 1.10^{a}	37.16± 1.22^{b}	81.8± 3.20^{c}
Plumule elongation velocity	0.456± 0.105^{a}	0.631± 0.093^{a}	0.308± 0.033^{ab}	0.00± 0.00^{b}
Radical elongation velocity	0.386± 0.046^{a}	0.435± 0.057^{a}	0.192± 0.047^{b}	0.00± 0.00^{c}
Length of plumule (cm)	6.85± 0.58^{ab}	9.47± 1.40^{a}	3.52± 0.59^{bc}	0.00± 0.00^{c}
Length of radical (cm)	5.80± 0.704^{a}	6.52± 0.874^{a}	2.88± 0.709^{b}	0.00± 0.00^{c}
Total length of seedlings (cm)	12.65± 1.26^{ab}	15.99± 2.14^{a}	6.40± 1.83^{bc}	0.00± 0.00^{c}
Dry weight of plumule (gm)	0.070± 0.016^{ab}	0.107± 0.014^{a}	0.041± 0.020^{bc}	0.00± 0.00^{c}
Dry weight of radical (gm)	0.064± 0.011^{a}	0.061± 0.003^{a}	0.023± 0.004^{ab}	0.00± 0.00^{b}
Total dry weight of seedling	0.134± 0.044^{a}	0.168± 0.017^{a}	0.064± 0.004^{ab}	0.00± 0.00^{b}
Shoot/root	1.411± 0.202^{a}	1.717± 0.147^{a}	1.908± 0.238^{a}	0.00± 0.00^{b}

Note: Values in each columns with different letters are significantly different at P≤0.05. Values in rows with same letters are not significantly different.

CONCLUSION

This study mainly was focusing on effects of sewagewater and solid waste leachate on seed germination and plant growth characteristics of faba bean. The finding of the research evidence indicates that sewagewater had a positive influence on increasing of most vegetative growth characters of bean plant counter to leachate with very adverse effects and reduction or even stopping in the vegetative growth (numbers of legumes and nodules). Also, leachate had lowest germination rate and highest inhibition of germination compared with other used irrigated water.

References

ADAMCOVÁ, D.; VAVERKOVÁ, M. D.; BARTOˇN, S.; HAVLIˇCEK, Z. and BˇROUŠKOVÁ, E. 2016. Soil contamination in landfills: a case study of a landfill in Czech Republic. Solid Earth. 7: 239–247.

AHMAD1, K.; EJAZ, A.; AZAM, M.; KHAN, Z. I.; ASHRAF, M.; AL-QURAINY, F.; FARDOUS, A.; GONDAL, S.; BAYAT, A. R. & VALEEM, E. E. 2011. Lead, cadmium, and chromium contents of Canola irrigated with sewagewater. Pakistan J. of Botany. 43(2): 1403-1410.

AKBARI, G.; DADRESAN, M.; KHAZAEI, F. & KHANDAN, A. 2012. Effect of irrigation with urban sewage and aqueduct water on heavy metals accumulation and nutritional value of bean (*Phaseolus vulgaris* L.). ARPN Journal of Agricultural and Biological Science. 7(3): 169-176.

ALGHOBAR, M. A.; RAMACHANDRA, L. & SURESHA, S. 2014. Effect of sewage water irrigation on soil properties and evaluation of the accumulation of elements in Grass crop in Mysore city, Karnataka, India. American Journal of Environmental Protection. 3(5): 283-291.

APHA (AMERICAN PUBLIC HEALTH ASSOCIATION). 1998. Standard Methods for the Examination of Water and Wastewater. 20th Ed., APHA, 1015, 15th. Street, NW, Washington, DC 20005.

AYERS, R. S. & WESTCOT, D. W. 1985. Water Quality for Agriculture, FAO Irrigation and Drainage Paper 29, revision 1, Food and Agriculture Organization of United Nations, Rome, Italy.

CALDWELL, B.E. & GRANT, V. 1968. Nodulation interactions between soybean genotypes and serogroups of rhizobium japoni cum. Crop Science 8:680-682.

CHAIGNON, V. & HISSINGER, P. 2003. Heavy metals in environment- A biotest for evaluating copper bioavailability to plants in a contaminated soil. J. Environmental Quality. 32: 824- 833.

DUC, G. 1997 Faba bean (Vicia faba L). Field Crops Res. 53: 99–109.

EL-GHAMERY, A. A. & BASUONI, M. M. 2015. Evaluation of the cytotoxic and genotoxic effects of Cinnamon aqueous extract in *Allium cepa* and *Vicia faba*. Int. J. Adv. Res. Biol. Sci. 2(11): 209–224.

FAO (FOOD AND AGRICULTURE ORGANIZATION). 1992. Wastewater treatment and use in agriculture. FAO Irrigation Paper 47: Food and Agriculture Organization of the United Nations, Rome, Italy.

FAROMBI, E.O.; AKINTUNDE, J.K.; NSUTE, N.; ADEDARA, I.A. & AROJOJOYE, O. 2011. Municipal landfill leachate induces hepatotoxicity and oxidative stress in rats. Toxicol Ind Health. 28(6): 532-541.

FATHI, H.; MIRZANEJAD, M.; EBADI, A.; MORADI, H. & ARYANPOUR, H. 2014. Effects of wastewater irrigation on the growth of two bean spices and soil chemical properties under greenhouse conditions. International Journal of Soil and Crop Sciences. 2(2): 33-38.

GUPTA, A. & RAJAMANI, P. 2015. Toxicity assessment of municipal solid waste landfill leachate collected in different seasons from Okhala landfill site of Delhi. J. of Biomedical Science and Engineering. 8:357-369.

HIRICH, A. R.; FAHMI, C. H.; RAMI, A.; LAAJAJ, K.; JACOBSEN, S. & EL OMARI, H. 2014. Using deficit irrigation to improve crop water productivity

of sweet corn, chickpea, faba bean and quinoa: a synthesis of several field trials. Rev. Mar. Sci. Agron. Vét. 2 (1):15-22.

HIRICH, A.; CHOUKR ALLAH, R.; JACOBSEN, S. E.; EL YOUSSFI, L. & EL OMARI, H. 2012. Revista Científica UDO Agrícola. 12 (3): 570-583.

ISMAIEL, A. A.; HEGAZY, H. S. & AZB, M. A. 2014. Physiological response of *Vicia faba* L. to inoculation with *Rhizobium* and arbuscular mycorrhizal fungi: Comparative study for irrigation with Nile water and wastewater. Australian J. of Crop Science. 8(5):781-790.

KHAN, I. U.; KHAN, M. J.; KHAN, N. U.; KHAN, M. J.; RAHMAN, H. U.; BIBL, Z. & ULLAH, K. 2012. Wastewater impact on physiology, biomass and yield of Canola (*Brassica napus* L.). Pakistan Journal of Botany. 44(2): 781-785.

LI, G.; CHEN, J.; YAN, W. & SANG, N. 2017. A comparison of the toxicity of landfill leachate exposure at the seed soaking and germination stage on Zea mays L. (maize). J. of Environmental Science. 55:206- 213.

LI, G. K.; YUN, Y.; & SANG, N. 2008. Effect of landfill leachate on cell cycle, micronucleus, and sister chromatid exchange in *Triticum aestivum*. J. Hazard. Mater. 155 (1–2), 10–16.

MAPANDA, F.; MANGWAYANA, E.N.; NYAMANGARA, J. & GILLER, K. E. 2005. The effect of long- term irrigation using waste water on heavy metal contents of soils under vegetables in Harare, Zimbabwe. Agric. Ecosystem and environment.107:151-165.

McBEAN, E. A.; ROVERS, F. A. & FARQUHAR, G. J. 1995. Solid Waste Landfill Engineering and Design, Prentice Hall PTR, Englewood Cliffs, 521p.

MOHAMMAD, A. I. & EBEAD, B. M. 2012. Effect of irrigation with magnetically treated water on faba bean growth and composition. International Journal of Agricultural Policy and Research. 1(2):24-40.

MORRIS, B. 2003. Legumes Encyclopedia of food and culture. Ed. Solomon H. Katz. Vol. 3. New York: Charles Scribner and Sons.

OSUAGWU, G. G.; NWOKEOCHA, O. W.; MGBEZE, G.C.; INI, O.O. 2015. Effect of dump site soil on the growth of common bean (*Phaseolus vulgaris*). International Journal of Plant Science and Ecology. 1(5):213-217.

RYAN, J.; ESTEFON, G. & RASHID, A. 2001. Soil and plant analysis laboratory manual. 2nd Ed. *National Agriculture Research Center* (NARC). Islamabad, Pakistan.

SANG, N. & LI, G. 2004. Genotoxicity of municipal landfill leachate on root tips of *Vicia faba*. Mutagen Research. 560: 159-165.

SANG, N. & LI, G. 2004. Genotoxicity of municipal landfill leachate on root tips of *Vicia faba*. Mutagen Research. 560: 159-165.

SAS, 2004. Statistical Analysis System, SAS Institute, Inc. Cary, N.C. U.S A.

SHEKHA, Y.A. 2011. Household Solid Waste Content in Erbil City, Iraqi Kurdistan Region, Iraq. Zanco Journal. 23(3): 1-8.

SHEKHA, Y.A.; Al-ATTAR, M.S.M.; SALEEM, M.A.; TOMA, J.J. & ABDULLA, S.M. 2017. Effect of landfill leachates extract of Erbil city on abnormal sperm morphology and chromosomal aberrations in male albino mice. Zanco J. of Pure and Applied Science. 27(6): 18-27.

SRIVASTAVA, R.; KUMAR, D. & GUPTA, S. K. 2005. Municipal sludge- induced phytotoxicity. Atla. 33: 501- 508.

TAIZ, L. & ZEIGER, E. 2006. Plant physiology. 4th Ed. Siuaner Associates, Inc., Publisher. USA. 764pp.

TURKI, N. & BOUZID, J. 2017. Effects of landfill leachate application on crops growth and properties of a Mediterranean sandy soil. J. of Pollution Effects and Control. 5(2):

VISHNOI, N.; DIXIT, S. & SINGH, D.P. 2013. Phytotoxic effect of leachates of industrial solid waste on the growth of *Pisum sativum*. J. of Environmental Biology. 34:651- 656.

VOEGBORLO, R. B. & ABDULKABIR, M. O. 2006. Effect of municipal sewage effluent on soil and crops cultivated on a hyper- arid zone sandy soil. Journal of Science and Technology. 26(2):

YADAV, S. K. 2010. Heavy metals toxicity in plants: An overview on the role of glutathione and phytochelatins in heavy metal stress tolerance of plants. South African Journal of Botany. 76(2): 167- 179.

ZEID, I. M. & ABOU El-GHATE, H. M. 2007. Effect of sewage water on growth, metabolism and yield of bean. Journal of Biological Science. 7(1): 34-40.

ZANCO Journal of Pure and Applied Sciences
The official scientific journal of Salahaddin University-Erbil
https://zancojournals.su.edu.krd/index.php/JPAS

ISSN (print):2218-0230**, ISSN (online):** 2412-3986**, DOI: http://dx.doi.org/10.21271/zjpas**

RESEARCH PAPER

Theoretical study for the inhibition ability of some bioactive imidazole derivatives against the Middle-East respiratory syndrome corona virus (MERS-Co)

Hassan H. Abdallah[1]

[1]Department of Chemistry, College of Education, Salahaddin University-Erbil, Erbil, Iraq

A B S T R A C T:
The Severe Acute Respiratory Syndrome (SARS) is a serious viral life-threatening and mortal respiratory illness caused by SARS-CoV. SARS-CoV plays an essential role in the viral replication cycle. It is considered a potential target for SARS inhibitor development. A series of twenty eight bioactive imidazole compounds as possible SARS-CoV inhibitors were designed and evaluated using computational calculations. Possible binding interaction modes were proposed by molecular docking studies. Among all studied compounds, compounds **5**, **15** and **22** showed most potent inhibitory activity against SARS-CoV. These results indicated that these inhibitors could be potentially developed into anti-SARS drugs.

KEY WORDS: SARS, Corona viruses, imidazole, docking.
DOI: http://dx.doi.org/10.21271/ZJPAS.31.2.10
ZJPAS (2019) , 31(2);71-78 .

INTRODUCTION:

Coronaviruses are single stranded RNA viruses. They can infect humans and animals, such as bats, mice, birds, dogs, pigs, and cattle producing respiratory and enteric diseases (Perlman and Netland, 2009). It was believed that these viruses can only cause mild respiratory symptoms similar to common cold (Saif, 2004) however this idea changed after 2002-2003 outbreak of the severe acute respiratory syndrome (SARS) when it infected approximately 8000 and killed 774 people (Peiris et al., 2004).

* **Corresponding Author:**
Hassan H. Abdallah
E-mail: hassan.abdullah@su.edu.krd
Article History:
Received: 07/01/2019
Accepted: 18/02/2019
Published:23/04/2019

In the followed years hCoV-NL63 and hCoV-HKU1 human coronaviruses were discovered (van der Hoek et al., 2004, Woo et al., 2005). It is believed that bats are the major role in the process of interspecies transmission in all known human coronaviruses (To et al., 2013). The complete genome sequence of the coronavirus was obtained by different groups of scientists (van Boheemen et al., 2012), (de Groot et al., 2013).

The MERS-CoV common symptoms are fever followed by cough and shortness of breath then acute pneumonia and acute renal failure (Geng and Tan, 2013). Although the beginning of the MERS-CoV transmission to the human species was from an animal, the occurrence of new clusters suggests the human to human transmission.

Obviously, aerosol droplets, direct contact with biological secretions like stool, urine and blood are the main ways of virus transmission among humans (Danielsson and Catchpole, 2011).

To the moment, there are no effective anti-viral agents against human coronavirus (Chan et al., 2012) and the only available therapeutic interventions for SARS involve antibiotics, supportive care, antiviral agents and sometimes immunomodulatory therapy (Puzelli et al., 2013).
It is known that imidazole compounds are heterocyclic compounds or diazole compounds. There are a huge number of imidazole compounds that derived from natural product compounds like alkaloids or chemically synthesized. The imidazole ring compounds has a wide range of biological activity, such as certain antifungal drugs, the nitroimidazole series of antibiotics, and the sedative midazolam (Grimmett, 1997, Brown, 2012, Gilchrist, 1997, Rosemeyer, 2004, Katritzky et al., 1997) or available in biological molecules like histidine, and related hormone histamine. In addition imidazole represents an important part of many pharmaceuticals such as many fungicides and antifungal which includes ketoconazole, miconazole, and clotrimazole (Shargel and Swanson, 2004), antiprotozoal, and antihypertensive medications. Nevertheless, imidazole is found in tea leaves and coffee beans and in the anticancer medication mercaptopurine.

Computer-aided docking is one of the important tools for designing novel bioactive compounds and studying the binding interactions between a ligand (inhibitor) and its target receptor (protein or enzyme) (Anderson, 2003, Schneider, 2010). Computational methods are reliable methods that provide accurate results, cost-effective and time-saving technique for drug design and drug discovery process(Walters et al., 1998, Waszkowycz et al., 2001).

Recently, there are many articles targeting the inhibition of this virus theoretically (Maria, 2017, Radwan, 2018, Chafekar, 2018 and Kim 2018) however, to the best of our knowledge there is no theoretical of experimental study studying the inhibition activity of these compounds against corona virus.
In this study twenty eight bioactive imidazole compounds with known biological activity are studied theoretically to investigate the possibility of using these compounds against corona virus.

1. MATERIALS AND METHODS

A database of twenty eight bioactive imidazole compounds was built. The 2D and 3D structures of these imidazole derivatives were extracted from online databases, such as, PubChem, chemspider, drugbank websites. The structures were optimized to get the best 3D structure using Density Functional methods (DFT). The X-ray structure of SARS coronavirus 3CLpro was used as our initial protein model for docking as in Figure 1. Docking simulation of the fully optimized compounds was achieved using different computational methods. The protein structure was prepared using the Material Studio program. All water molecules were deleted from the protein structure before docking. The dimensions of the grid box are 60 x 60 x 60. The standard precision of Genetic Algorithm scoring functions was used to rank the binding pose and the limit of 100 conformations was used for each inhibitor.

2. RESULTS AND DISCUSSION

Twenty eight bioactive imidazole derivatives, some of them are pharmaceutical drugs and some are still under testing were extracted from literature. 2D structures for the bioactive imidazole compounds were downloaded from online databases such as, Chemspider, PubChem, and Zinc. The 2D structures of the studied bioactive imidazole derivatives are shown in Figure 2. The chemical formula, chemical names and the biological activity are listed in Table 1.

All the selected bioactive compounds have at least one imidazole ring however they have a variety of substituted groups. For example, in compound **1** the imidazole ring is connected with unsubstituted aromatic rings. Compounds **2**, **4**, and **6** have a substituted aromatic ring with chloride. Compounds **9**, **10**, **17** and **26** have no aromatic ring while compounds 10 and 25 have a nitro group. Compounds **9** and **21** have acidic properties with a carboxylic group while compounds **13** and **15** have a sulfur atom. In addition compounds **18**, **21** and **22** have a fluoride while others have amide or hydrophobic properties.

The protein crystal structure of the corona virus (SARS-CoV) was downloaded from protein data bank and the structure is viewed using discovery studio program. As shown in Figure 1, the secondary structure of the protein is composed mainly of beta sheets and helixes. The active site

of the protein is found by the same program discovery studio in which the inhibitor is located as shown in Figure 1. The active site of the protein is consist of the following amino acids; Asn142, Gly143, Leu141, Ser144, Cys145, Met49, Gln189, Met165, Arg188, Gln192 and Phe140.

In order to predict the best conformation of the studied compounds, rotation around the single bonds was allowed. Before docking, the crystalized ligand was re-docked at the active site of the protein of corona virus and the new conformation and binding site were compared. The same procedure was followed for the rest of the compounds. For each compound, 100 conformations were tested and the calculated binding free energies were ranked accordingly. Table 2, is showing the list of studied inhibitors (ligands) and the binding energies of the best three conformations. As shown in Table 2, the binding energies (E_{bind}) or docking free energy, of the best three conformations were listed and the repetition number for each confirmation was added between brackets. Generally, all the studied imidazole inhibitors have shown a good ability to bind to the active site of the protein where the binding energy between -4.57 and -9.64 kcal/mol.

In this study, we are going to focus on the best three inhibitors with the best docking score, namely, the inhibitors, **5**, **15** and **22** as highlighted in Table 2. The common characters between these inhibitors are aromatic ring, relatively big size (branched) and one or more of the following heteroatoms, O or F or N or Cl.

At the active site normally, there are different interactions between the ligand and the protein such as hydrogen bonds, pi-pi interactions, electrostatic interactions, hydrophobic and hydrophilic interactions. The more interactions with the active site the more binding forces made with the protein, the more stable complex formed between the protein and the inhibitor and the more inhibition ability. In addition, interactions made between the inhibitor and the active site depends on the substituted groups of the inhibitor, the characters of the amino acids at the active site and the size and conformation of the inhibitor.

Ligand **5**, is connected with the active site by two types of interactions, hydrogen bonds and pi-pi interaction. These interactions are due to the groups, OH and aromatic ring of the ligand. The calculated binding free energy is -9.16 kcal mol. Hydrogen bonds are made with Arg188, Leu141 and Ser144 with distances, 3.28, 2.97 and 3.25 Å, respectively, as shown in Figures 2 and 3. The hydrophobic group ($-(CH_2)_3-CH_3$) of the inhibitor seems to be not important in binding with the active site of the protein. In a similar manner, ligand **15** has an aromatic ring with Cl, O and S heteroatoms. The binding free energy is -9.64 kcal/mol. The most important interactions with the active site are the hydrogen bond formed with the amino acids Ser144 and Leu141 with a distances of 3.15 and 3.05 Å respectively and pi-pi interaction with the aromatic ring.

Ligand **22** has made a hydrogen bond interaction with the amino acids Ser144 and Leu141 with a distances of 3.09 and 3.20 Å respectively. The other interaction is pi-pi interaction in which two aromatic rings in parallel conformation is made between the aromatic ring of the ligand and the amino acid His41 at the active site of the protein of corona virus.

As shown from the previous results, the highest binding free energy or inhibition activity is due to the interaction with the amino acids at the active site. Hydrogen bonds and pi-pi interactions are the dominant interactions with the protein. For that we may conclude that the inhibition activity or the high binding free energy for those active compounds is due to the formations of strong interactions with the active site of the protein.

3. CONCLUSIONS

Twenty eight bioactive imidazole compounds with pharmaceutical application were docked against corona virus. Compounds **5**, **15** and **22** were found to be the best inhibitors against corona virus among the studied compounds. Interactions of the docked compounds were visualized and discussed. Hydrogen bonds and pi-pi interactions were the dominant interactions with the amino acids of the protein active site. The results of this study may help to develop novel drugs against corona virus.

Acknowledgements

This study was supported by Salahaddin University-Erbil.

Conflict of Interest

There is no conflict of interest

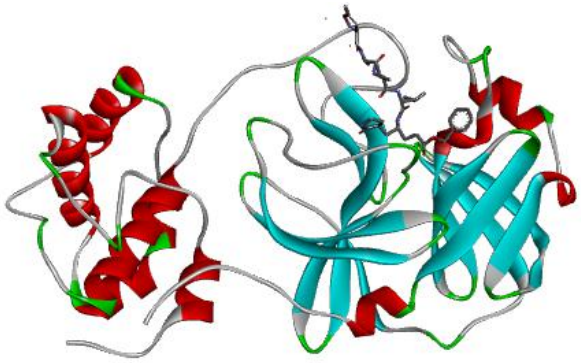

Figure (1) Crystal structure of SARS-CoV in complex with inhibitor

Table (2) The best three conformations and the values of binding energy in kcal/mol

Ligand	E_{Bind1}	E_{Bind2}	E_{Bind3}
1	**-8.57 (50)**	**-8.40 (15)**	**-8.05 (33)**
2	**-6.71 (48)**	**-6.65 (45)**	**-6.65 (6)**
3	**-8.12 (38)**	**-8.10 (9)**	**-7.80 (9)**
4	**-8.67 (3)**	**-8.00 (22)**	**-7.88 (31)**
5	**-9.16 (1)**	**-8.95 (5)**	**-8.81 (5)**
6	**-8.98 (4)**	**-8.93 (19)**	**-8.46 (14)**
7	**-8.12 (12)**	**-5.46 (20)**	**-4.59 (15)**
8	**-8.16 (12)**	**-7.99 (5)**	**-7.74 (20)**
9	**-4.66 (70)**	**-4.16 (11)**	**-3.91 (2)**
10	**-4.57 (44)**	**-4.35 (9)**	**-4.26 (3)**
11	**-6.08 (27)**	**-5.95 (24)**	**-5.93 (5)**
12	**-6.76 (27)**	**-5.99 (10)**	**-5.99 (2)**
13	**-8.55 (7)**	**-8.38 (17)**	**-8.09 (14)**
14	**-8.24 (19)**	**-8.16 (6)**	**-8.06 (51)**
15	**-9.64 (14)**	**-8.88 (33)**	**-8.72 (6)**
16	**-6.19 (18)**	**-6.18 (53)**	**-5.92 (28)**
17	**-7.46 (49)**	**-7.13 (19)**	**-6.89 (10)**
18	**-6.88 (31)**	**-6.06 (3)**	**-5.97 (20)**
19	**-8.59 (3)**	**-8.18 (5)**	**-8.15 (13)**
20	**-7.37 (6)**	**-7.12 (4)**	**-6.96 (6)**
21	**-5.40 (18)**	**-5.16 (11)**	**-5.01 (10)**
22	**-9.08 (78)**	**-8.95 (22)**	**-----**
23	**-6.08 (25)**	**-5.95 (19)**	**-5.89 (2)**
24	**-7.64 (8)**	**-7.64 (11)**	**-7.06 (18)**
25	**-6.67 (4)**	**-5.51 (9)**	**-5.48 (4)**
26	**-4.96 (3)**	**-4.86 (7)**	**-4.50 (9)**
27	**-5.52 (12)**	**-5.18 (9)**	**-4.95 (17)**
28	**-7.56 (32)**	**-7.26 (14)**	**-7.07 (6)**

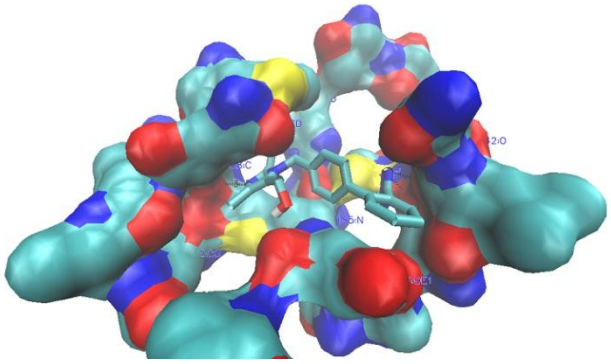

Figure (3) Ligand **5** at the active site of the protein.

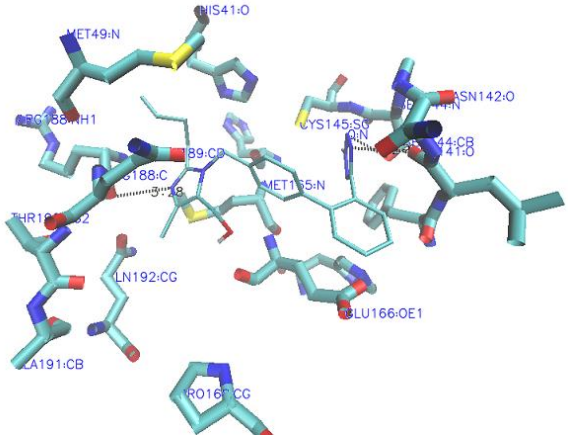

Figure (4) Ligand **5** at the active site of the protein making HB and pi-pi interactions.

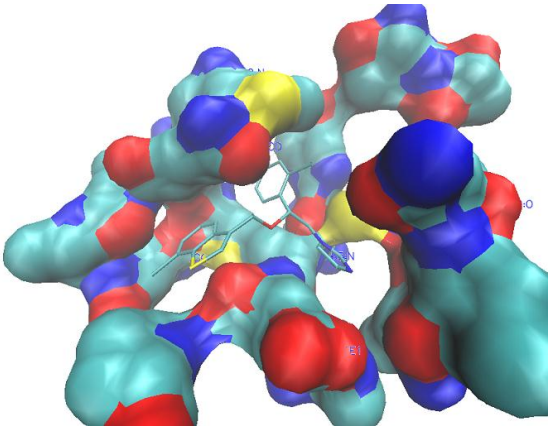

Figure (5) Ligand **15** at the active site of the protein

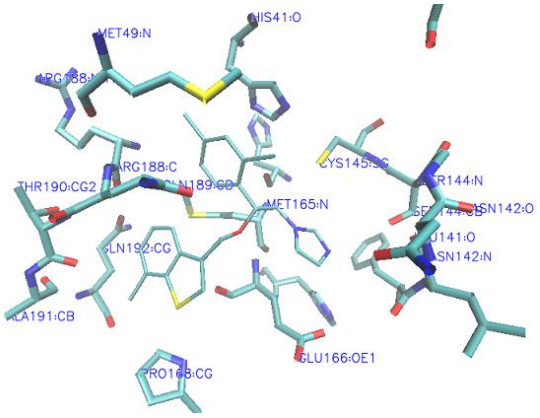

Figure (6) Interactions of ligand **15** at the active site of the protein.

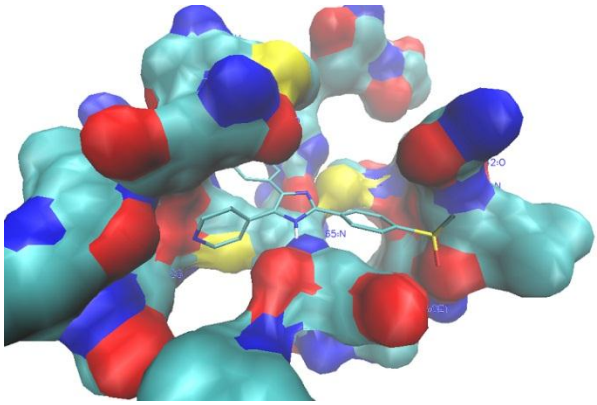

Figure (7) Ligand **22** at the active site of the protein.

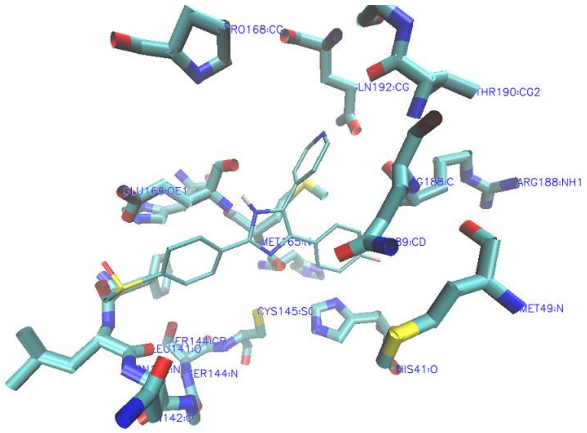

Figure (8) Interactions of ligand **22** at the active site of the protein.

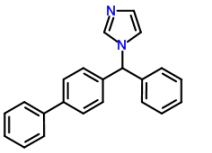

1

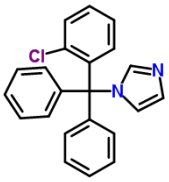

2

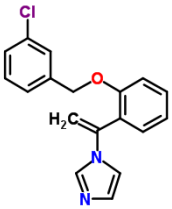

3

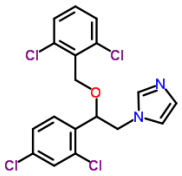

4

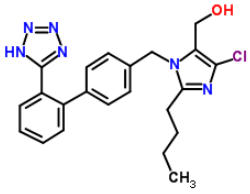

5

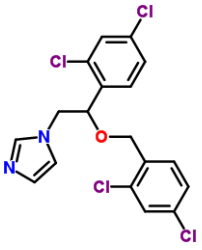

6

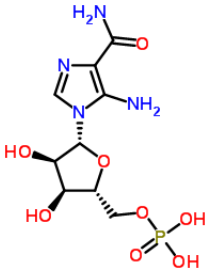

7

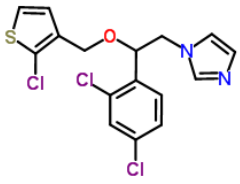

8

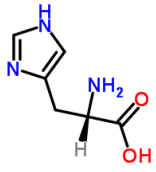

9

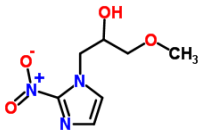

10

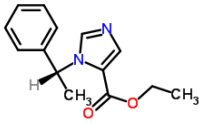

11

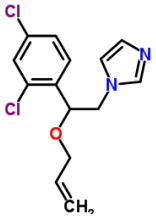

12

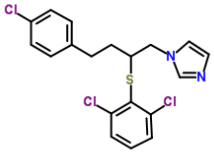

13

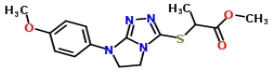

14

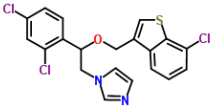

15

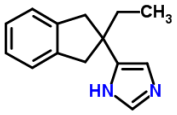

16

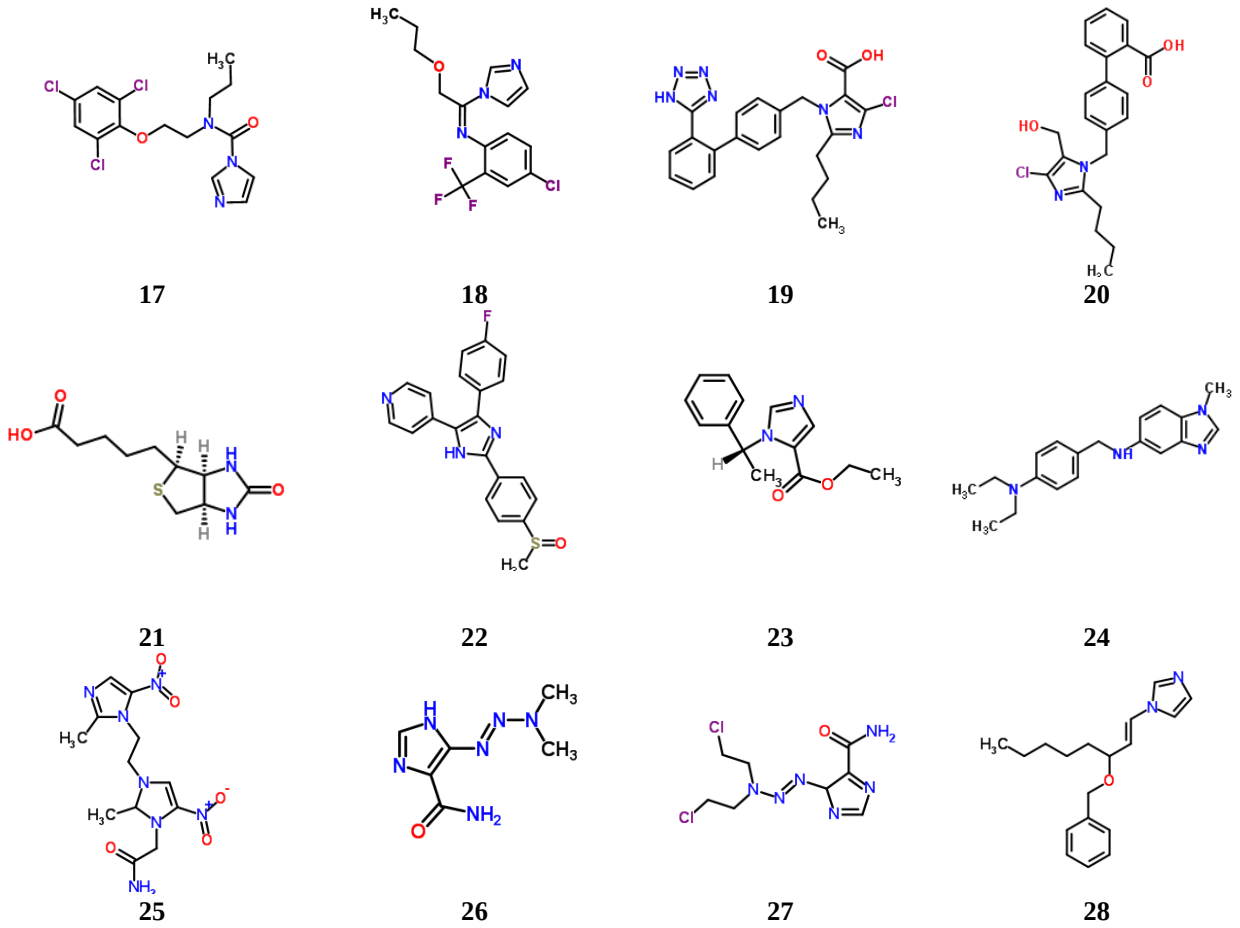

Figure (2) Structures of the bioactive imidazole compounds

Table (1) Molecular formula, chemical name and the biological activity of the studied bioactive imidazole compounds

Lig.	Molecular Formula	Chemical Names	biological activity
1	$C_{22}H_{18}N_2$	Bifonazole**,** Trifonazole	Inhibiting the production of ergosterol
2	$C_{22}H_{17}ClN_2$	Clotrimazole, Lotrimin, Mycosporin	Antimycotic activity, inhibits biosynthesis of the sterol ergostol.
3	$C_{18}H_{15}ClN_2O$	Croconazole, Croconazolum	no specific biological action
4	$C_{18}H_{14}Cl_4N_2O$	Isoconazole, Travogen, Fazol	Antifungal drug that has similar to clotrimazole in the treatment of foot and vaginal infections.
5	$C_{22}H_{23}ClN_6O$	Losartan, Lortaan, Cozaar, Hyzaar	Antagonist of angiotensin type 1 receptor with antihypertensive activity
6	$C_{18}H_{14}Cl_4N_2O$	Miconazole, Monistat, Daktarin IV, Minostate	An imidazole antifungal agent that is used topically and by intravenous infusion.
7	$C_9H_{15}N_4O_8P$	Amino imidazole carboxamide ribonucleotide,	Nucleotide transport and metabolism
8	$C_{16}H_{13}Cl_3N_2OS$	Tioconazole, Trosyd	Antifungal medication
9	$C_6H_9N_3O_2$	Histidine, Glyoxaline-5-alanine	L-histidine is an essential amino acid that is required for the production of Histamine.
10	$C_7H_{11}N_3O_4$	Misonidazole, Misonidazolum	Nitroimidazole that sensitizes normally radio-resistant hypoxic cells.
11	$C_{14}H_{16}N_2O_2$	Etomidate, Amidate, Radenarcon	Anesthetic and hypnotic with little effect on blood gases, ventilation.
12	$C_{14}H_{14}Cl_2N_2O$	Imazalil Chloramizol, Deccozil, Fungaflor	Brown solidified oil, non-corrosive, fungicide.
13	$C_{19}H_{17}Cl_3N_2S$	Butoconazole, Femstat	Imidazole antifungal used in gynecology.
14	$C_{15}H_{18}N_4O_3S$	Methyl 2-{[7-(4-methoxyphenyl)-6,7-dihydro-5H-imidazo[2,1-c][1,2,4]triazol-3-	no specific biological action

		yl]sulfanyl}propanoate	
15	$C_{20}H_{15}Cl_3N_2OS$	Sertaconazole, Sertaconazolum	Antifungal medication to treat skin infections
16	$C_{14}H_{16}N_2$	Atipamezole, Antisedan, 4-(2-ethyl-2,3-dihydro-1h-inden-2-yl)-1h-imidazole	no specific biological action
17	$C_{15}H_{16}Cl_3N_3O_2$	Prochloraz, Mirage, Octave	no specific biological action
18	$C_{15}H_{15}ClF_3N_3O$	Triflumizole, Procure	no specific biological action
19	$C_{22}H_{21}ClN_6O_2$	Losartan carboxylic acid	no specific biological action
20	$C_{22}H_{23}ClN_2O_3$	4'-{[2-Butyl-4-chloro-5-(hydroxymethyl)-1H-imidazol-1-yl]methyl}-2-biphenylcarboxylic acid	In vivo inhibitory activity against angiotensin II
21	$C_{10}H_{16}N_2O_3S$	Biotin, D-biotin, Vitamin H, Coenzyme R, Vitamin B7	Enzyme co-factor present in minute amounts in liver, kidney, pancreas, yeast, and milk.
22	$C_{21}H_{16}FN_3OS$	4-(4-(4-fluorophenyl)-2-(4-(methylsulfinyl)phenyl)-1H-imidazol-5-yl)pyridine	no specific biological action
23	$C_{14}H_{16}N_2O_2$	Etomidate, (R)-Ethyl-1-(1-phenylethyl)-1H-imidazole-5-carboxylate	Anesthetic and hypnotic with little effect on blood gases or the cardiovascular system.
24	$C_{19}H_{24}N_4$	N-[4-(Diethylamino)benzyl]-1-methyl-1H-benzimidazol-5-amine	no specific biological action
25	$C_{12}H_{17}N_7O_5$	2-{2-Methyl-3-[2-(2-methyl-5-nitro-1H-imidazol-1-yl)ethyl]-5-nitro-2,3-dihydro-1H-imidazol-1-yl}acetamide	no specific biological action
26	$C_6H_{10}N_6O$	Dacarbazine, Imidazole carboxamide	Antineoplastic agent has significant activity against melanomas.
27	$C_8H_{12}Cl_2N_6O$	4-[(1E)-3,3-Bis(2-chloroethyl)-1-triazen-1-yl]-4H-imidazole-5-carboxamide	no specific biological action
28	$C_{18}H_{24}N_2O$	Midazogrel, Midazogrelum, (E)-1-(3-Benzyloxyocten-1-yl)imidazole	no specific biological action

References

ANDERSON, A. C. 2003. The process of structure-based drug design. *Chemistry & biology,* 10**,** 787-797.

ASSIRI, A., MCGEER, A., PERL, T. M., PRICE, C. S., AL RABEEAH, A. A., CUMMINGS, D. A., ALABDULLATIF, Z. N., ASSAD, M., ALMULHIM, A. & MAKHDOOM, H. 2013. Hospital outbreak of Middle East respiratory syndrome coronavirus. *New England Journal of Medicine,* 369**,** 407-416.

BROWN, E. G. 2012. *Ring nitrogen and key biomolecules: The biochemistry of N-heterocycles*, Springer Science & Business Media.

CHAFEKAR, A., FIELDIN, F.C., 2018, MERS-CoV: Understanding the Latest Human Coronavirus Threat. *Viruses*, 10(93), 2-22.

CHAN, J. F., LI, K. S., TO, K. K., CHENG, V. C., CHEN, H. & YUEN, K.-Y. 2012. Is the discovery of the novel human betacoronavirus 2c EMC/2012 (HCoV-EMC) the beginning of another SARS-like pandemic? *Journal of Infection,* 65**,** 477-489.

DANIELSSON, N. & CATCHPOLE, M. 2011. Novel coronavirus associated with severe respiratory disease: Case definition and public health measures. *Euro surveillance: bulletin Europeen sur les maladies transmissibles= European communicable disease bulletin,* 17**,** 395-405.

DE GROOT, R. J., BAKER, S. C., BARIC, R. S., BROWN, C. S., DROSTEN, C., ENJUANES, L., FOUCHIER, R. A., GALIANO, M., GORBALENYA, A. E. & MEMISH, Z. A. 2013. Middle East respiratory syndrome coronavirus (MERS-CoV): announcement of the Coronavirus Study Group. *Journal of virology,* 87**,** 7790-7792.

GENG, H. & TAN, W. 2013. A novel human coronavirus: Middle East respiratory syndrome human coronavirus. *Science China Life sciences,* 56**,** 683-687.

GILCHRIST, T. L. 1997. *Heterocyclic chemistry*, Prentice Hall.

GRIMMETT, M. R. 1997. *Imidazole and benzimidazole synthesis*, Academic press.

GUBERINA, H., WITZKE, O., TIMM, J., DITTMER, U., MULLER, M., DROSTEN, C. & BONIN, F. 2014. A patient with severe respiratory failure caused by novel human coronavirus. *Infection,* 42**,** 203-206.

GUERY, B., POISSY, J., EL MANSOUF, L., SEJOURNE, C., ETTAHAR, N., LEMAIRE, X., VUOTTO, F., GOFFARD, A., BEHILLIL, S. & ENOUF, V. 2013. Clinical features and viral diagnosis of two cases of infection with Middle East Respiratory Syndrome coronavirus: a report of nosocomial transmission. *The Lancet,* 381**,** 2265-2272.

KATRITZKY, A., POZHARSKI, A. & SOLDATENKOV, A. 1997. Heterocycles in life and society. Wiley: NewYork.

KIM, Y.S., SON, A., KIM, J.H., KWON, S.B., KIM, M.H., KIM, P., KIM, J.E., BYUN, Y.H., SUNG, J.M., LEE, J.H., YU, J.E., PARK, C., KIM, Y.S., CHO, N.H., CHANG, J. SEONG, B.L. 2018. Chaperna-Mediated Assembly of Ferritin-Based Middle East Respiratory Syndrome-Coronavirus Nanoparticles. *Front. Immunol.* 9, 1093.

MAILLES, A., BLANCKAERT, K., CHAUD, P., VAN DER WERF, S., LINA, B., CARO, V., CAMPESE, C., GUERY, B., PROUVOST, H. & LEMAIRE, X. 2013. First cases of Middle East Respiratory Syndrome Coronavirus (MERS-CoV) infections in France, investigations and implications for the prevention of human-to-human transmission, France, May 2013. *Middle East Respiratory Syndrome Coronavirus (MERS-CoV),* 12**,** 19.

MEMISH, Z. A., ZUMLA, A. I. & ASSIRI, A. 2013. Middle East respiratory syndrome coronavirus infections in health care workers. *New England Journal of Medicine,* 369**,** 884-886.

MARIA, B., SHAH, M., PATRA, M.C., YESUDHAS, D. 2017. Structural insights into the Middle East respiratory syndrome coronavirus 4a protein and its dsRNA binding mechanism. *Sci Rep,* 7, 11362.

PEIRIS, J., GUAN, Y. & YUEN, K. 2004. Severe acute respiratory syndrome. *Nature medicine,* 10**,** S88-S97.

PERLMAN, S. & NETLAND, J. 2009. Coronaviruses post-SARS: update on replication and pathogenesis. *Nature Reviews Microbiology,* 7**,** 439-450.

PUZELLI, S., AZZI, A., SANTINI, M., DI MARTINO, A., FACCHINI, M., CASTRUCCI, M., MEOLA, M., ARVIA, R., CORCIOLI, F. & PIERUCCI, F. 2013. Investigation of an imported case of Middle East respiratory syndrome coronavirus (MERS-CoV) infection in Florence, Italy, May to June 2013. *Euro Surveill,* 18**,** 20564.

RADWAN, A.A., ALANAZI, F.K. 2018. In silico studies on novel inhibitors of MERS-CoV: Structure-based pharmacophore modeling, database screening and molecular docking. *Trop. J. Pharm. Res.* 17(3), 513-517.

ROSEMEYER, H. 2004. The chemodiversity of purine as a constituent of natural products. *Chemistry & biodiversity,* 1**,** 361-401.

SAIF, L. 2004. Animal coronaviruses: what can they teach us about the severe acute respiratory syndrome? *Revue scientifique et technique (International Office of Epizootics),* 23**,** 643-660.

SCHNEIDER, G. 2010. Virtual screening: an endless staircase? *Nature Reviews Drug Discovery,* 9**,** 273-276.

SHARGEL, L. & SWANSON, L. N. 2004. *Comprehensive pharmacy review*, Lippincott Williams & Wilkins.

TO, K. K., HUNG, I. F., CHAN, J. F. & YUEN, K.-Y. 2013. From SARS coronavirus to novel animal and human coronaviruses. *Journal of thoracic disease,* 5**,** S103-S108.

VAN BOHEEMEN, S., DE GRAAF, M., LAUBER, C., BESTEBROER, T. M., RAJ, V. S., ZAKI, A. M., OSTERHAUS, A. D., HAAGMANS, B. L., GORBALENYA, A. E. & SNIJDER, E. J. 2012. Genomic characterization of a newly discovered coronavirus associated with acute respiratory distress syndrome in humans. *MBio,* 3**,** e00473-12.

VAN DER HOEK, L., PYRC, K., JEBBINK, M. F., VERMEULEN-OOST, W., BERKHOUT, R. J., WOLTHERS, K. C., WERTHEIM-VAN DILLEN, P. M., KAANDORP, J., SPAARGAREN, J. & BERKHOUT, B. 2004. Identification of a new human coronavirus. *Nature medicine,* 10**,** 368-373.

WALTERS, W. P., STAHL, M. T. & MURCKO, M. A. 1998. Virtual screening—an overview. *Drug Discovery Today,* 3**,** 160-178.

WASZKOWYCZ, B., PERKINS, T. D. J., SYKES, R. A. & LI, J. 2001. Large-scale virtual screening for discovering leads in the postgenomic era. *IBM Systems Journal,* 40**,** 360.

WOO, P. C., LAU, S. K., CHU, C.-M., CHAN, K.-H., TSOI, H.-W., HUANG, Y., WONG, B. H., POON, R. W., CAI, J. J. & LUK, W.-K. 2005. Characterization and complete genome sequence of a novel coronavirus, coronavirus HKU1, from patients with pneumonia. *Journal of virology,* 79**,** 884-895.

ZANCO Journal of Pure and Applied Sciences
The official scientific journal of Salahaddin University-Erbil
https://zancojournals.su.edu.krd/index.php/JPAS

ISSN (print):2218-0230**, ISSN (online):** 2412-3986**, DOI: http://dx.doi.org/10.21271/zjpas**

RESEARCH PAPER

Some Biological Aspects Of *Carpocoris coreanus* Distant (Hemiptera: Pentatomidae) In Kurdistan Region-Iraq

Banaz Sedik Abdulla [1,]Nabel Abdulkader Moulod[2,] Abdulbaset M. Amin Mohammed[3]

[1] Department of Biology- College of Education- Salahaddin University-Erbil, Kurdistan region, Iraq.
[2].Department of Plant protection -College of Agriculture-Salahaddin University-Erbil, Kurdistan Region-Iraq.
[3]Department of Forestry -College of Agriculture -Salahaddin University- Erbil, Kurdistan Region-Iraq.

A B S T R A C T:
The biological study of *Carpocoris coreanus* Distant carried out in March 2011 on wild mustard *Brassica nigra* (L.) at 25 Cº and 33% R.H. It has been found that the overwintered adult in the hibernated region of stink bug C. coreanus began their activity in the March of 2011, which overwinters inside the adult stage. The mean period of pre-oviposition, oviposition and post-oviposition were reached 8.2, 34.8 and 4 days, respectively. The average of adult longevity on mustard was 37.2 days for male and 46.6 days for female. The egg is barrel, brownish when newly laid, usually deposited in masses egg mass number of C. coreanus in this study averaged 8 masses/female, with an average 15.7 eggs/mass. The mean incubation period was 12 days, and egg hatching ratio approached 79.4%. The nymphs completed their development within five instars, with the mean period of 6.5±0.83, 7.8±1.15, 7.3±0.66, 9.3±0.66 and 12.8±0.96 days for the 1st, 2nd, 3rd, 4th and 5th nympal instars, respectively. It was found that stink bug C. coreanus has one generation per year.

KEY WORDS: Sunn bug, egg, nymph, developmental time .
DOI: http://dx.doi.org/10.21271/ZJPAS.31.2.11
ZJPAS (2019) , 31(2);79-88 .

INTRODUCTION :

Pentatomidae, is member of the order Hemiptera, suborder Hetroptera, they occur in the super family Pentatomoidea, commonly known as stink bugs, are worldwide in distribution with approximately 760 genera and 4l00 described species (Schuh and Slater,1995). The majority of economical important stink bugs belong to subfamily Pentatominae Panizzi, 1997).

Members of this family are characterized by round or oval bodies, with five-segmented antenna, tibia bristly rather than spiny, three-segmented tarsus and scutellum that is more or less triangular in shape almost rarely covering the abdomen (Panizzi, 1997, Panizzi *et al.*, 2000). They are called stink bugs because they discharge a strong disagreeable scent (odor), by means of their scent gland (Alston and Reding, 2003).

The stink bugs undergo incomplete metamorphosis, their eggs hatch to nymphs that develop to adults (McBrien and Millar, 1999). They have single generation annually and in almost all species the adult is the overwinter stage (Dolling, 1999). The Family is very important

* **Corresponding Author:**
Abdulbaset M. Amin Mohammed
E-mail: abdulbaset.mohammed@su.edu.krd or profabed57@yahoo.com
Article History:
Received: 08/10/2018
Accepted: 18/02/2019
Published: 28/10 /2018

from an agricultural point of view, they feed by inserting their styletes into the food source to suck up nutrients so they cause injury
to plant tissue, resulting the plant wilt (Pannizi, 1997, McBrien and Millar, 1999, Panizzi *et al*.,2000). Because some feed on several plant species of economic importance they are regarded as major pests. Among the more widespread species are the *Dolycoris baccarum* (L.) *Piezodorus lituratus* (Fab.), *Carpocoris mediterraneus* (Tam), *C. Purpureipennis* (Degeer), *Eurydema ornatum* (Linnaeus), *Codophila varia* (Fabr.) and *Aelia acuminate* (Linnaeus) (Dolling, 1999, Nihataktak 1999). The aim of this work is to study some biological aspects of *Carpocoris coreanus* which was important for integral pest management.

Materials and Methods

The biological study of *C. coreanus* Distant was performed in the Erbil City by rearing the insects from eggs to adult inside wooden cages (30×30×60 cm) the front side made of glass and the other sides covered by mesh. The adult bugs were collected from different sites in Erbil county Kurdistan region, and transferred to wooden cages for biological study. Each couple were captured in one cage, the cage contain fresh plants of mustard *Brassica nigra* (L.) were placed in small tubes filled with water, (with five replication) to determine oviposition; egg incubation period; nymph development and adult life span. Young sugar beet plants, shelled sunflower seeds, moist cotton served as a source of food and water. Eggs on leaves were carefully transferred to Petri-dishes with moist filter paper and moist cotton, recorded observation daily till hatching the eggs. One day first nymphal instar remained on their egg shells, while second nymphal instar moved more freely inside the petri-dish. Fresh plants of mustard and sunflower seeds were provided every second or third day during nymphal growth period. In addition of cotton soaked in water or in 10% of honey solution, sprinkled with a small amount of yeast extract (Conradi-larsen and Somme 1973.

Overwintering.

To find the sites as habitat for winter hibernation, a survey was done in many places, in Erbil governorate. Many visits were performed in different time in those places. The visits were done during November 2011 to March 2012. This process included the observation of all parts of the fruit, non-fruit trees, wild plants and shrubs grow in these regions (Mohammed, 2009).

Results and Discussions

1-Pre oviposition, oviposition and post oviposition periods.

The pre-oviposition period ranged (Nihataktak 1999, Mcpherson, 1982) from March 10 to March 20/ 2011. The females started laying eggs on March 18 and continued until April 25/ 2011, the oviposition period ranged from (33 - 36) days and the post-oviposition period ranged from (3 - 5) days, with an average of 8.2, 34.8 and 4 respectively for pre-oviposition, oveposition and post oviposition periods at 25 C° and 33% R.H as shows in Table-1. Mating started in spring and eggs are laid in masses on leaves and twigs of host plants (Mcpherson, 1982). Mating is done back to back, usually begins with the male courtshiping the females, but eventually concert rating on or near the tip female abdomen this may be sufficient to stimulate the female to raise the tip of female abdomen for aedeagus insertion. If successful, copulation last for several hours, in this end to end position, and both individuals may feed during this time (Mcpherson and Mcpherson, 2000). These results agreed with that of (Hallnan *et al.,* 1992) who mentioned that the mean of pre-oviposition period of *Acrosternum marginatum* reached to 10.1 ± 1.31 days. Nielsen *et al.,* (2008) found that the pre-ovipositon period for *Halymorpha halys* (Stal.) averaged 13.35. Mohammed , (2009) indicated that the pre-oviposition period ranged between 3-6 days for the first generation of *A. amygdali*, but the overwintered females of the second generation have along pre-oviposition period began to lay their eggs after hibernation.

Table (1): Pre-oviposition, oviposition and post-oviposition periods of *C. coreanus* Distant, in outdoor conditions in Erbil City at 25 C° and 33% R.H.

Cage No.	Pre – oviposition period		Oviposition period		Post- oviposition period		Total days
	Dates	Days	Dates	Days	Dates	Days	
1	10/3-18/3/2011	8	19/3-23/4/2011	36	24/4-28/4/2011	5	49
2	10/3-17/3/2011	7	18/3-19/4/2011	33	20/4-23/4/2011	4	44
3	10/3-20/3/2011	10	21/3-25/4/2011	36	26/4-28/4/2011	4	50
4	10/3-19/3/2011	9	20/3-23/4/2011	35	24/4-26/4/2011	3	47
5	10/3-17/3/2011	7	18/3-20/4/2011	34	21/4-24/4/2011	4	45
Avg.		8.2		34.8		4	47

2- Adult Longevity.

The life span of adult in outdoor cages takes an average of 43.3 and 37.2 days for female and male respectively, at 25 C° and 33% R.H (Table -2). The result indicated that the females lived longer time than the male. This result nears with that of Panizzi *et al.,* (2000) who indicated that the longevity for male and female *P. lituratus* on broom was 59 and 100 days, respectively. The female of *Acrosternum marginatum* lived mean of 44.4 ± 2.84 days (Hallnan *et al.,* 1992, Singii and Malik, 1993) found that the female and male adults of painted bug survived for 25.9 and 20.9 days respectively.

Table (2): Longevity of adult C.coreanus Distant in outdoor conditions in Erbil city at 25 C° and 33% R.H.

Cage No.	Female life span		Male life span	
	period	Days	period	Days
1	10/3-28/4/2011	43	10/3-19/4/2011	41
2	10/3-23/4/2011	44	10/3-14/4/2011	36
3	10/3-28/4/2011	40	10/3-5/4/2011	37
4	10/3-26/4/2011	45	10/3-28/4/2011	32
5	10/3-24/4/2011	44	10/3-10/5/2011	40
Avg.		43.3		37.2

3-Female oviposition behavior.

Eggs are barrel-shaped with a detachable cap (pseudoperculum), dull brownish color when freshly laid, then changed to light color and laid in masses, closely packed in four irregular rows (Fig.1-A). There are differences in the number of mass and the number of eggs per mass which are laid by each female. These results confirmed with that of Southwood , (1956) who pointed that the Pentatomide eggs, always oviposited in clusters, they are characterized by their shapes (barrel and cylindrical or spherical), and variable degree of chorion ornamentation and with Javahery , (1994) mentioned that the eggs of *C. coreanus* are barrel-shaped, brownish and laid in masses of 14 eggs in four rows. From the data obtained in the (Table -3 number of masses ranged between (5-10) mass, with an average of 8 masses average number of eggs per mass ranged from (14 -17.2) eggs at 25 C° and 33% R.H. which firmly stuck together and adhere to the host by a sticky secretion from the accessory glands, with a total of (86 - 148) eggs per female.

Eggs are laid in various parts of host particularly on the lower surface of leaves and the wall of the petri dish. These results agreed with Mcpherson, (1982) who indicated that the eggs are laid in masses on various exposed parts of the plant, particularly on leaves, and fixed by sticky secretion. Also with Todd, (1989) who suggested that the southern stink bugs laid eggs under surface of leaves. And with Candan and Suludere, (1999) who reported that each female of *C. pudicus* generally deposited 14 barrel-shaped eggs in a mass. Stink bug eggs are deposited on host plants in polygonal masses. Each mass may contain several to more than 70 barrel-shaped eggs that are tightly packed in rows (Bunddy and Mcpherson, 2000). Mcpherson and Mcpherson , (2000) reported that the green stinkbug *Nezara viridula* deposited lemon yellow to pea green eggs in loosely uniform rows, each egg masses have been consisting of a maximum of 40 to 69 eggs. In another biological study. Panizzie et al,. (2000) found that *Piezorous lituratus* eggs are barrel-shaped, blackish color with two circles of white or creams band. Bernon , (2000) observed that the stink bug *Acrosternum hilare* always laid egg masses on underside of leaves, not near the leaf margin. Matesco *et al* ., 2007) found that each female of *Chinavia pengue* (Roston) laid an average of 15.9±4.18 egg mass and 218.8 ±48.69 eggs with a marked peak at 14 eggs per egg mass. Mohammed, (2009) observed that the female of *A. amygdali* laid its eggs in masses usually 14 eggs per each mass.

Table (3): Oviposition behavior of *C. coreans* Distant in outdoor conditions in Erbil City at 25 C° and 33% R.H.

Cage No.	Egg Masses	Avg. No. Eggs per mass	Total eggs
1	7	16±1.3	112
2	5	17.2±0.16	86
3	10	14.8±0.91	148
4	10	14.0±0.77	140
5	8	16.5±0.72	132
Avg.	8	15.7	123

4-Eggs hatching.

(Table -4) shows that the mass contains an average of 15 eggs, and takes an average 12 days of incubation period at 25 C° and 33% R.H the percentage of hatching ranged from 66.6 to 88.8% with the average 79.4% at 25 C° and 33% R.H. Eggs were found in both of plant parts and the wall of the petri-dish. Hatching begin with peristaltic contraction of the body of the hatched nymph from the posterior to anterior which forces the blunt sclerotized tooth of the egg burster, against the anterior pole of the eggs. Egg bursters of *C. coreanus* are T-shaped and dark color as shows in (Photo.1-B). The egg burster is a median sclerotized area of the embryonic cuticle that is present in 35 species of pentatomoidea (Javahery 1994). These results agreed with Southwood, (1956) who pointed that the pentatominae egg-burster is well

marked and T-shaped. Also with Puchkoval, (1961) who indicated that the inverted T-shaped egg burster found in eggs of

various species of pentatomoidea such as *Sciocoris sulcaus, Bagrada stolata*, *Palomena prasina* and *Pentatoma rufipers*; other species like *D. baccarum* and *Piezodorus lituratus* have Y-shaped egg burster. Candan and Suludere, (1999) in their studies on the external morphology of *C. pudics* eggs founded that the T-shaped egg bursters are dark and sclerotized. The incubation period of *A. hilari* eggs takes (10 – 15) days (Bensebbane, 1981). Javahery, (1994) indicated that the incubation period takes 14 to15 days of *C. fuscispinus* eggs in the field. *N. viridula* eggs require 6 days of incubation at 33 C° (Mcpherson and Mcpherson, 2000). According to Mohammed, (2009) the mean incubation period for *A. amygdali* eggs on the apricot tree was 3.5 days at 36.05 C° and 31% R.H.

Saruhan*et al* ., (2010) in their biological studies on the development of *Palomena prasina,* showed the incubation period and hatching ratio were 5.47 days and 90.7 %, respectively at 28 C° .

Table (4): Number of eggs per mass, incubation period and hatching percent of *C. coreanus* Distant in outdoor conditions in Erbil City at 25 C° and 33% R.H. .

Eggs masses No.	No. of eggs/masses	Incubation period (Days)	Hatching %
1	**18**	**14**	**88.8**
2	**14**	**10**	**78.5**
3	**16**	**12**	**66.6**
4	**15**	**12**	**76.9**
5	**13**	**10**	**78.9**
6	**14**	**14**	**87.5**
Avg.	**15**	**12**	**79.4**

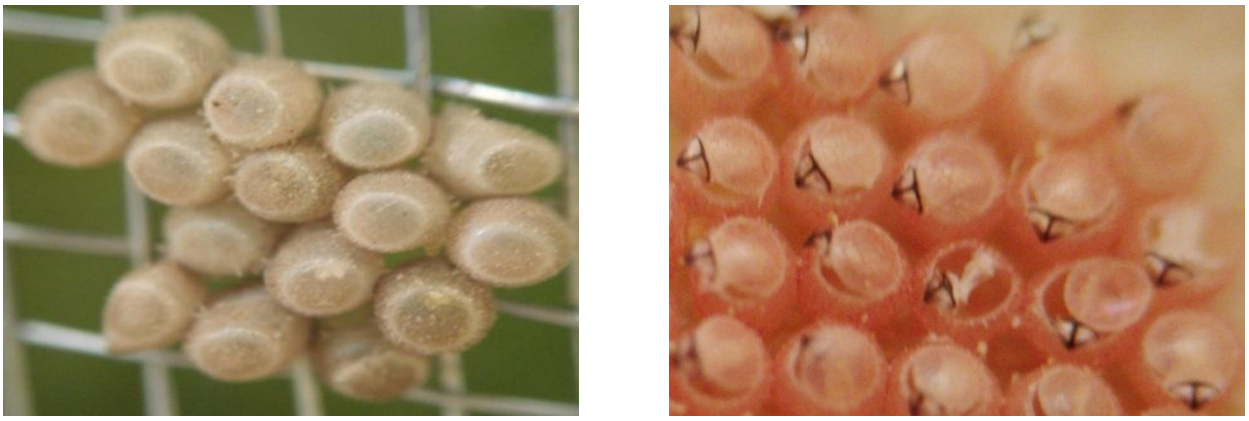

Figure (1): Egg masses of *C. coreanus* Distant (A) New laid eggs; (B) Hatched eggs.

5- Nymphal development.

Data in the (Table-5) shows the nymphal stages specific development rate. The mean duration in day of 1st, 2nd, 3rd, 4th and 5th instars was 6.5 ± 0.83, 7.8 ± 1.15, 7.3 ± 0.66, and 9.3 ± 0.66 and

12.8 ± 0.96 days, respectively. Nymphal development takes 42.7 days at 25 C° and 33%

R.H. Nymphs of *C. coreanus* hatch from the eggs and pass through five instars before becoming adults. First nymphal instar (Figure.2-A), aggregated and remain clustered around egg masses until molting to the second instar and remain inactive without feeding, feeding activity begins during the second instar, and generally a quire food by puncturing plant tissues with their piercing sucking mouthparts and removing cell content, as the bugs pass through the remaining instars (Figure. 2-A, B, C, D, E and F) until change occurs in the marking, patterns, and number of punctures, setae and development of the wing pads (Panizzi 1997). Wing pads are distinctive in the fourth and fifth instar, that they can be used to distinguish these instars from each other and from younger instar (Mcpherson and Mcpherson, 2000). Aggregation is believed to occur as a defensive strategy against predator uptake of symbionts from the eggs, or for improved humidity control and is believed to development time (26,11,27 and 13) . Dolling (1991) suggested they stay clustered on the remains of the egg-mass, ingesting the symbiotic bacteria that the female smeared on the eggs as she laid them. This result agreed with Todd , (1989) who suggested that the first instar nymph enclose within five days, and remain aggregated on or near the egg mass without feeding, then the nymph begin to disperse slightly and feed after the first molt, but aggregation may continue through the third molt, this nymphal aggregation up to the fourth instars may provide a measure of protection from predator. Conradi- Larsen and Somme , (1973) recorded that the development from egg to adult of *D. baccarum* at 21 C° takes 48 to 52 days. Nymphal development from 1st to 5th instars in *C. fuscispinus* takes 45 days (Javahery, 1994). Gyeitshen *et al* ., (2005) indicated that the brown marmored stink bug *Halys dentatus* (F.) has five nymphal instars, and each stages lasts approximately one week, depending upon temperature. mentioned that the period of the five nymphal instar of *A. amygdali* lasted a mean period of 4.0, 7.7, 7.8, 8.7 and 9.3 days for the 1st, 2nd, 3rd, 4th and 5th nympal instars, respectively.

Table (5): Duration in days of the nymphal instars of *C. coreanus* Distant in outdoor conditions in Erbil City at 25 C° and 33% R.H.

Instars	No. of nymph	Nymphal period(days)	
		Range	Average
1st	20	5-7	6.5±0.83
2nd	19	6-9	7.8±1.15
3rd	17	6-8	7.3±0.66
4th	14	8-10	9.3±0.66
5th	12	12-14	12.8±0.96
Total	82	37-48	42.7

(D) (40X) (E) (40X) (F) (20X)

Figure (2): Nymphal instars of *C. coreanus* Distant (A) first nymphal instar (B) First nymphal instar aggregation (C) Second nymphal instar (D) Third nymphal instar (E) Fourth nymphal instar (F) Fifth nymphal instar.

(A)

Dorsal view **Ventral view**

(4X

(B)

Dorsal view **Ventral view**

Figure(3):*C. coreanus* Distant adult stage (A) Male (B) Female.

6 - Overwintering.

Field observation indicated that the *C. coreanus* overwinter in adult stage and has only one generation per year. They hide under many wild plants and debris through aestivation and hibernation, it has been found that aestivation spend underneath the plants like *Astragallus russelli, Thymbra vlugris* (Thyme), also under, the falling leaves of *Quercus aegiliops* L. and *Pistacia atlantica* These plants grow naturally on

the top of the mountains at different altitudes, generally higher than 1900 meters they do not exist in mountain side or at the base, and in addition to providing shelter to adult they protect the insect from critical conditions of temperature, relative humidity, wind, sunlight and natural enemies. Stink bugs move from wild host plants to cultivated field crops coincides with seed development stages of the hosts, then become active in the spring, and have been observed as early in March. Kobayashi, (1972) suggested that *D. baccarum* has a bivoltine life cycle in. Jones and Sullivan, (1981) reported winter mortality levels and spring emergence pattern among several hemipterans from various overwintering habitats. Adult species of *Carpocoris* enter aestivation on the mountain summit and then they resume their movement from the top to the mountain sides toward to the base of the mountain for overwintering. They hide under fallen leaves and rooks for months, this migration perform by the insects to protect itself against the winter condition. Javahery, (1994) indicated that *C. fuscispinus* migrate to higher altitudes during early summer and returns to the breeding areas during the following spring. Overwintered adults appear in the field during April to May and feed on green shoots, leaves and stems. Yousif, (1995) found that the stink bug *A. amygdali* spend the winter in adult stage from the 4th week of November 1993 till the end of April 1994. Mcpherson and Mcpherso, (2000) indicated that the brown stink bugs are bivoltin, while green stink bugs have been reported as both univoltin and bivoltin depending upon its geographical location. Mohammed, (2002) reported that the stink bug *D. baccarum* used Safeen Mountain in Erbil governorate for hibernation. Bernon , (2004) observed adults of stink bug *H. halys* were leaving overwintering sites at the end of April near the Rodale tree farm site, and not observed on host plants at the monitoring site until late May. Mehmet and Ozlem , (2005) reported that prediapausing adults of *D. baccarum* and *P. lituratus* spend the summer in fields, while diapausing individual spend the winter in overwintering localities under stones and wild plants. Adults of *D. baccarum* started reproduction soon after adult emergence under long-day condition while they entered diapauses under short-day condition (Nakamura and Numata , 2006).

References:

Alston, D. G. and Reding, M. E. (2003). Cat-Facing insects (Lygus bugs, stink bugs and box elder bugs) on tree fruits. Extension entomology, department of biology, London, UT 84322. Uton state university.

Bernon, G. (2004). Biolog of Halyomorpha halys, the Brown Marmorated stink bug (BMSB). Final report –U.S Dep. Agric. APHIS CPHST http://cphst.aphis.usda.gov/docs/Bernonfinal report T3P01.

Bensebbane, C.G. (1981). Les punaisis des bles en. Algeric. Bull. OEPP. 71: 33-38.

Bunddy, C. S. and McPherson, R. M. (2000). Morphological examination of stink bugs (Heteroptera: Pentatomidae) eggs on cotton and soybean with a key to genera. Ann. Entomol. Soc. Am., 93:616-624.

Candan, S. and Suludere, Z. (1999). External morphology of eggs of Carpocoris pudicus (Poda, 1761) (Heteroptera: Pentatomidae). J. Entomol. Soc. Res., 1(2):21-26.

Conradi-larsen, E. and Somme, L. (1973). Note on the biology of Dolycoris baccarum L. (Heteroptera: Penatomidea) Nor. Entomol. Tidsskr. 20:245-247.

Dolling, W. R. (1991). The Hemiptera. Oxford: Oxford University press 274pp.

Gyeltshen, J.; Bernon, G. and Hodes, A. (2005). Brown marmorated stink bug Halyomorpha halys Stal (Insecta: Hemiptera: Pentatomidae). Floridia Cooperative Extension service.Unvercity of Floridae.,p.

Hallnan, G. J; Morales, C. G. and Dugue, M. C. (1992). Biology of Acrosternum marginatum (Heteropters:

Pentatomidae) on common bean. Florida Entomologist, 75(2): 190-197.

Javahery, M. (1994). Development of eggs in some true bugs (Hemiptera-Heteroptera). Part 1, Pentatomiodea, Can. Entomol., 126: 401-433.

Jones, W. A. and Sullivan, M. J. (1981). Overwintering habits, spring emergence patterns and winter mortality of some South Carolina Hemiptera. Environ. Entomol., 10: 409-414.

Kobayashi, T. (1972). Biology of insect pests of soybean and their control. JARQ., 6 (4):212-218.

Matesco, V. C.; Schwertner, C. F. and Grazia, J. (2007). Morphology of the immature and Biology of Chinavia pengue (Rolston) (Hemiptera: Pentatomidae). Revista Brasileira de Entomologia, 51(1): 93-100.

McBrien, H. L. and Millar, J. G. (1999). Phytophagous bugs. In: Hardy, J. and Minks, A. K (Eds) Pheromones of non-lepidopteran insects associated with agricultural plants. CABI International. Wallingford. Oxon OX10 8DE, UK. : 277-304.

McPherson, J. E. (1982). The pentatomidea (Hemiptera) of North America with emphasis on the found of Illinois. Southern Illinois Univ. press. Carbondale and Edwardsville – 240pp.

McPherson, J. E. and McPherson, R. M. (2000). Stink bugs of economic importance in America North of Mexico. CRC Press II.C .271pp.

Mehmet, B. and OZlem, C. (2005). Change in chomposition of phospholipid and Triacylglycerol fatty acid prepared from prediapausing and diapausing adults of Dolycoris baccarum (L.) and Piezodorus licturatus (F.) (Heteroptera: Pentatomidae). Ann. Entomol. Soc. Am., 98 (4): 575-579.

Muhammad, A. M. (2002). The occurance of the sun pest Dolycoris baccarum (L.) in hibernated location on Safeen Mountain in Erbi- Iraq. J. of Duhuk Univ., 5(2): 53-60.

Mohammed, S. H. (2009). Bio-Ecological study and control of Apodiphus amygdali (Germar). (Heteroptera: pentatomidae) on some fruit trees in certain localities of Erbil governorate. PhD. Thesis, college of Science Education Salahaddin University – Erbil – Iraq. 108 pages.

Nakamura, K. and Numata, H. (2006). Effect photoperiod and temperature on the induction of adult diapause in Dolycoris baccarum (L.) (Heteroptera: pentatomidae) from Osaka and Hokkaido, Japan. APPL. Entomol., 41(1):105-109.

Nielsen, A.; George, C.; Hamilton, C. and Matadha, D. (2008). Developmental rate estimation and life table analysis for Halymorpha halys (Hemiptera: pentatomidae). Environ. Entomol., 37(2):348-355.

Nihataktak, M. F. (1999). Taxonomic and faunistic studies of the fauna Pentatomidae (Heteroptera) in the region of Erdin. Tr. J. Zool., 23(2): 377-395.

Panizzi, A. R. (1997). Wild host of pentatomids: Ecological significance and role in their pest status on crops. Ann. Rev. Entomol., 42: 99-122.

Pannizi, A. R.; McPherson, J. E.; James, D. G.; Javahery, M. and McPherson, R. M. (2000). Stink bugs (pentatomidae). 421-474 pp. In Scheafer, C. W. and Panizzi, A. R., (eds) Heteroptera of Economic Importance. Boca Raton: CRC Press, 828pp.

Puchkoval, L.V. (1961).The eggs of Hemiptera VI. Pentatomoidea; 2. Pentatomidae and Plataspidae. Rev. Entomol., 40:131-141.

Saruhan, I.; Tuncer, C. and Akca, I. (2010). Development of green shield bug Palomena prasina L. (Heteroptera: Pentatomidae) in different tempreture. Zemdiobyste - Agriculture, 97(1): 55-60.

Schuh, R. T and Slater, J. A. (1995). True bugs of the world (Hemiptera: Heteroptera). Classification and Natural History. Ithaca and London: Cornell University press Xii 349pp.

Singii, H. and Malik, V. S. (1993). Biology of painted bug Bagrada cruciferarum. Indian, J. Agric. Sci., 63(10):672-674.

Southwood, T. R. E. (1956). The structure of the eggs of the terrestrial Heteroptera and its relationship to the classification of the group.Trans. R. Entomol. Soc. Lond., 108:163-221.

Todd, J.W. (1989). Ecology and behavior of Nezara virdula. Ann. Rev. Entomol., 34:274-292.

Yousif, A. H. (1995). Ecological and Biologica Istudi lstudies of the Fruit tree bark bug Apodiphus amygdali (Germar) (Hemiptera: Pentatomidae).M.Sc. Thesis University of Bagdad, Iraq.46pp.

ZANCO Journal of Pure and Applied Sciences
The official scientific journal of Salahaddin University-Erbil
https://zancojournals.su.edu.krd/index.php/JPAS

ISSN (print):2218-0230**, ISSN (online):** 2412-3986**, DOI: http://dx.doi.org/10.21271/zjpas**

RESEARCH PAPER

Impact of bicalutamide, an anti-androgen on rat testis

Azheen S. Abdulrahman* and Inaam A. Mustafa

Department of Biology, College of Science, Salahaddin University-Erbil, Kurdistan Region, Iraq.

A B S T R A C T:

Bicalutamide/Casodex is a non-steroidal anti-androgen drug which used in treatment of prostate cancer. Castration by using anti-androgens such as bicalutamide became a successful strategy for prostate cancer metastasis suppression. The goals of the present work were to study the body weight, biochemical, histological and immunohistochemical changes induced by daily administration of bicalutamide 0.8mg/Kg body weight of rats. Treatment with bicalutamide caused non-significant decrease in relative testis weight, disturbing the histological architecture of the testis, decrease of sperm count, germinal layer depletion, increasing the apoptotic index of germinal layer cells and a decrease in testosterone level compared to control. In conclusion, bicalutamide treatment induced various biochemical, histological and immunological changes in rat testis.

KEY WORDS: Bicalutamide; Testes; Testosterone; Anti-androgen
DOI: http://dx.doi.org/10.21271/ZJPAS.31.12
ZJPAS (2019), 31(2);89-100 .

1. INTRODUCTION

Anti-androgen drugs have prospective to interfere abnormality in both human and animal male reproductive system development as well as functions (Sharpe, 2006, Metzdorff *et al.*, 2007). Bicalutamide is an orally active and non-steroidal anti-androgen drug which used with luteinizing hormone-releasing hormone agonist to decrease symptoms in patients with a metastatic prostate neoplasm and used mostly during the initiation of androgen deprivation therapy (Hussain *et al.*, 2014). The chemical formula of bicalutamide is (2RS)-4´- cyano-3-(4-fluorophenylsulphonyl)-2-hydroxy-2-methyl-3´ (trifluoromethyl)-propionanilide (Fig. 1) (Fradet, 2004).

* **Corresponding Author:**
Azheen S. Abdulrahman
E-mail: Azheen.abdulrahman@su.edu.krd
Azheen.subhi@yahoo.com

Article History:
Received: 27/01/2019
Accepted: 26/02/2019
Published:23/04 /2019

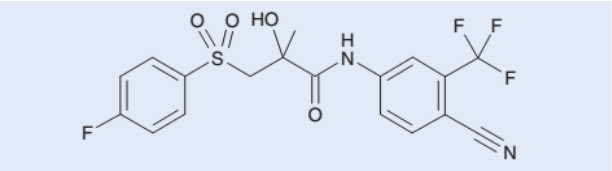

Figure 1: The chemical formula of bicalutamide (Fradet, 2004).

The combination of anti-androgen drugs and castration inhibit androgen synthesis by testes and block residual adrenal androgens at the level of receptor (Hussain *et al.*, 2014), thereby blocking the negative feedback mechanism that regulates testosterone hormone concentration (McLeod and Iversen, 2000), bicalutamide is a competitive inhibitor of androgens at the level of receptor (Furr *et al.*, 1987) and it is pure anti-androgen that exhibits only antagonist activity (Térouanne *et al.*, 2000).

Bicalutamide certainly reduced the mean testicular weight in the adult Sprague –Dawley rats (Khurshid *et al.*, 2014). Researches on male rats have revealed that bicalutamide drug had few

effects on serum luteinizing hormone and testosterone hormone concentrations (Freeman *et al.,* 1989, Furr and Tucker, 1996). Bicalutamide had adverse effects like prostate, testis and seminal vesicle atrophy, as well as Leydig cell hyperplasia which resulting from suppressing of pituitary feedback by testosterone hormone (Iswaran *et al.,* 1997). Reduction of testicular weight and associated histological changes were noted after administration of anti-androgen in an androgen-stimulated testis of rats (Kennel *et al.,* 2003).

Although more information about use of bicalutamide in clinical research and castration mechanism available(Lee *et al.,* 2018, Stanisławska *et al.,* 2018, Sekino *et al.,* 2019), there is more information we should know about castration by this anti-androgen drug and it's histological and biochemical effects in the testes of experimental animals, therefore, the present investigation aimed to evaluate the histological and biochemical effects induced by bicalutamide which may be behind its castration and anti-androgenic role.

2. MATERIALS AND METHODS

2.1. Experimental Animals

Current investigation was carried out by using 12 adult healthy Wistar rats. They were weighing 200-270gm and 8-10 weeks old. The animals were bred in controlled temperature and light of 24 ± 3℃ and 12/12 hrs light/dark respectively. Biology department animal house in college of science-Salahaddin University was used to conduct the study and all experiments were performed according to the protocols approved by the animal care ethic committee of Salahaddin University-College of Science (Erbil-Iraq).

2.2. Bicalutamide (Casodex)

Bicalutamide 50mg film-coated tablets (manufactured by AstraZeneca UK). Each tab contains 50mg of bicalutamide and during the current study, one dose of bicalutamide has been chosen which was 0.8mg/Kg of rat which orally administrated daily by gavage.

2.3. Experimental design

Rats were classified randomly into two groups, Group 1 (control group) which received 1 ml distilled water and Group 2 (treated group) which received bicalutamide at dose of 0.8mg/kg of rat dissolved in distil water (0.2 mg per rat which dissolved in 1 ml distilled water), and given orally via gavage for 45 days.

2.4. Relative testicular weight determination

From anesthetized and sacrificed rats, both testes were removed and then testicles were excised free of surrounding tissues and weighed by balance. Relative testes weight was calculated by following equation: Relative testis weight = (testis weight/body weight) x 100 (Mossa *et al.,* 2015).

2.5. Determination of testosterone concentration

Serum testosterone concentration of all rats were estimated by using Cobas 6000 instrument in Bio Lab private, Erbil. The assay principle of estimate testosterone hormone was combines an enzyme immunoassay competition method with a final fluorescent detection. Finally, the serum testosterone concentration results were calculated in relation to the calibration curve and the results were expressed by ng/ml.

2.6. Histological preparations

2.6.1. Paraffin method

After anesthetising rats, testes were surgically removed by opening abdomen, cleaned, directly fixed in 10% buffered formalin for 48 hrs, then dehydrated through gradually increased ethanol concentrations (50%, 70%, 80%, 95%, 100% and 100%). Xylene used for clearing and after infiltration by using paraffin wax, paraffin blocks were prepared from pieces of testes by embedding in the same wax. About four micrometer thick slices were acquired by using rotary microtome machine (Bright, MIC) from paraffin block and then stained by using haematoxylin and eosin stains (H&E) (Bancroft *et al.,* 1977). Specimens were viewed and photographed by using digital light microscope (digital binocular compound microscope 40x 2000x, built-in 3MP USB camera).

2.6.2. Immunohistochemistry

The DakoCytomation En Vision®+Dual link system-HRP(DAB+) staining procedure was used for immunostaining to detect p53 protein and was applied to paraffin embedded testes tissue which

fixed by formalin. After preparing of slides, deparaffinization, rehydration, monoclonal mouse anti-human p53 protein antibody, incubation with enzyme and substrate-chromogen solution diaminobenzidine have been done. Sections were rinsed with distilled water and counterstained with haematoxylin stain. After wash with running tap water, testes sections on slides were dehydrated via gradually increased ethanol concentration and examined under digital light microscope.

2.6.3. Plastic method

Small pieces of testes which about 1 mm^3 were fixed in primary fixative which it is 2.5% glutaraldehyde in 0.1 cacodylate buffer pH 7.2-7.4 for 1 hr, postfixed in secondary fixative which it is 1% osmium tetroxide for 1 hr, dehydrated through gradually increased of acetone concentrations (50%, 70%, 80%, 95%, 100% and 100%). Then infiltrated by using acetone with resin mixture (3:1) for 1 hr, acetone with resin mixture (1:1) for 1 hr, acetone with resin mixture (1:3) for overnight, and eventually embedded only in resin medium to make plastic block (Durcupan ACM mixture epoxy resin: 10gm; Hardener: 10gm; Accelerator (dimethoxypropane) DMP 30: 0.3gm; and Di-n-butyl phthalate Plasticizer: 0.2gm). All of these chemicals have been got from Fluka AG, Bucha SG. Oven at 60°C for 72 hrs used to polymerization. Plastic blocks were sectioned by ultra-microtome into 1μm thick sections and then stained by using 1% toluidine blue in 1% Borax for light microscopic examination (Glauret, 1965).

2.7. Apoptotic index

The counting of apoptotic cells was achieved by using a 40x objective lens in which 100 numbers of cells were counted randomly throughout the field of the testis and then the number and percentage of apoptotic cells have been calculated. To get an accurate result, counting of cells repeated ten times in different fields.

2.8. Sperm counting

After sacrifice of rats, cauda epididymis were removed and cut to release sperms into 20ml of normal saline in small petri dish and then carefully minced by using manual glass homogeniser. Sperm numbers were measured by using haemocytometer slide and expressed by a number of sperm per millilitre.

2.9. Measurement of seminiferous tubule diameter and germinal layer thickness

About 10 seminiferous tubules were chosen randomly from each rat testes paraffin section which they were round or nearly round. Seminiferous tubule diameter and germinal layer thickness were measured at 100x magnification by using a scale of a digital light microscope.

2.10. Statistical analysis

All data were expressed as means ± standard error of mean (M ± SE) and statistical analyses were done by using statistically available software of Graph Pad Prism 6. To find significant differences between groups, T-test was performed.

3. RESULTS AND DISCUSSION

3.1. Relative testes weight

In the current study, no change was observed in the color, consistency and appearance of testes in both control group and bicalutamide treated group. However, the difference was noted in the weight of the testes. The present investigation showed a non-significant decrease in relative testes weight of bicalutamide treated rats when compared with control group rat testes (Fig. 3.1). This result was compatible with other studies that showed bicalutamide reduced the mean testicular weight in the adult Sprague – Dawley rats (Khurshid *et al.,* 2014). In another investigation conducted by (Leonelli *et al.,* 2011), concerning the effect of flutamide (another anti-androgen) on rats, a significant reduction in testicular weight was noted. Similarly, reduction of testicular weight and associated histological changes were noted after administration of anti-androgen in an androgen-stimulated testes of rats (Wason *et al.,* 2003).

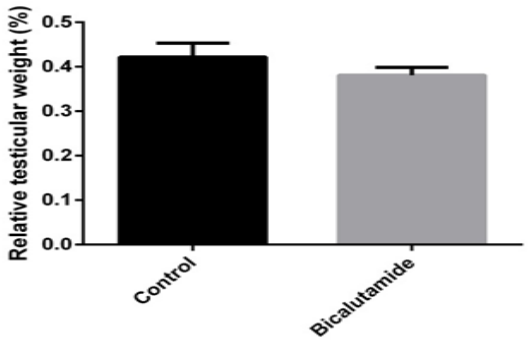

Figure 3.1: Effect of bicalutamide on relative testes weight.

3.2. Effect of bicalutamide on serum testosterone concentration

Orally administration bicalutamide decreased testosterone level in treated group rats when compared with control group rats (Fig. 3.2). The result of the current investigation was similar to the results of Hashimoto et al. (2010) on bicalutamide. Another study which achieved on human, used another type of pure non-steroid anti-androgens has been shown a decrease in testosterone levels (Morse *et al.,* 1973), while another study found no change in testosterone level, after treatment with bicalutamide (Chandolia *et al.,* 1991, Morgante *et al.,* 2001). Recently, bicalutamide treatment caused decrease level of testosterone hormone slightly (Han *et al.,* 2018). Bicalutamide has effect through the competitive inhibition of androgen receptors, and it was shown to have slight impact on serum testosterone hormone concentration (Furr and Tucker, 1996). Bicalutamide might affect Leydig cells and this may be the reason behind testosterone decrease as other drugs did (Chiao *et al.,* 2002).

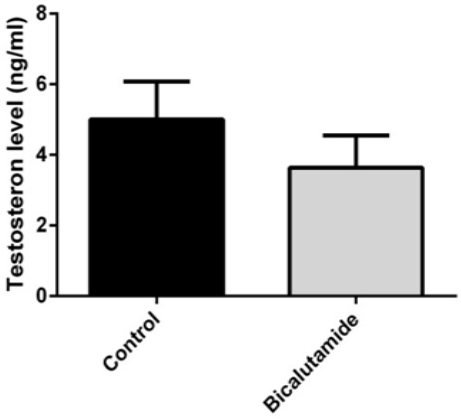

Figure 3.2: Effect of bicalutamide on serum testosterone level.

3.3. Histological effect of bicalutamide on testis.

The histological structure of seminiferous tubules in control group rats was normal with well-formed spermatozoa in their lumen (Fig. 3.3). Administration of bicalutamide caused alteration of the histological structure of testes such as the appearance of vacuoles and sloughing of germ cells from the germinal layer of seminiferous tubules into their lumens which caused decrease of germinal epithelium thickness. Spermatids detachment and accumulation of the desquamated spermatocytes together with spermatids and cellular debris were seen in the seminiferous tubule lumens (Fig. 3.4). In plastic sections, dying germ cells, the formation of the apoptotic body, peripheral chromatin condensation in nuclei which are the characteristic of cell death were noted and apoptotic cells were shed into the seminiferous tubule lumen (Fig. 3.5). Bicalutamide caused a decrease in testosterone concentration which led to sperm death. Deprivations of gonadotropin or testosterone induce apoptosis in germ cells(Sinha Hikim *et al.,* 1997). In some seminiferous tubules of the experimental rat group, detachment of the seminiferous tubule epithelial cells, presence of immature germinal cell and loss of germ cells was observed following administration of bicalutamide (Chandolia *et al.,* 1991). Long-term bicalutamide monotherapy showed to have a little effect on the structure of testes, maturation of sperms and morphology of Sertoli and Leydig cells (Morgante *et al.,* 2001). Administration of bicalutamide led to significant decrease of germ cells number and impacts of bicalutamide on the development of germ cells were due to contribute with testicular androgen actions (Russell and Clermont, 1977). Viguier-Martinez et al. (1983) noticed a slight decrease of spermatocyte count after administration of flutamide.

3.4. Immunohistochemical analysis

Immunohistochemistry technique for detection of p53 was done to demonstrate cells died by apoptosis mode of cell death in testes. As illustrated in Figure (3.6), sections of the control group was shown negative reaction, while bicalutamide treated rat testes was shown a positive p53 reaction (brown to black color cells) in the cytoplasm and nuclei of germinal layer

cells. The multinucleated giant cells of the germinal layer were seen having a strong reaction. In adult rats, germ cell apoptosis due to bicalutamide could be associated with an increase in the expression and activation of p53. Expression and activation of enzymes such as caspases have a major role in apoptosis. Most of the characteristics of apoptosis such as cell shrinkage and nuclear condensation were observed in the current study. Apoptosis is essential to control cell number in adults, development in early life of multicellular organisms such as human and protects the organism by removing or eliminating cells which damaged by aging, disease, genetic mutation, infection, and exposure to toxic substances (Saikumar and Venkatachalam, 2009). P53 was first reported to be expressed and to promote apoptosis in primordial germ cells (Matsui *et al.*, 2000), type A1 spermatogonia (Beumer *et al.*, 1998) and primary spermatocytes (Yin *et al.*, 1998). Exposure to flutamide which caused apoptosis in germ cells related with increase in the expression and activation of caspases-3 and caspases-6 enzymes in rats, which they are two major elements in the process of apoptosis (Omezzine *et al.*, 2003).

As shown in Figure (3.7), bicalutamide caused a significant increase ($P<0.0002$) of apoptotic cells in testes of rats in comparison to the control group rats. The percentage of apoptosis in testes of bicalutamide treated rats was six folds when compared to the testes in control group. Bicalutamide caused decrease in testosterone level which is essential to growth of germ cells in testes. Omezzine *et al.* (2003) found that the number of apoptotic germ cells in adult rat testes were increased significantly after flutamide exposure. Decline of testosterone hormone level induced apoptotic cell death mode of germ cells (Sinha Hikim *et al.*, 1997). Giant multinucleated cells (most often round spermatids, occasionally spermatocytes) result from failed integrity of the cellular bridges serving as partitions, which appeared in the bicalutamide treated rat seminiferous tubule which are a kind of apoptotic germ cells (Anton, 2003, Rasul and Aziz, 2012, Luo *et al.*, 2013, Vidal and Whitney, 2014,).

3.5. Sperm counting

Daily administration of bicalutamide showed a statistically significant decrease ($p<0.0001$) of sperm count in bicalutamide treated group when compared with control group (Fig. 3.8). Spermatozoa produced from germ cells in a germinal layer of seminiferous tubules were consistently decreased after administration of bicalutamide (Chandolia *et al.*, 1991). Morse et al. (1973) showed decrease sperm count in human after administration of cyproterone acetate (which is another type of anti-androgen drug). The reduction in sperm count might be via the partial arrest of spermatogenesis and also due to oxidative stress induced by the drug (Ghosh *et al.*, 2002, Srinivasulu and Changamma, 2017).

3.6: Effect of bicalutamide on seminiferous tubule diameter and germinal layer thickness

Seminiferous tubule diameter and germinal layer thickness were shown statistically significant differences between two groups. Bicalutamide drug led to statistically significant increase ($p<0.0001$) in the diameter of seminiferous tubules, while it caused statistically significant decrease in the germinal layer thickness ($p<0.05$) in treated group as compared with control group (Table1). Other studies showed marked reduction in the germinal layer thickness in the experimental group of animals that received bicalutamide as compared to the control group (Khursheed *et al.*, 2011). Flutamide, which it is another anti-androgen, didn't cause change in diameter of seminiferous tubules in experimental group while it led to a significant reduction in the germinal layer thickness (Bustos-Obregón *et al.*, 2006). Degeneration of the germinal cells in response to bicalutamide administration may the reason behind the depletion in germinal layer thickness.

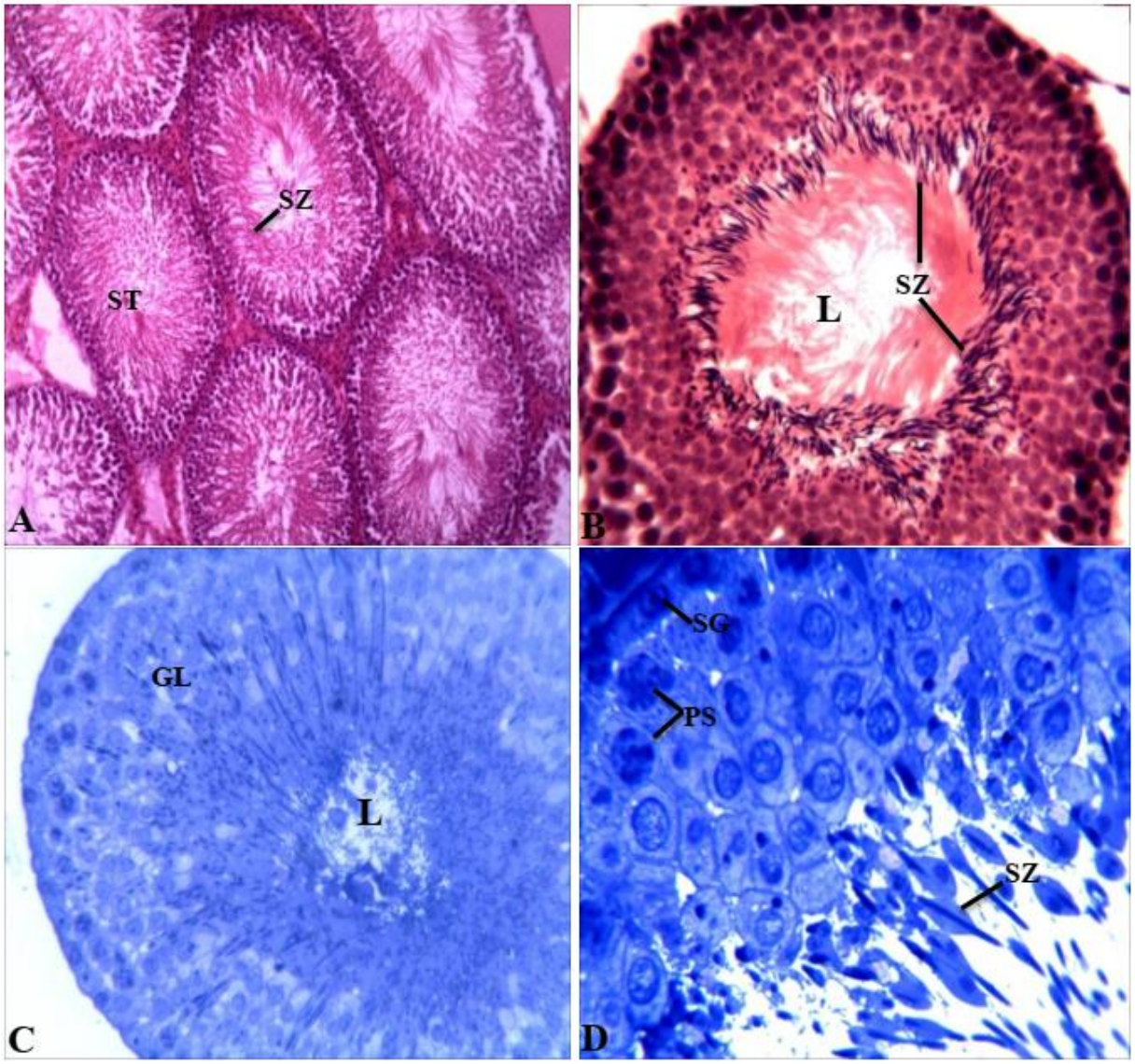

Figure 3.3: Sections in the testes of control adult rats. A and B) Paraffin sections revealed normal histological structures of seminiferous tubules and spermatozoa in their lumen, H&E. 100x and 400x respectively. C and D) Plastic sections through the seminiferous tubules showing healthy features of the germinal epithelial cells, toluidine blue. 400x and 1000x respectively. ST Seminiferous tubule, SZ Spermatozoa, L Lumen, GL Germinal layer, SG spermatogonia and PS Primary spermatocyte.

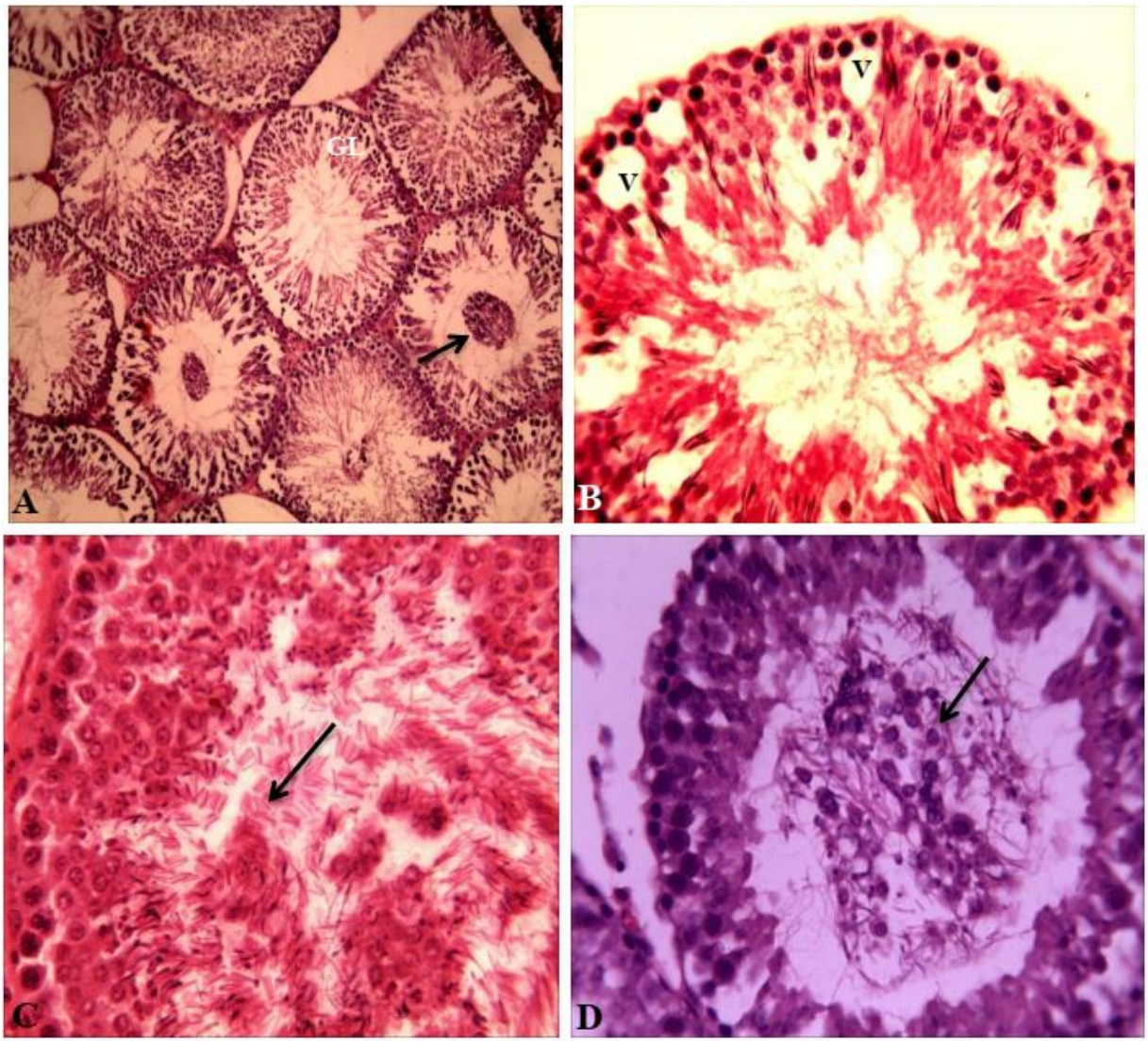

Figure 3.4: Sections of seminiferous tubules in the testes of rats treated with bicalutamide A) Paraffin section shows certain histological alterations such as decreased thickness of the germinal epithelium layer (GL), decrease of spermatids number and accumulation of cellular debris (arrow) in the center of the seminiferous tubules. H&E. 100x B) Vacuoles (V) and depleted germinal layer with reduction of sperm number have been shown in the seminiferous tubule. H&E. 400x, C) Damaged spermatozoan tails forming clusters of filaments (arrow). H&E. 400x, D) Damaged germinal layer and cellular debris (arrow) are noted in the seminiferous tubule lumen. H&E. 400x.

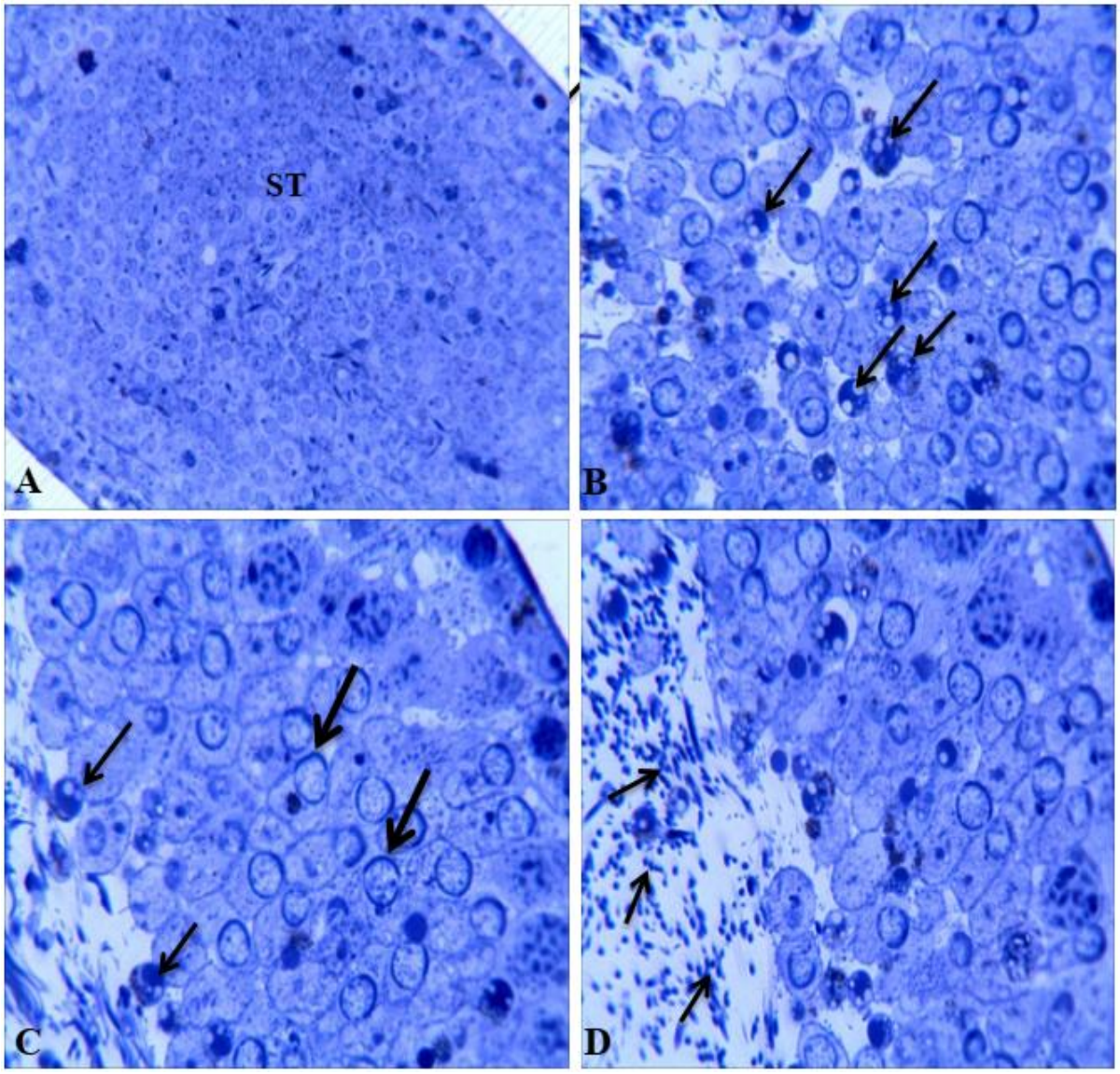

Figure 3.5: Plastic sections of seminiferous tubules in the testes of rats treated with bicalutamide A) Approximately no spermatids were seen in seminiferous tubule (ST). Toluidine blue 400x. B) The appearance of apoptotic nuclei with marginated chromatin (arrows). Toluidine blue 1000x C) Apoptotic bodies shed (thin arrow) into seminiferous tubule lumen. In the germinal layer, a number of apoptotic-like nuclei with marginated chromatin (thick arrow) are seen. Toluidine blue 1000x. D) Destructed sperms (arrows) in the lumen of the seminiferous tubule were noted. Toluidine blue 1000x.

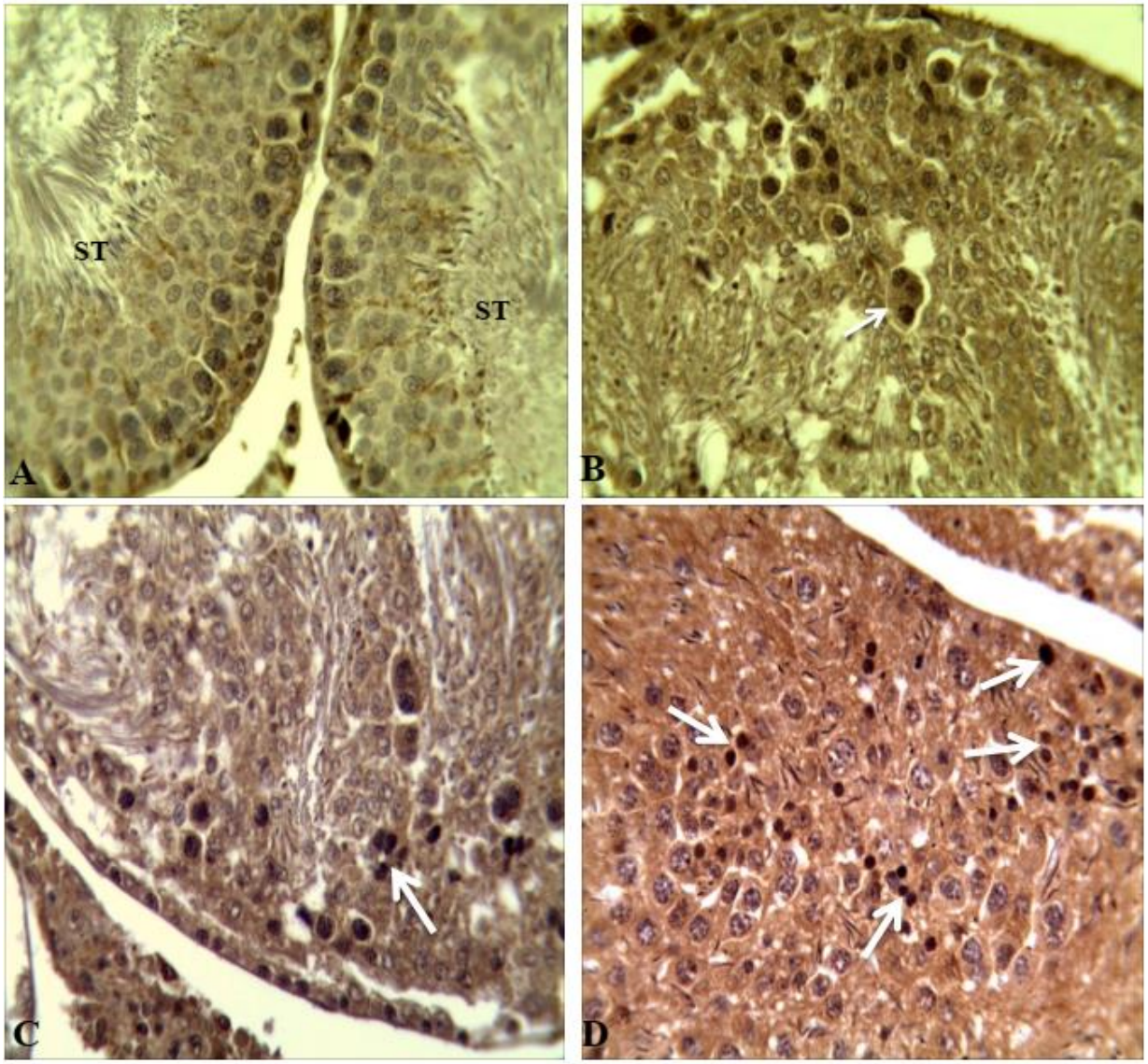

Figure 3.6: Sections of seminiferous tubules demonstrating the immunohistochemical reaction of p53. A) Control group revealed no p53 immunohistochemical reaction. 400x. B, C and D) Treated group showed positive immunohistochemical reactions in the cells of germinal layer epithelium of seminiferous tubules. Reactions are seen in the germ dead cells (thick arrow) and multinucleated giant cells (thin arrow) 400x.

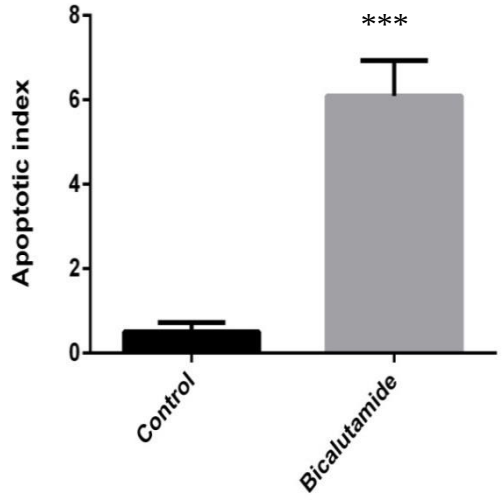

Figure 3.7: Apoptotic index in both control and bicalutamide treated rats.
*** indicates that the value is significant compared to control at *P*<0.0002

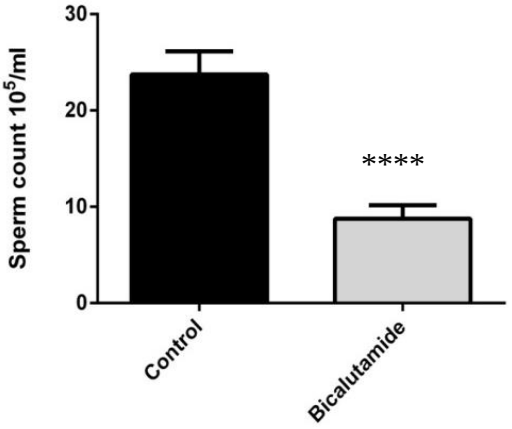

Figure 3.8: Effect of bicalutamide on sperm count.
**** indicates that the value is significant compared to control at *P*<0.0001

Table 1. Effect of bicalutamide on seminiferous tubules diameter and germinal layer thickness.

Measured regions(µm)	**Control**	**Bicalutamide**
80.62 ± 1.708 **Seminiferous tubules diameter**	**80.62 ± 1.708**	**106.0 ± 1.322 ******
Germinal layer thickness	**16.19 ± 0.5500**	**14.47 ± 0.4631 ***

Data represented as mean ± S.E. * mean significant differences at level P<0.05, **** mean significant differences at level *P*<0.0001 compared with control.

4. CONCLUSIONS

According to the present results, bicalutamide treatment caused castration in rats represented by the appearance of various biochemical, histological and immunohistochemical changes.

Acknowledgements

We wish to thank members of biology department, college of science, Salahaddin university especially Dr. Falah M. Aziz, Dr. Chnar Najmadden, Mrs Shang Z. abdulqadir and Mr. Khder Hussein Rasul for their help and supports.

Conflict of Interest

I do not have any conflict of interest.

5. REFERENCES

ANTON, E. 2003. Arrested apoptosis without nuclear fragmentation produced by efferent duct ligation in round spermatids and multinucleated giant cells of rat testis. Reproduction, 125, 879-887.

BANCROFT, J. D., D;, S. & S, D. I. M. 1977. Theory and Practices of Histological Techniques. Edinburg, London, New York. ChurchillLivingstone.

BEUMER, T. L., ROEPERS-GAJADIEN, H. L., GADEMAN, I. S., VAN BUUL, P. P., GIL-GOMEZ, G., RUTGERS, D. H. & DE ROOIJ, D. G. 1998. The role of the tumor suppressor p53 in spermatogenesis. Cell death and differentiation, 5, 669.

BUSTOS-OBREGÓN, E., ESPONDA, P. & SARABIA, L. 2006. Effect of flutamide in mouse spermatogenesis and on the function of seminal vesicle and prostate.

CHANDOLIA, R. K., WEINBAUER, G. F., BEHRE, H. M. & NIESCHLAG, E. 1991. Evaluation of a peripherally selective antiandrogen (Casodex) as a tool for studying the relationship between testosterone and spermatogenesis in the rat. The Journal of steroid biochemistry and molecular biology, 38, 367-375.

CHIAO, Y.-C., CHO, W.-L. & WANG, P. S. 2002. Inhibition of testosterone production by propylthiouracil in rat Leydig cells. Biology of reproduction, 67, 416-422.

FRADET, Y. 2004. Bicalutamide (Casodex®) in the treatment of prostate cancer. Expert review of anticancer therapy, 4, 37-48.

FREEMAN, S., MAINWARING, W. & FURR, B. 1989. A possible explanation for the peripheral selectivity of a novel non-steroidal pure antiandrogen, Casodex (ICI 176,334). British journal of cancer, 60, 664.

FURR, B. & TUCKER, H. 1996. The preclinical development of bicalutamide: pharmacodynamics and mechanism of action. Urology, 47, 13-25.

FURR, B., VALCACCIA, B., CURRY, B., WOODBURN, J., CHESTERSON, G. & TUCKER, H. 1987. ICI 176,334: A NOVEL NON–STEROIDAL, PERIPHERALLY SELECTIVE ANTIANDROGEN. Journal of Endocrinology, 113, R7-R9.

GHOSH, D., DAS, U., GHOSH, S., MALLICK, M. & DEBNATH, J. 2002. Testicular gametogenic and steroidogenic activities in cyclophosphamide treated rat: a correlative study with testicular oxidative stress. Drug and chemical toxicology, 25, 281-292.

GLAURET, A. 1965. The fixation and embedding of biological specimen. In: Techniques for electron microscopy. D.H. Key, ed. Davis Co., Philadelphia, PP. 166-212. .

HAN, J.-H., SHIN, M.-S., LEE, J.-M., KIM, T.-W., JIN, J.-J., KO, I.-G., KIM, S.-E., KIM, C.-J., KIM, M. & ROH, J. H. 2018. Long-term chemical castration induces depressive symptoms by suppressing serotonin expression in rats. Animal Cells and Systems, 22, 29-36.

HASHIMOTO, K., MASUMORI, N., HASHIMOTO, J., TAKAYANAGI, A., FUKUTA, F. & TSUKAMOTO, T. 2010. Serum testosterone level to predict the efficacy of sequential use of antiandrogens as second-line treatment following androgen deprivation monotherapy in patients with castration-resistant prostate cancer. Japanese journal of clinical oncology, 41, 405-410.

HUSSAIN, S., HAIDAR, A., BLOOM, R. E., ZAYOUNA, N., PIPER, M. H. & JAFRI, S.-M. R. 2014. Bicalutamide-induced hepatotoxicity: A rare adverse effect. The American journal of case reports, 15, 266.

ISWARAN, T., IMAI, M., BETTON, G. & SIDDALL, R. 1997. An overview of animal toxicology studies with bicalutamide (ICI 176, 334). The Journal of toxicological sciences, 22, 75-88.

KENNEL, P., PALLEN, C., BARALE-THOMAS, E., ESPUÑA, G. & BARS, R. 2003. Tamoxifen: 28-day oral toxicity study in the rat based on the Enhanced OECD Test Guideline 407 to detect endocrine effects. Archives of toxicology, 77, 487-499.

KHURSHEED, A., MINHAS, L. A. & NIAZ, W. A. 2011. Histomorphometric study of effects of bicalutamide on spermatogenesis in male rats. Pak Armed Forces Med J, 61, 325-9.

KHURSHID, A., HAMID, S. & NIAZ, A. 2014. Effect of bicalutamide; an antiandrogen on testicular weight in adult rats. Pak Armed Forces Med J, 64, 204-207.

LEE, J., MUN, S., PARK, A., KIM, D., HEUN CHA, B. & KANG, H.-G. 2018. Bicalutamide enhances fodrin-mediated apoptosis through calpain in LNCaP. Experimental Biology and Medicine, 1535370218779780.

LEONELLI, C., GARCIA, P. C. & PEREIRA, O. C. 2011. Copulatory efficiency and fertility in male rats exposed perinatally to flutamide. Reproductive Toxicology, 31, 10-16.

LUO, L., LI, Y., YANG, Y., HE, Y., WANG, Y., XU, Z. & ZHANG, Y. 2013. Multinucleated cells are involved in normal development and apoptosis in mouse testes. Molecular medicine reports, 8, 865-870.

MATSUI, Y., NAGANO, R. & OBINATA, M. 2000. Apoptosis of fetal testicular cells is regulated by both p53-dependent and independent mechanisms. Molecular Reproduction and Development: Incorporating Gamete Research, 55, 399-405.

MCLEOD, D. G. & IVERSEN, P. 2000. Gynecomastia in patients with prostate cancer: a review of treatment options. Urology, 56, 713-720.

METZDORFF, S. B., DALGAARD, M., CHRISTIANSEN, S., AXELSTAD, M., HASS, U., KIERSGAARD, M. K., SCHOLZE, M., KORTENKAMP, A. & VINGGAARD, A. M. 2007. Dysgenesis and histological changes of genitals and perturbations of gene expression in male rats after in utero exposure to antiandrogen mixtures. Toxicol Sci, 98, 87-98.

MORGANTE, E., GRADINI, R., REALACCI, M., SALE, P., D'ERAMO, G., PERRONE, G., CARDILLO, M., PETRANGELI, E., RUSSO, M. & DI SILVERIO, F. 2001. Effects of long-term treatment with the anti-androgen bicalutamide on human testis: an ultrastructural and morphometric study. Histopathology, 38, 195-201.

MORSE, H., LEACH, D., ROWLEY, M. & HELLER, C. 1973. Effect of cyproterone acetate on sperm concentration, seminal fluid volume, testicular cytology and levels of plasma and urinary ICSH, FSH and testosterone in normal men. Journal of reproduction and fertility, 32, 365-378.

MOSSA, A.-T. H., SWELAM, E. S. & MOHAFRASH, S. M. 2015. Sub-chronic exposure to fipronil induced oxidative stress, biochemical and histopathological changes in the liver and kidney of male albino rats. Toxicology reports, 2, 775-784.

OMEZZINE, A., CHATER, S., MAUDUIT, C., FLORIN, A., TABONE, E., CHUZEL, F., BARS, R. & BENAHMED, M. 2003. Long-term apoptotic cell death process with increased expression and activation of caspase-3 and-6 in adult rat germ cells exposed in utero to flutamide. Endocrinology, 144, 648-661.

RASUL, K. H. & AZIZ, F. M. 2012. The Effect of Sustanon (Testosterone Derivatives) Taken by Athletes on the Testis of Rat. Jordan journal of biological sciences, 5.

RUSSELL, L. D. & CLERMONT, Y. 1977. Degeneration of germ cells in normal, hypophysectomized and hormone treated hypophysectomized rats. The Anatomical Record, 187, 347-365.

SAIKUMAR, P. & VENKATACHALAM, M. A. 2009. Apoptosis and cell death. Basic Concepts of Molecular Pathology. Springer.

SEKINO, Y., OUE, N., MUKAI, S., SHIGEMATSU, Y., GOTO, K., SAKAMOTO, N., SENTANI, K., HAYASHI, T., TEISHIMA, J. & MATSUBARA, A. 2019. Protocadherin B9 promotes resistance to bicalutamide and is associated with the survival of prostate cancer patients. The Prostate, 79, 234-242.

SHARPE, R. M. 2006. Pathways of endocrine disruption during male sexual differentiation and masculinization. Best Pract Res Clin Endocrinol Metab, 20, 91-110.

SINHA HIKIM, A. P., RAJAVASHISTH, T. B., HIKIM, I. S., LUE, Y., BONAVERA, J. J., LEUNG, A., WANG, C. & SWERDLOFF, R. S. 1997. Significance of apoptosis in the temporal and stage-specific loss of germ cells in the adult rat after gonadotropin deprivation. Biology of reproduction, 57, 1193-1201.

SRINIVASULU, K. & CHANGAMMA, C. 2017. A Study on the Effect of Ocimum sanctum (Linn.) Leaf Extract and Ursolic Acid on Spermatogenesis in Male Rats. Indian Journal of Pharmaceutical Sciences, 79, 158-163.

STANISŁAWSKA, I. J., PIWOWARSKI, J. P., GRANICA, S. & KISS, A. K. 2018. The effects of urolithins on the response of prostate cancer cells to non-steroidal antiandrogen bicalutamide. Phytomedicine.

TÉROUANNE, B., TAHIRI, B., GEORGET, V., BELON, C., POUJOL, N., AVANCES, C., ORIO JR, F., BALAGUER, P. & SULTAN, C. 2000. A stable prostatic bioluminescent cell line to investigate androgen and antiandrogen effects. Molecular and cellular endocrinology, 160, 39-49.

VIDAL, J. D. & WHITNEY, K. M. 2014. Morphologic manifestations of testicular and epididymal toxicity. Spermatogenesis, 4, e979099.

VIGUIER-MARTINEZ, M., DE REVIERS, M. H., BARENTON, B. & PERREAU, C. 1983. Endocrinological and histological changes induced by flutamide treatment on the hypothalamo-hypophyseal testicular axis of the adult male rat and their incidences on fertility. Acta endocrinologica, 104, 246-252.

WASON, S., POHLMEYER-ESCH, G., PALLEN, C., PALAZZI, X., ESPUÑA, G. & BARS, R. 2003. 17α-methyltestosterone: 28-day oral toxicity study in the rat based on the "enhanced OECD test guideline 407" to detect endocrine effects. Toxicology, 192, 119-137.

YIN, Y., STAHL, B. C., DEWOLF, W. C. & MORGENTALER, A. 1998. p53-mediated germ cell quality control in spermatogenesis. Developmental biology, 204, 165-171.

ZANCO Journal of Pure and Applied Sciences
The official scientific journal of Salahaddin University-Erbil
https://zancojournals.su.edu.krd/index.php/JPAS

ISSN (print):2218-0230**, ISSN (online):** 2412-3986**, DOI: http://dx.doi.org/10.21271/zjpas**

RESEARCH PAPER

L-arginine and tetrahydrobiopterin modulate endothelin-1A receptor activity in isolated rat aorta

Zhikal O. Khidhr*, Ismail M. Maulood.

Department of Biology, College of Science, Salahaddin University-Erbil, Kurdistan Region, Iraq.

A B S T R A C T:

Endothelin-1 (ET-1), is a potent endogenous vasoconstrictor secreted by endothelial cells. It acts as the natural counterpart of the vasodilator effect of nitric oxide (NO). ET-1 exert it is the vasoconstrictor activity through two types of receptors, ET-1A and ET-1B receptors that are located on vascular smooth muscle cells (VSMCs). The present study was designed to evaluate the effect of L-arginine (LA), tetrahydrobiopterin (BH4), and their combination on ET-1A receptor activity in rat aortic rings. The study involved pre-incubation of rat aortic rings with LA, BH4, and their combination. Then, the vascular response to a cumulative dose of the ET-1A receptor antagonist (BQ-123) and in the second set of experiment cumulative doses of Acetylcholine (ACh) were applied to each group. BQ-123 potency increased after LA pre-incubation, but LA and BH4 in combination significantly potentiated BQ-123 potency and maximum response. In the second set of experiment, ACh potency does not change, while ACh efficacy markedly increased during pre-incubation of LA, BH4, and their combination. In conclusion, LA and BH4 may offer some pharmacological tools to modulate the ET-1A receptor activity and treat cardiovascular disease beyond pulmonary arterial hypertension.

KEY WORDS: Acetylcholine; BQ-123; Endothelin-1; L-arginine; Rat aorta; Tetrahydrobiopterin.
DOI: http://dx.doi.org/10.21271/ZJPAS.31.2.13
ZJPAS (2019) , 31(2);101-108 .

1. INTRODUCTION:

Endothelial cell and other cells in the body produce ET-1, a 21-amino acid peptide which is acts as one of the most powerful vasoconstrictors identified to play a vital role in the generation of hypertension (Hamad *et al.*, 2016), that was recognized by Yanagisawa *et al.* (1988). ET-1A and ET-1B are the two pharmacological receptors for ET-1.

* **Corresponding Author:**
Zhikal O. Khidhr
E-mail: zhikal.khudhur@su.edu.krd
Article History:
Received: 06/03/2019
Accepted: 30/03/2019
Published: 23/04 /2019

VSMCs have ET-1A and ET-1B receptors while endothelial cells have only ET-1B receptors (Vignon-Zellweger et al., 2012). ET-1 regulates its activity by binding to either ET-1A or ET-1B receptors, which are receptors with G protein-coupled to Gαq/11. After binding ligand to its receptor, there are secondary messenger system activated within VSMCs involves Gq, Gs and Gi small G proteins (In addition to the heterotrimeric G proteins, other forms of G proteins play important roles in cell function. These proteins belong to a large superfamily often referred to as "small G proteins" based on their low molecular weight (20,000 to 35,000) prompting provoke activation of phospholipase C. The back to back creation of inositol triphosphate (IP3) and diacylglycerol (DAG) expands the convergence of

calcium ion (Ca2+) within the cell which is released from the sarcoplasmic reticulum by stimulation of the IP3 receptor, and outer Ca2+ rushes into the sarcoplasm through the opening of the Ca2+ channels on the sarcolemma (Barrett et al., 2010). The enzymes NADPH oxidase and/or uncoupled nitric-oxide synthase (NOS) which are located on blood vessels is activated by increased levels of ET-1, then the production of superoxide and constriction of blood vessels occur while the vasodilation might be regulated by endothelial ET-1B receptors through releasing NO (Kowalczyk et al., 2015).

BQ-123 is a powerful and specific blocker for ET-1A receptors in various distinctive tissues and cells. The capacity of BQ-123 to stop the impacts of ET-1 in rabbit aorta, Schneider proposes that the contractile impacts of ET-1 are incitement because of ET-1A receptors (Schneider et al., 2007). Preliminary studies on BQ-123 showed that BQ-123 inhibited angiotensin II-induced contractions in isolated rabbit aorta (C Kowala et al., 2004). The effects of ET-1 that are mediated via ET-1A receptors are sensitive to blockade by BQ-123, whereas those that are mediated via ET-1B receptors are BQ-123-insensitive (Martínez-Revelles et al., 2012).

The chemical precursor of NO is a semi-essential amino acid which is known as LA, causes vasodilation of blood vessels so NO termed vasodilator (Soderman, 2013). Endothelial NOS (eNOS) is the enzyme that mediates the conversion of LA to L-citrulline and NO (Endemann and Schiffrin, 2004). NO activates the enzyme guanylyl cyclase which is regarded as a soluble receptor for NO (Friebe and Koesling, 2003). ACh can mobilize a stored NO pool, which, synergistically with prostacyclin, can relax precontracted aortic rings Patients with hypercholesterolemia and atherosclerosis get benefit from supplementation of LA amino acid which enhances NO production and reestablish endothelial function (Tsuboi et al., 2018) but other studies recorded that LA does not improve endothelial function in rabbit aortic rings (Sagach et al., 2006).

Tetrahydrobiopterin (BH4) act as eNOS cofactor, the coupling and stability of NOS homodimer maintains by binding two BH4 to the two NOS homodimer because it provides stability of the homodimer through numerous hydrogen bonds and it makes intimate coupling between LA substrate and the heme site of the eNOS oxygenase domain that binds to the oxygenase domain adjacent to the heme active site (Chen et al., 2010). The relaxation of blood vessels which is stimulated by ACh, augmented by BH4 (100 mM) (Jiang et al., 2000). The using LA with BH4 together shows a synergistic effect and elevates the production of NO and restore endothelial function (Tratsiakovich et al., 2013b). To the best of our knowledge, combined administration of LA and BH4 with the purpose to decrease the ET-A receptor has never been tested before. Therefore, the present study aimed to investigate the impact of NO precursor, BH4 and their combination of ET-1A receptor activity.

2. MATERIALS AND METHODS

2.1: Chemicals

ET-1 was purchased from Bachem (Bubendorf, Switzerland); BH_4 from Nootropic (Arizona, USA); BQ-123 selective ET-1A Receptor antagonist from Selleckchem (Houston, Texas, USA); ACh from Sigma-Aldrich, LA was provided by Scharlab S.L/Sentmenat Spain.

2.2: Animals

Twenty male albino rats weighing 200-300 gm were housed and kept in standard laboratory conditions of light and temperature about 12 hours light: 12 hours dark photoperiod and 22 ± 4 ^{o}C. The experimental protocol was approved by the ethics committee and animal care committee in the College of Science; Salahaddin University – Erbil. The study was carried out in the Biology department, College of Science from March/ 2018 to October/ 2018.

2.3: Aortic rings preparation

Rats were anaesthetized by intraperitoneal injection of a mixture of ketamine: xylasine 90 mg/kg: 10 mg/kg, respectively (Rameshrad *et al.*, 2016). Thoracic aorta was immediately ectomized, set in a cold Krebs solution and cleaned from surrounding adipose and connective tissues, then cut into 4-segments, each about 2-2.5mm in length.

2.4: Vascular reactivity measurement

Two metal rods were passed through the lumen of the rings**,** one of the hooks was fixed to the bottom of organ bath chamber**,** and the other was connected to the force transducer through a thread to record vasoreactivity in organ bath (Automatic organ bath-Pan lab, Harvard apparatus USA, AD Instrument Power lab 8/35-Australia) that is filled with 10-ml of Krebs bicarbonate solution in (mM/L NaCl,119; $MgSO_4$, 1.2; $CaCl_2$, 1.5; $NaHCO_3$; KCl, 4.7; KH_2PO_4 1.2; glucose 11.1. The solution in the organ bath was kept up at 37 ^oC and aerated with a mixture of about 95% O_2 and 5% CO_2. After 60 to 90 minutes of equilibration, each aortic rings was exposed to KCl (60mM) as a viability test. Each ring was washed with a fresh medium and re-equilibrate for at least 30 minutes before adding any substances.

2.5: Experimental protocol

Prepared aortic rings have been used to evaluate the possible contribution of some substances to vascular action of BQ-123 and ACh. Two sets of experiments were carried out as follows:

Experiment 1: The prepared aortic rings were incubated for 45 minutes with LA (1µM), BH_4 (100Mm), and their combination, then pre-contracted by ET-1 (0.01µM), and after stabilization of contractile response. The BQ-123 relaxation -response curves were generated (from 10^{-11} to 10^{-6} M). The relaxations are expressed in percent of pre-contractile tone

Experiment 2: After pre-incubation of aortic with LA (1µM), BH_4 (100Mm), and their combination for 45 minutes, rings were pre-contracted by ET-1 (0.01µM). Endothelium-dependent relaxations were determined by application of ACh (from 10^{-9} to 5* 10^{-4} M). The relaxations are expressed in percent of pre-contractile tone.

2.6: Statistical analysis

All results are presented as means ± standard error of the mean (SEM). Statistical analysis was carried out by GraphPad Prism (Version 7), the concentration-response curves of BQ-123 and ACh were fitted nonlinearly. Two-way analysis of variance (ANOVA) was applied to know the difference, followed by Sidak multiple comparison tests as an individual mean comparison, and Tukey-test as the potency difference (pD_2) and maximum response (Emax) comparison between groups with each other. Values were considered to be statistically significant at $P < 0.05$.

3. RESULTS

The result showed that pre-incubation of aortic rings with LA, BH_4, and the combination of LA and BH_4 significantly improved the relaxation that was evoked by BQ-123 and ACh.

Table 1: The maximum response (Emax) and the potency difference (pD_2) to BQ-123 in rat aortic rings

Groups	N	Emax %KCL	pD_2
Control	7	21.64 ± 2.892	-8.156 ± 0.100
LA	6	18.57 ± 2.854	-8.797 ± 0.1277**
BH_4	6	14.89 ± 1.786	-8.512 ± 0.06505
LA+BH_4	6	10.51 ± 1.967*	-8.9214 ± 0.07798*** ¤

The studied groups were compared with each other (ANOVA was applied with Tukey test). *, **, *** represents statistical differences at P<0.05, P<0.01 P<0.001 versus the corresponding control group, and ¤ Significant differences between groups vs BH_4 group at $p < 0.05$.

3.1: The effect of NO precursor on vascular response to BQ-123

To find out the role of NO precursor in vascular response to BQ-123, LA was used. Figure (fig.) 1A showed that LA noticeably magnified the relaxant effect of BQ-123 with a significant change in BQ-123 potency, however, BQ-123 efficacy remained significantly unchanged table 1.

3.2: The effect of BH_4 on vascular response to BQ-123

To investigate the effect of NOS cofactor, BH_4 was applied. The results showed that the altitude of the vascular response to BQ-123 was significantly unchanged in the presence of BH_4.

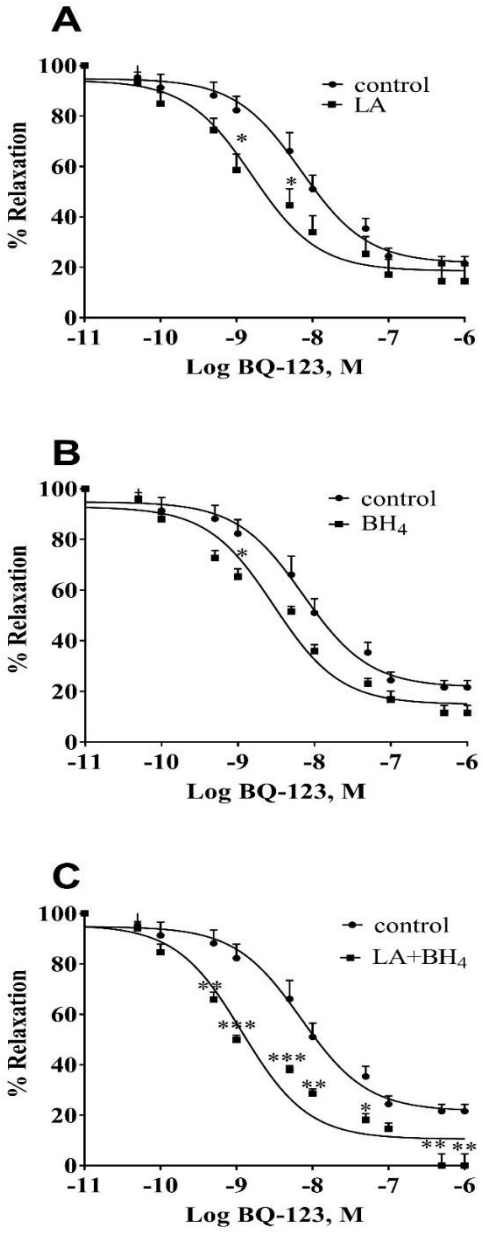

Figure 1. Concentration-response curves showing relaxation induced by BQ-123 in rat thoracic aortic rings under control condition and after pre-incubation with (A) LA, (B) BH_4, and (C) the combination of LA and BH_4. The relaxations are expressed in per cent of the pre-contracted tone induced by 0.01 µM ET-1.The asterisks; *, **, *** represents statistical differences at P<0.05, P<0.01 P<0.001versus the corresponding control group

3.3: The combined effect of LA and BH_4 on vascular response to BQ-123

The data analysis of the present study showed a synergistic role of LA and BH_4 in altering the vascular reactivity of BQ-123 to left. As it can be seen in table 1 LA and BH_4 in the combination showed the significant difference in BQ123 potency and efficacy. Furthermore, combination of LA and BH_4 has a greater impact than each substance alone.

Table 2: The maximum response (Emax) and the potency difference (pD_2) to ACh in rat aortic rings.

Groups	N	Emax (%KCL)	pD_2
Control	7	36.83 ± 1.732	-6.867 ± 0.07907
LA	5	12.99 ± 1.932***	-7.087 ± 0.06988
BH_4	5	15.25 ± 2.071***	-6.913 ± 0.073
LA+BH_4	5	2.761 ± 2.154***# ¤¤	-7.132 ± 0.07023

The studied groups were compared with each other (ANOVA was applied with Tukey test). *** represent statistical differences at P<0.001versus the corresponding control group, # Significant differences between groups vs LA group at $p < 0.05$, and ¤¤ Significant differences between groups vs BH_4 group at $p < 0.01$.

3.4: The effect of NO precursor on vascular response to Ach

The present study showed that using LA as NO precursor significantly increased ACh efficacy while ACh potency did not change as shown in fig. 2 and table 2.

3.5: The effect of BH_4 on vascular response to Ach

To scrutinize the effects of BH_4 on ACh vascular actions and the possible role of eNOS, BH_4 (100µM) was used. The result showed that BH_4 noticeably magnified the vasorelaxant response to ACh with significant changes in efficacy although, ACh potency remained significantly unchanged (table 2).

3.6: The combined effect of LA and BH_4 on vascular response to Ach

To determine the influence of LA and BH_4 in combination on the vascular response of aortic rings to ACh. The ACh reactivity following after 45 min of LA and BH_4 pre-incubation and ET-1 pre contraction was significantly elevated the maximum response significantly rise (table 2) , While ACh potency was stable.

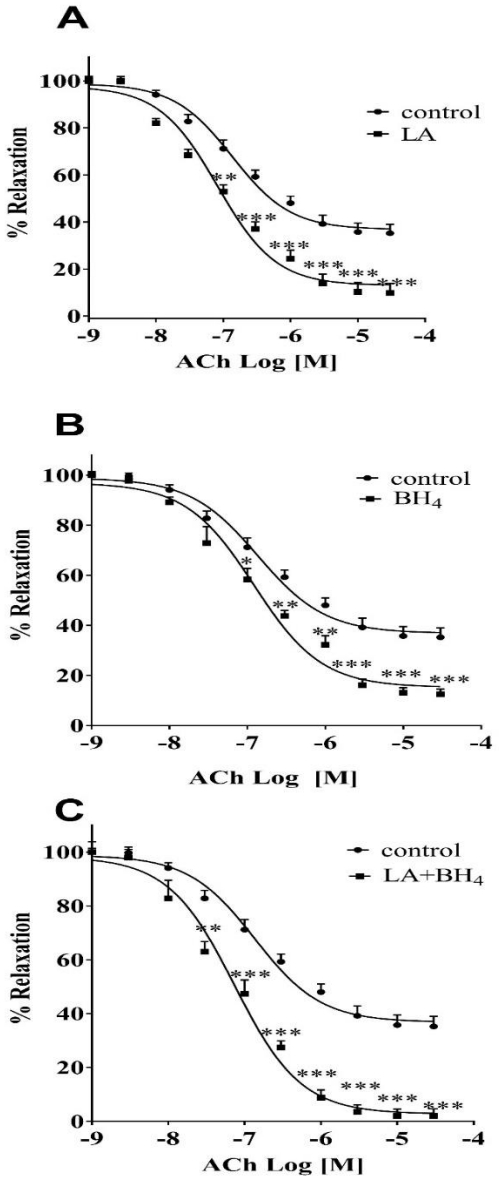

Figure 2. Concentration-response curves showing relaxation induced by ACh in rat thoracic aortic rings under control condition and after pre-incubation with (A) LA, (B) BH_4, and (C) the combination of LA and BH_4. The relaxations are expressed in per cent of the pre-contracted tone induced by 0.01 µM ET-1.The asterisks; *, **, *** represents statistical differences at P<0.05, P<0.01 P<0.001 versus the corresponding control group.

4. DISCUSSION

The major findings of this study illustrated that LA and BH_4 significantly increased the relaxation effect of both BQ-123 and ACh. The current results demonstrate that pre-incubation of ET-1 in contact aortic rings cause activation of the ET-1A receptor stimulates phospholipase C to IP_3 and DAG from phosphatidylinositol 4.5-bisphosphate. IP_3 induces Ca^{2+} outflow from intracellular stores in the sarcoplasmic reticulum. Furthermore, the ET-1A receptor acts on nonselective plasmalemmal Ca^{2+} channels causing Ca^{2+} input from the extracellular space. Consequently, increased concentrations of Ca^{2+} leads to the contraction of VSMCs. The activated ET-1A receptor also stimulates cell growth. Production of DAG activates protein kinase C, which increases VSMCs contraction (Hynynen and Khalil, 2006, Lima *et al.*, 2010, Khalil, 2011). Aortic rings that pre-contracted by ET-1 followed by BQ-123 as dose-response curves (DRC) caused the attenuation of vascular reactivity of ET-1.

From the result of this study, it could be concluded that BQ-123 produces blood vessel dilation *via* blocking ET1A receptor and subsequently preventing calcium release from the sarcoplasmic reticulum and entering calcium to the cell (Callera *et al.*, 2003). Briyal, who is a researcher, detected that ET-1 induces the synthesis of superoxide anion through ET-1A receptors that cause lipid peroxidation (Briyal *et al.*, 2011).

BQ-123 pre-incubation in arteries and veins significantly block the increased production of superoxide in ET-1-induced oxidative stress (Cerrato *et al.*, 2012), Another possible mechanism by which BQ-123 causes vascular relaxation is that BQ-123 associated with a significant increase in the concentration of total glutathione and superoxide dismutase (SOD) activities (Briyal *et al*., 2011). Over all, it can be concluded that ET-1A receptor blockade will improve the function of the aorta (Tirapelli *et al.*, 2008). Blockade of ET-1A receptor allows ET-1B receptor to release more NO in the endothelial cells and hence, vasorelaxation.

Besides the aforementioned effect of BQ-123, as obtained from the present result, pre-incubation of LA increased the potency of BQ-123. In addition, LA significantly shifted BQ-123 DRC to left. LA is only substrate in the biosynthesis of NO, and NO plays an important role in the diverse physiological process including vasorelaxation through cyclic guanosine monophosphate (cGMP) pathway. In addition, BH_4 pre-incubation did not change in DRC of BQ-123 compared to such changes occurred by LA pre-incubation.

The present investigation showed that pre-incubation of rat aortic rings with LA and BH_4 in combination caused the marked increase in BQ-123 efficacy and potency. Schreiber *et al.* (2017) recorded that LA is the main substrate in the production of NO. Binding BH_4 exert allosteric action to stabilize the active dimeric form of eNOS (Shinozaki *et al.*, 2000) and increases the enzymatic turnover of LA. Jiang *et al*. (2000) demonstrated that combined pre-incubation of LA and BH_4 induced a pronounced enhancement of ACh-induced relaxation.

Several mechanisms have been suggested to explain how ACh produces relaxation in rat aortic rings. ACh exerts a direct effect on vascular tone by binding to muscarinic receptors present on vascular endothelium, and hence, the activation of eNOS and prostaglandin production (Kellogg *et al.*, 2005) and subsequently NO mediates relaxation through activation of potassium channels (Salihi *et al.*, 2016). The current results showed that LA pre-incubation increased the efficacy of ACh significantly as shown in table 2 (fig.2A), because by the activity of eNOS change to NO and L-citrulline, as previously we mentioned that increasing of NO increase vasorelaxant effect of ACh (Tratsiakovich *et al.*, 2013a). In the same manner, pre-incubation of BH_4 increased ACh maximum response because of its cofactor for NO production and protective eNOS as an active dimer as shown in fig.2B as previously reported by Jiang *et al*. (2000). Interestingly, pre-incubation of LA and BH_4 in combination in high significant shifted the DRC of ACh to the left (fig.2C), and this finding indicates that LA and BH_4 in combination has a greater effect on ACh relaxation than each substance alone that is co-coordinated with Gunnett *et al.* (2005).

5. CONCLUSIONS

The present results demonstrated that pre-incubation of LA and BH_4 alone and in their combination shift the BQ-123 DRC to left. It can be suggested that the above agents reduce the ET-1A activity. These effects are markedly changed by LA and BH_4 combination then each substance alone. The results also indicated that the relaxation response curve of ACh that depends on NO, and prostacyclin pathways increased by LA and BH_4 in combination. In summary, LA and BH_4 may offer some pharmacological tools to modulate the ET-1A receptor activity and treat cardiovascular disease beyond pulmonary arterial hypertension.

Acknowledgements

Great thanks to Prof. Dr. A. M. Rasheed for Lab support, Mr. A. H. Ahmad for organ bath training and technical support.

Conflict of Interest

I do not have any conflict of interest or any other relevant connection or shared interest.

6. References

A KHALIL, R. J. C. M. P. 2011. Modulators of the vascular endothelin receptor in blood pressure regulation and hypertension. 4**,** 176-186.

BARRETT, K. E., BARMAN, S. M. & BOITANO, S. 2010. *Ganong's review of medical physiology*, New Delhi: McGraw Hill, 2010.

BRIYAL, S., PHILIP, T. & GULATI, A. J. J. O. A. S. D. 2011. Endothelin-a receptor antagonists prevent amyloid-β-induced increase in ET A receptor expression, oxidative stress, and cognitive impairment. 23**,** 491-503.

C KOWALA, M., MURUGESAN, N., TELLEW, J., CARLSON, K., MONSHIZADEGAN, H., RYAN, C., GU, Z., KANE, B., FADNIS, L., BASKA, R., BEYER, S., ARTHUR, S., DICKINSON, K., ZHANG, D., PERRONE, M., FERRER, P., GIANCARLI, M., BAUMANN, J., BIRD, E. & E MACOR, J. 2004. *Novel Dual Action AT1 and ETA Receptor Antagonists Reduce Blood Pressure in Experimental Hypertension*.

CALLERA, G. E., TOUYZ, R. M., TEIXEIRA, S. A., MUSCARA, M. N., CARVALHO, M. H. C., FORTES, Z. B., NIGRO, D., SCHIFFRIN, E. L. &

TOSTES, R. C. J. H. 2003. ETA receptor blockade decreases vascular superoxide generation in DOCA-salt hypertension. 42**,** 811-817.

CERRATO, R., CUNNINGTON, C., CRABTREE, M., ANTONIADES, C., PERNOW, J., CHANNON, K. & BÖHM, F. J. L. S. 2012. Endothelin-1 increases superoxide production in human coronary artery bypass grafts. 91**,** 723-728.

CHEN, Q., KIM, E. E. J., ELIO, K., ZAMBRANO, C., KRASS, S., TENG, J. C.-W., KAY, H., PERKINS, K.-A., PERSHAD, S. & MCGRAW, S. J. A. I. P. S. 2010. The role of tetrahydrobiopterin and dihydrobiopterin in ischemia/reperfusion injury when given at reperfusion. 2010.

ENDEMANN, D. H. & SCHIFFRIN, E. L. 2004. Endothelial dysfunction. *Journal of the American Society of Nephrology,* 15**,** 1983-1992.

FRIEBE, A. & KOESLING, D. J. C. R. 2003. Regulation of nitric oxide-sensitive guanylyl cyclase. 93**,** 96-105.

GUNNETT, C., LUND, D., MCDOWELL, A., FARACI, F., HEISTAD, D. J. A., THROMBOSIS, & BIOLOGY, V. 2005. Mechanisms of inducible nitric oxide synthase–mediated vascular dysfunction. 25**,** 1617-1622.

HAMAD, S. H. A., MAULOOD, I. M. J. Z. J. O. P. & SCIENCES, A. 2016. Hemodynamic and Renal Effects of Bosentan and Losartan in Endothelin-1 And Angiotensin II Induced Hypertensive Rats. 28**,** 152-160.

HYNYNEN, M. M. & KHALIL, R. A. J. R. P. O. C. D. D. 2006. The vascular endothelin system in hypertension-recent patents and discoveries. 1**,** 95-108.

JIANG, J., VALEN, G., TOKUNO, S., THORÉN, P. & PERNOW, J. J. B. J. O. P. 2000. Endothelial dysfunction in atherosclerotic mice: improved relaxation by combined supplementation with L-arginine- tetrahydrobiopterin and enhanced vasoconstriction by endothelin. 131**,** 1255-1261.

KELLOGG JR, D., ZHAO, J., COEY, U. & GREEN, J. J. J. O. A. P. 2005. Acetylcholine-induced vasodilation is mediated by nitric oxide and prostaglandins in human skin. 98**,** 629-632.

KOWALCZYK, A., KLENIEWSKA, P., KOLODZIEJCZYK, M., SKIBSKA, B. & GORACA, A. J. A. I. E. T. E. 2015. The role of endothelin-1 and endothelin receptor antagonists in inflammatory response and sepsis. 63**,** 41-52.

LIMA, V. V., GIACHINI, F. R., HARDY, D. M., WEBB, R. C., TOSTES, R. C. J. A. J. O. P.-R., INTEGRATIVE & PHYSIOLOGY, C. 2010. O-GlcNAcylation: a novel pathway contributing to the effects of endothelin in the vasculature. 300**,** R236-R250.

MARTÍNEZ-REVELLES, S., CARACUEL, L., MÁRQUEZ-MARTÍN, A., DANTAS, A., OLIVER, E., D'OCON, P. & VILA, E. 2012. Increased endothelin-1 vasoconstriction in mesenteric resistance arteries after superior mesenteric ischaemia-reperfusion. *British journal of pharmacology,* 165**,** 937-950.

RAMESHRAD, M., BABAEI, H., AZARMI, Y. & FOULADI, D. F. 2016. Rat aorta as a pharmacological tool for in vitro and in vivo studies. *Life sciences,* 145**,** 190-204.

SAGACH, V., BONDARENKO, A., BAZILYUK, O. & KOTSURUBA, A. 2006. Endothelial dysfunction: Possible mechanisms and ways of correction. *Experimental and clinical cardiology,* 11**,** 107-110.

SALIHI, A. B., SHEKHA, M. S., MAULOOD, I. M., MAHMUD, A. M. & AL-HABIB, O. A. 2016. Nitric Oxide Donor Dilates Aorta in Salt Loaded Rats via Activation of Inward-Rectifier Potassium Channels. *ZANCO Journal of Pure and Applied Sciences,* 28**,** 69-77.

SCHNEIDER, M. P., BOESEN, E. I. & POLLOCK, D. M. 2007. Contrasting actions of endothelin ET(A) and ET(B) receptors in cardiovascular disease. *Annual review of pharmacology and toxicology,* 47**,** 731-759.

SCHREIBER, C., EILENBERG, M. S., PANZENBOECK, A., WINTER, M.-P., BERGMEISTER, H., HERZOG, R., MASCHERBAUER, J., LANG, I. & BONDERMAN, D. J. P. C. 2017. Combined oral administration of L-arginine and tetrahydrobiopterin in a rat model of pulmonary arterial hypertension. 7**,** 89-97.

SHINOZAKI, K., NISHIO, Y., OKAMURA, T., YOSHIDA, Y., MAEGAWA, H., KOJIMA, H., MASADA, M., TODA, N., KIKKAWA, R. & KASHIWAGI, A. 2000. Oral administration of tetrahydrobiopterin prevents endothelial dysfunction and vascular oxidative stress in the aortas of insulin-resistant rats. *Circ Res,* 87**,** 566-73.

SODERMAN, R. 2013. *Over-the-counter L-arginine supplements to improve human performance.*

TIRAPELLI, C. R., LEGROS, E., BROCHU, I., HONORÉ, J. C., LANCHOTE, V. L., UYEMURA, S. A., DE OLIVEIRA, A. & D'ORLÉANS- JUSTE, P. J. B. J. O. P. 2008. Chronic ethanol intake modulates vascular levels of endothelin- 1 receptor and enhances the pressor response to endothelin- 1 in anaesthetized rats. 154**,** 971-981.

TRATSIAKOVICH, Y., GONON, A. T., KISS, A., YANG, J., BÖHM, F., TORNVALL, P., SETTERGREN, M., CHANNON, K. M., SJÖQUIST, P.-O. & PERNOW, J. J. I. J. O. C. 2013a. Myocardial protection by co-administration of L-arginine and tetrahydrobiopterin during ischemia and reperfusion. 169**,** 83-88.

TRATSIAKOVICH, Y., GONON, A. T., KISS, A., YANG, J., BOHM, F., TORNVALL, P., SETTERGREN, M., CHANNON, K. M., SJOQUIST, P. O. & PERNOW, J. 2013b. Myocardial protection by co-administration of L-arginine and tetrahydrobiopterin during ischemia and reperfusion. *Int J Cardiol,* 169**,** 83-8.

TSUBOI, T., MAEDA, M. & HAYASHI, T. 2018. Administration of L-arginine plus L-citrulline or L-citrulline alone successfully retarded endothelial senescence. *PloS one,* 13**,** e0192252-e0192252.

VIGNON-ZELLWEGER, N., HEIDEN, S., MIYAUCHI, T. & EMOTO, N. 2012. Endothelin and endothelin receptors in the renal and cardiovascular systems. *Life sciences*, 91**,** 490-500.

YANAGISAWA, M., KURIHARA, H., KIMURA, S., TOMOBE, Y., KOBAYASHI, M., MITSUI, Y., YAZAKI, Y., GOTO, K. & MASAKI, T. 1988. A novel potent vasoconstrictor peptide produced by vascular endothelial cells. *Nature*, 332**,** 411-5.